Technical Report Documentation Page

1. Report No. FHWA-RD-96-207	2. PB97-179451	3. Recipient's Catalog No.
4. Title and Subtitle IMPROVED CONCRETES FOR CORROSION RESISTANCE		5. Report Date May 1997
		6. Performing Organization Code
7. Author(s) Neil G. Thompson and David R. Lankard		8. Performing Organization Report No.
		10. Work Unit No. (TRAIS) 3D4C
9. Performing Organization Name and Address Cortest Columbus Technologies, Inc., 6141 Avery Road, Dublin, OH 43016-8761		11. Contract or Grant No. DTFH61-93-C-00028
12. Sponsoring Agency Name and Address Office Of Engineering R&D, Federal Highway Administration, 6300 Georgetown Pike, McLean, Virgina 22101-2296		13. Type of Report and Period Covered Interim Report, August 12, 1996
		14. Sponsoring Agency Code

15. Supplementary Notes

Contracting Officer's Technical Representative (COTR): Y. Paul Virmani, HNR-10, assisted by John Hardy

16. Abstract A major cause of concrete deterioration on bridge structures is the corrosion of the embedded steel reinforcement. In response to the continued problem of corrosion, FHWA initiated this research aimed at (1) quantifying the corrosive conditions fostering concrete bridge deterioration and (2) identifying concrete materials which consistently provide superior performance when used in bridge applications. The experimental phase of this research project was divided into three tasks: Task A - Corrosive Environment Studies, Task B - Concrete Chemical and Physical Properties, and Task C - Long-Term Corrosion Performance. This Interim Report reviews the results of tasks A and B and provides recommendations for performing task C.

In task A, laboratory experiments were conducted to characterize the corrosive environment and to establish boundary conditions for environmental variables of moisture content, chloride concentration, and temperature. Special test specimen design and test procedures were developed to permit uniform chloride diffusion to the steel surface. A full factorial matrix of experiments were performed for three levels each of chloride concentration, relative humidity, and temperature. A regression model was developed to predict corrosion rate and corrosion potential as a function of environment for two different concretes.

In task B, experiments were performed to identify the chemical components of concretes and to determine how they effect corrosion induced deterioration of concrete structures. The dependent variables of interest in examining corrosion induced deterioration of concrete are corrosion rate, corrosion potential, chloride permeability, electrical resistivity, and physical properties. The independent concrete design mix variables examined included: water-cement ratio, air content, coarse aggregate type, fine aggregate type, mineral admixture, and cement type. Because of the large number of independent variables and the number of levels of interest for the variables, an optimized experimental design was developed to permit the estimate of the main-effect terms for each independent variable. Models were developed to predict the effect of the independent variables on corrosion rate and corrosion potential in each of two environments, chloride permeability, resistivity, and compressive strength. The data developed was used to make recommendations for the concretes to be tested in the task C long-term experiments.

17. Key Words Concrete, mortars, reinforcing steel, corrosion rate, corrosion potential, model predictions, chloride, temperature, relative humidity, permeability, compressive strength, resistivity, water-cement ratio, air content, aggregate, mineral admixture, cement.	18. Distribution Statement No restrictions. This document is available to the public through the National Technical Information Service, Springfield, VA 22161

19. Security Classif. (Of this report) Unclassified	20. Security Classif. (Of this page) Unclassified	21. No. Of Pages 176	22. Price

Form DOT F 1700.7 (8-72) Reproduction of completed page authorized

SI* (MODERN METRIC) CONVERSION FACTORS

APPROXIMATE CONVERSIONS TO SI UNITS

Symbol	When You Know	Multiply By	To Find	Symbol
		LENGTH		
in	inches	25.4	millimeters	mm
ft	feet	0.305	meters	m
yd	yards	0.914	meters	m
mi	miles	1.61	kilometers	km
		AREA		
in^2	square inches	645.2	square millimeters	mm^2
ft^2	square feet	0.093	square meters	m^2
yd^2	square yards	0.836	square meters	m^2
ac	acres	0.405	hectares	ha
mi^2	square miles	2.59	square kilometers	km^2
		VOLUME		
fl oz	fluid ounces	29.57	milliliters	mL
gal	gallons	3.785	liters	L
ft^3	cubic feet	0.028	cubic meters	m^3
yd^3	cubic yards	0.765	cubic meters	m^3
NOTE: Volumes greater than 1000 l shall be shown in m^3.				
		MASS		
oz	ounces	28.35	grams	g
lb	pounds	0.454	kilograms	kg
T	short tons (2000 lb)	0.907	megagrams (or "metric ton")	Mg (or "t")
		TEMPERATURE (exact)		
°F	Fahrenheit temperature	5(F-32)/9 or (F-32)/1.8	Celcius temperature	°C
		ILLUMINATION		
fc	foot-candles	10.76	lux	lx
fl	foot-Lamberts	3.426	candela/m^2	cd/m^2
		FORCE and PRESSURE or STRESS		
lbf	poundforce	4.45	newtons	N
lbf/in^2	poundforce per square inch	6.89	kilopascals	kPa

APPROXIMATE CONVERSIONS FROM SI UNITS

Symbol	When You Know	Multiply By	To Find	Symbol
		LENGTH		
mm	millimeters	0.039	inches	in
m	meters	3.28	feet	ft
m	meters	1.09	yards	yd
km	kilometers	0.621	miles	mi
		AREA		
mm^2	square millimeters	0.0016	square inches	in^2
m^2	square meters	10.764	square feet	ft^2
m^2	square meters	1.195	square yards	yd^2
ha	hectares	2.47	acres	ac
km^2	square kilometers	0.386	square miles	mi^2
		VOLUME		
mL	milliliters	0.034	fluid ounces	fl oz
L	liters	0.264	gallons	gal
m^3	cubic meters	35.71	cubic feet	ft^3
m^3	cubic meters	1.307	cubic yards	yd^3
		MASS		
g	grams	0.035	ounces	oz
kg	kilograms	2.202	pounds	lb
Mg (or "t")	megagrams (or "metric ton")	1.103	short tons (2000 lb)	T
		TEMPERATURE (exact)		
°C	Celcius temperature	1.8C + 32	Fahrenheit temperature	°F
		ILLUMINATION		
lx	lux	0.0929	foot-candles	fc
cd/m^2	candela/m^2	0.2919	foot-Lamberts	fl
		FORCE and PRESSURE or STRESS		
N	newtons	0.225	poundforce	lbf
kPa	kilopascals	0.145	poundforce per square inch	lbf/in^2

* SI is the symbol for the International System of Units. Appropriate rounding should be made to comply with Section 4 of ASTM E380.

(Revised September 1993)

U.S. Department
of Transportation
**Federal Highway
Administration**

Research and Development

Turner-Fairbank Highway
Research Center
6300 Georgetown Pike
McLean, Virginia 22101-2296

ERRATA

Improved Concretes for Corrosion Resistance

Publication No. FHWA-RD-96-207

Because of an oversight, recipients of the above referenced publication are asked to make the following pen-and-ink changes to their copies of the report:

Location	Change
Figure 1-6 on unnumbered page 17	**Change the figure number from** "Figure 1-6" **to** "Figure 3."
Unnumbered page 17	**Write in the correct page number** as page "17" at the bottom of the page.

We apologize for any inconvenience this may have caused you.

TABLE OF CONTENTS

TABLE OF CONTENTS (Continued)

LIST OF FIGURES

Figure **Page**

LIST OF FIGURES (Continued)

Figure **Page**

LIST OF TABLES

LIST OF TABLES (Continued)

Table **Page**

CHAPTER 1. INTRODUCTION

The deterioration of various reinforced concrete (R/C) bridge components containing conventional black steel reinforcement is the most important problem facing U.S. highway agencies. A major cause of this concrete deterioration (cracking, delamination, and spalling) is the corrosion of the embedded steel reinforcement, initiated by chloride ions from deicing salts and salt-water spray which have penetrated the concrete cover. A similar problem exists for prestressing steel in prestressed concrete (PS/C) bridge components exposed to deicing salts and marine environments. For PS/C bridge components, in addition to the corrosion-induced concrete deterioration, corrosion induced hydrogen embrittlement of prestressing steel may eventually compromise the structure's safety and its ability to carry the normal structural loads.

The historical approach to this problem has involved small-area patching on all bridge components, and complete overlays on bridge decks. These conventional rehabilitation methods have involved a wide variety of repair strategies, and dozens of different repair materials. No one repair procedure/material has evolved as the optimum solution to the problem.

In response to this situation, the Federal Highway Administration (FHWA), in 1992, issued a Broad Agency Announcement (no DTFH61-92-R-000137) to solicit research proposals aimed at improving rehabilitation technology for corrosion induced deterioration of bridges. FHWA initiated this research project directed at the quantitative identification of the corrosive conditions fostering concrete bridge deterioration, and at the identification of concrete materials which consistently provide superior performance when used for bridge deck overlays and for the repair of other concrete bridge members. It was also envisioned that this work would lead to the identification of concretes which are cost-effective for the construction of new bridge members, in addition to successfully resisting corrosion-induced concrete deterioration in the presence of well-defined corrosive conditions.

The present research project was initiated during January 1993, in answer to this need. The research approach was structured to address the three principal rate phenomena that control corrosion-induced deterioration of concrete bridge components. These phenomena are identified as:

1. Diffusion of chloride ions to the level of the reinforcing steel (chloride diffusion rate).
2. Corrosion of the reinforcing steel once passivity has been destroyed by the presence of the chloride ion (rate of corrosion).
3. Cracking/spalling distress in the concrete as a result of the build-up of steel corrosion products (rate of deterioration).

The experimental phase of the research was divided into three tasks which include:

1. Task A - Corrosive Environment Studies.
2. Task B - Concrete Chemical and Physical Properties.
3. Task C - Long-Term Corrosion Performance.

In task A laboratory experiments were conducted to characterize the corrosive environment and to establish boundary conditions for moisture content, chloride content, and temperature levels for corrosion initiation and propagation.

Task B focused on an identification of the chemical and physical characteristics of concretes as they relate to the rate of corrosion of embedded reinforcing steel. Corrosive environments used in task B were selected on the basis of results obtained in the task A work.

Task C will provide simulation and measurement of all three of the phenomena that control corrosion induced deterioration of concrete structures. These include the chloride diffusion rate in the concrete, the rate of corrosion of the steel once corrosion is initiated, and the rate of deterioration of the concrete during the build-up of corrosion products.

Task C will encompass long-term tests of small reinforced concrete slabs under conditions that simulate bridge structures in well-defined corrosive environments. Independent variables for the task C work will be selected on the basis of findings from task A and task B.

The present interim report describes the methodology used and the results obtained in the task A and task B work.

CHAPTER 2. BACKGROUND

Over the past 60 years or so, an enormous amount of energy has been expended in laboratory and field studies of reinforced concrete to characterize the nature of the corrosion-induced damage phenomenon, and to identify preventative and remedial solutions. Despite this effort, it is still not possible to identify the "ideal" concrete to provide "optimum" performance in a particular corrosive environment situation.

What has been learned in the previous and ongoing research investigations is that there are many material, design, and environmental variables that can affect both the corrosion process itself, and the extent of damage resulting from the corrosion process. In the vast majority of cases, the field and laboratory results are empirical in nature. A fundamental study of the effect of these variables (table 1) on the corrosion phenomenon, and on the damage resulting from the corrosion in reinforced concrete structures, is needed if true advances are to be made.

It is widely known and accepted that reinforcing steel in "uncontaminated," uncarbonated, and uncracked Portland cement concrete will either show no corrosion or will corrode at such a slow rate that cracking and spalling distress is never manifested. It is only when these three requirements for corrosion protection are violated that disruptive corrosion of reinforcing steel can initiate and be sustained. This violation can take the form of either (1) a chemical violation or (2) a mechanical violation. In the chemical violation mode, the normally protective environment of the Portland cement concrete can be compromised by (1) intrusion of chloride-bearing solutions to the level of reinforcing steel, and/or (2) carbonation of the concrete to the level of the reinforcing steel. In the mechanical mode, cracking of the concrete over the reinforcing steel can hasten the onset of corrosion by providing a direct access of oxygen, water, and chlorides to the reinforcing steel.

Figure 1 shows a simplified deterioration model relating to the corrosion of steel reinforcement in reinforced concrete.[1] Initially, there is an initiation period during which time the concrete is undergoing carbonation, or an influx of chloride-laden waters. During this period the reinforcing steel remains in a passive state.

Because of the dominant role played by chloride ion in the corrosion process, the vast majority of research designed to make concrete more "protective" focuses on changes to the concrete that can reduce the rate of chloride ion diffusion. Once the chloride ion reaches the level of reinforcing steel in moist concrete, corrosion is inevitable, if oxygen is available. However, following the initiation of corrosion, both the rate of corrosion and the subsequent rate of damage arising from the corrosion process depend upon many factors that, at present, are not well understood. It is a primary objective of the present research to increase the state of knowledge here.

Much of the treatment of the steel corrosion problem in the literature is concerned with material and design variables that will increase the time required for chloride ion to reach the level of reinforcing steel. A lesser amount of the literature

Table 1. Material, environmental, and design variables known to influence the corrosion induced damage of steel reinforced concrete structures.

Material Variables	Environmental Variables	Design Variables
A. Concrete Chemistry 1. pH of pore water 2. Chemistry of pore water (Cl^-/OH^-) 3. Chloride binding capability B. Concrete Engineering Properties 1. Permeability 2. Porosity 3. Compressive Strength 4. Bond Strength 5. Tensile Strength 6. Elastic Properties 7. Inelastic Properties 8. Electrical Properties C. Water-Cement Ratio D. Hardened Concrete Free Water Content	A. Source of Aggressive ions, e.g. chloride (from deicing salts and sea water) and sulfate. B. Temperature Extremes and Cycling C. Relative Humidity D. Moisture Content and Cycling E. Live Loads	A. Depth of Cover B. Cracking C. Size and Spacing of Rebar D. Drainage Efficiency

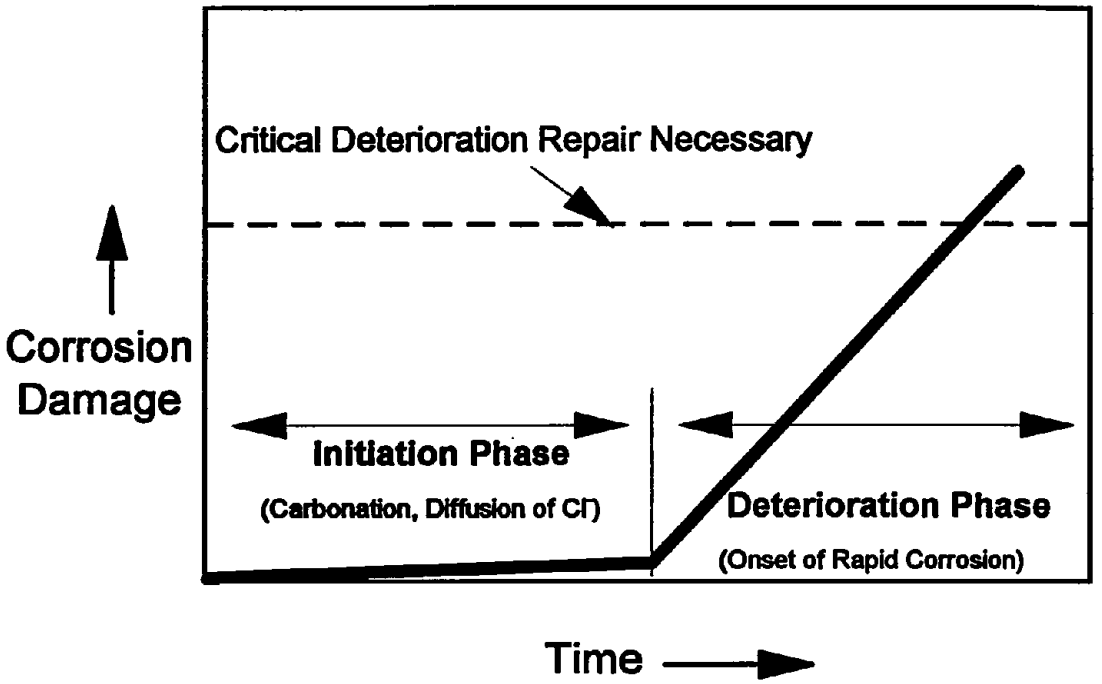

Figure 1. Simple deterioration model for corrosion of steel in concrete.

(mostly of relatively recent vintage) is concerned with chemical factors that influence the onset and rate of corrosion once the chloride has reached the steel level. With the exception of the depth of concrete cover over the steel reinforcement, there is very little in the literature to date dealing with the ability of the concrete to eliminate or minimize damage once the corrosion process is operative.

FACTORS AFFECTING CHLORIDE ION DIFFUSION RATE

In practice, chlorides that get into concrete come primarily from one of two sources: (1) deicing salts and (2) seawater. In both of these instances, little control can be exerted over the source of the chloride ion. For this reason, individuals responsible for addressing the corrosion issue have focused on modifications to the concrete that will reduce the rate of chloride ion diffusion. The concrete property controlling diffusion rate is its permeability. Reduced permeabilities in concrete have been achieved by:

1. Reduction in water-cement ratio.
2. Use of pozzolonic and pozzolonic/cementitious mineral admixtures.
3. Use of polymer modifiers.

The ability of these material modifications/additions to reduce chloride ion permeability is well documented.[2-9]

It is widely believed that reduced permeability is achieved through a reduction in connected porosity attributed to the decreased water-cement ratio, and to the in situ formation of additional cementitious material (CSH) when pozzolonic and pozzolonic/ cementitious mineral admixtures are used. An additional benefit is provided by the submicron particle size of mineral admixtures such as silica fume. These small particles fit into spaces in the concrete that previously could only be occupied by water, thereby creating a denser, less permeable matrix. With respect to the ability to decrease the diffusion rate of chloride ion, reductions in water-cement ratio alone is not as effective as the use of latex polymer modifiers or the use of mineral admixtures (particularly silica fume) in conjunction with reduced water-cement ratios.

It can be reasoned that aggregate porosity/permeability should also affect the chloride ion diffusion rate in concrete. If porosity in the aggregates is connected, and assuming that the pores can become saturated with pore water solution, then it is expected that, as aggregate connected porosity increases, an increase should also occur in chloride ion diffusion rate. To date, there have been no studies to directly address this issue.

Although permeability is the dominant factor controlling chloride diffusion, other factors may be involved, including (1) the surface charge on the hydrated cement phases, (2) the formation of porous transition zones at aggregate/cement paste interfaces, and (3) microcracking in the concrete's matrix phase.

It has been suggested that diffusion of chloride ions is retarded by the surface charge of the hydrated cement gel pastes with a low-capillary porosity.[10] In contrast,

the hydrated cement gel is much more permeable to the similarly-sized neutral oxygen molecule. This study showed that the use of a mineral admixture (fly ash) had a significantly greater effect on the chloride diffusion than on the oxygen diffusion in concrete. The size of the oxygen molecule and the chloride ion are similar, and their diffusion coefficients in bulk aqueous solutions are comparable. The two species might be expected to diffuse at similar rates in very porous hydrated cement pastes. The fact that they don't suggests that chloride diffusion kinetics in these pastes are generally restricted by the interactions between the migrating chloride ion and the electrostatically charged pore walls, or by the electrical double-layer at the interface between the pore walls and pore solution.

The amount of microcracking that occurs in concrete structures subjected to cyclic loadings can increase the rate of chloride permeability into the structures.[11] Static compressive stresses appear to have little effect on chloride permeability of concrete. Compressive load repetitions in the 60 to 80 percent of ultimate strength range gave rise to a significant increase in the chloride permeability of the concrete. Chloride permeability increases at an increasing rate as the residual strengths decrease.

It has been shown that the introduction of aggregates (sand particles) into cement paste results in a higher chloride ion transport coefficient.[12] This porous transition zone formed at the aggregate-cement paste interface affects the pore size distribution. This, in turn, affects the chloride ion diffusion rate.

Tests that are used to measure the chloride ion diffusion rate include short-term tests in which chloride ions are driven through concrete by an electrical potential difference, and long-term tests in which concretes ponded on concrete surfaces are allowed to diffuse in naturally. Andrade showed that chloride penetration into concrete, as defined by the Rapid Chloride Permeability Test, provides values for chloride diffusivities that agree quite well with values obtained under both steady- and non-steady-state conditions.[13] However, the agreement with values obtained from natural diffusion tests (i.e., ponding) is still not adequate, and further experimentation is needed to clarify this point. Andrade also showed that chloride diffusivities can be calculated from concrete resistivity measurements, providing the concentration of chlorides in the pore solution is measured or assumed.

Johansen cautions that the use of Fick's Second Law to describe chloride penetration in concrete can result in values of the diffusion coefficient that apparently decrease with increasing time.[14] Application of such data to estimate chloride-induced corrosion of reinforcement has been found to be very conservative. Johansen contends that this does not mean that Fick's Second Law is not valid; only that the description of concrete as a homogeneous medium with respect to transport of dissolved species is too simple a model. Chatterji further cautions that any attempt to predict the long-term penetration depth of chloride ion in concrete, on the basis of diffusivity as measured by any method, may be very uncertain.[15] The assumption of a constant chloride ion diffusivity through concrete is seldom satisfied in practice.

FACTORS AFFECTING CORROSION RATE

Factors that have been shown to affect the corrosion of embedded reinforcing steel in concrete, once chloride ions reach the steel, include:

1. The amount of chloride ion present in the pore water (typically expressed as Cl^-/OH^- ratio).
2. Ionic conductivity/resistivity of the concrete.
3. Temperature.
4. Relative humidity (external and internal).
5. Concrete microstructure.

Cl\OH⁻ Ratio

In 1981, Barneyback and Diamond described a device for retrieving pore solution from hardened cement paste samples.[16] Since that time, measurements of the type and amount of chemical species in pore solutions have become commonplace.[17-22] Particular interest is focussed on measurements of the Cl^-/OH^- ratio. It is now well-established that the depassivation of embedded steel, where it occurs, is a function not only of Cl^- concentration, but also of OH^- concentration. Diamond showed that, for pH values representative of those in concrete pore solutions, the maximum Cl^-/OH^- that can be tolerated without depassivation is 0.29 at pH 12.6 and 0.30 at pH 13.3.[17] Goni and Andrade showed that the Cl^-/OH^- ratio is the only parameter which unequivocally corresponds to the mean corrosion current (I_{corr}) value, which indicates that higher Cl^-/OH^- ratios induce a higher corrosion rate.[23]

It is likely that other features of cement pore water chemistry also influence the nature of the steel corrosion products and the rate of corrosion. These important parameters of the cement pore water chemistry may include (1) ionic strength, (2) pH, (3) redox potential, and (4) cation composition. The ionic strength effects ionic exchange reactions of the pore solution with the cement hydrate phases. It has been found that cement pore solutions have fairly high ionic strengths (up to 0.3), with pHs in the range of 12.4 to 13.5.[24] The redox potential determines the oxidation state for multivalent elements. In general, pore solutions of Portland cements are oxidizing (positive redox potentials), except for those containing blast furnace slag. For standard Portland cements (including those containing slag, silica fume, and fly ash), the dominating cations in the pore solutions are sodium and potassium. The calcium contents of the pore solution are significantly lower than sodium or potassium. For calcium aluminate cements, sodium and aluminum dominate the cement pore solution.

It is indicated that the alkali concentrations of pore solutions are not affected by the presence of aggregate.[25] However, over a long time period, the presence of alkali reactive aggregates could affect the alkali concentration as alkalis are entrapped in the reaction products, resulting in a depletion of alkalis in the pore solution.

In recent years, considerable attention has been given to the so-called chloride binding ability of concretes, with respect to the influence of this feature on the Cl^-/OH^-

ratio. Chloride-binding refers to the chemical reaction between cement hydration products and chloride ions in solution to form insoluble chloride phases. This effectively removes chloride ion from pore water, eliminating its participation in the depassivation phenomenon. Many researchers have proposed a correlation between the tricalcium aluminate (C_3A) content of cement and the cement's ability to bind chlorides through the formation of insoluble calcium chloroaluminates.[26-31] Typically, it is reported that higher C_3A cements bind more chlorides, thereby lowering the chloride ion concentration in the pore solution. This general conclusion is, however, challenged by Arya, et al., for chlorides that were externally derived relative to chlorides added at the time of mixing.[28,32] They showed that cement type, the type and proportion of cement replacement material, associated cations, and total chloride content were the most important factors governing the binding of chlorides. Binding of internal chlorides also increased with increases in water-cement ratio, curing temperature, and age. Furthermore, Arya showed that for external chloride, the associated cation had a dramatic influence on chloride binding phenomenon; calcium chloride, and particularly magnesium chloride, produced massive increases in binding in relation to sodium chloride.

Byfors also cautions that differences in chloride binding among cements cannot be attributed simply to differences in C_3A content.[33] Chloride binding also appears to be related to both the original alkalinity of the cement and its specific surface area. For bound chlorides, some are irreversibly combined into hydrated products by chemical reaction, and others can unbind as the free chloride concentration decreases.

It has been suggested that tetracalcium aluminoferrite participates in chloride binding in the form of a chloro-complex $C_3F \cdot CaCl_2 \cdot 10H_2O$.[34] Principal chloride binding, however, is still attributed by these authors to the formation of Friedel's salt, derived from the tricalcium aluminate hydrates.

The effect of chemical admixtures on the chloride binding capacity has not been widely studied. It has been suggested that the presence of a superplasticizer in concrete can lower chloride binding capacity.[35] This conclusion was based on the finding that the Cl^-/OH^- ratio is considerably lower in solutions that have been obtained by decanting, relative to pore water that has been extracted under pressure from the hydrated cement (expressed solutions).

The results of chloride binding studies have provided guidelines regarding the design of experiments intended to study the corrosion process in concrete. Enevoldzen, et al., addressed the method of chloride addition to experimental concretes; that is, whether or not the chloride is added as the initial mix ingredient or allowed to diffuse naturally into the hardened concrete.[32,36] The study was done in connection with electrochemical removal of chlorides from concrete. They showed that more of naturally-ingressed chloride could be removed more easily from concrete relative to concretes in which the chloride had been added to the initial mix. They concluded that this supports a hypothesis that some of the admixed chlorides become physically trapped in the CSH gel during hydration; whereas, chloride penetrated from the environment enters and leaves the paste exclusively via the capillary pores.

There are two factors that may compromise or trivialize the importance of pore water chemistry, as related to its importance as an independent variable in studies of the corrosion of embedded reinforcing steel in concrete. One is the question surrounding the validity of chemical analyses of expressed pore solutions. Another is the fact that, in many service environments, there is a nearly inexhaustible supply of chloride ion.

Chatterji questions the validity of chemical analyses of expressed pore solutions.[37] This question arises from the fact that polyvalent ions are expected to preferentially accumulate at the interface between cement hydration products and pore water. This arises from the fact that both cement hydration products and reactive silica particles are negatively charged in alkaline solutions (such as in a cement paste condition).

As previously discussed, it is now well-established that high Cl^-/OH^- ratios correspond to high corrosion currents, which translate into high corrosion rates. In practice, the availability of chloride ion from external sources may overwhelm any effect that the intrinsic concrete pore water chemistry has on the corrosion process. Arya and Xu concluded that chloride binding is not related, in any simple way, to the rate of corrosion.[32] They showed that mineral admixtures (ground granulated blast furnace slag, fly ash, silica fume) did have an effect on the chloride binding ability of the cementitious phase. However, corrosion rates increased with increasing chloride content for all mixes due (they concluded) to a simple increase in the amount of free chloride. Al-Amoudi showed that, in a high chloride environment, a high C_3A content in plain cement concrete is rendered ineffective.[8] These findings may explain why there have been no studies that have actually proven that a high chloride binding potential in concrete translates into improved corrosion protection in field-placed concrete.

Ionic Conductivity

The corrosion of steel in concrete is an electrochemical phenomenon. Thus, it is widely assumed that the electrical conductivity (and resistivity) of the concrete exerts an influence on the nature and rate of corrosion of embedded reinforcing steel. This phenomenon is clearly operative in those instances where the electrical conductivity of the concrete is at a low level as a result of the removal of free (evaporable) water due to low values of ambient relative humidity or artificial drying.

Although acknowledged as a contributing factor, only a few studies have been conducted to attempt to relate concrete resistivity with the corrosion rate of embedded reinforcing steel.[38-41] Conditions such as a high pore water content and the presence of electrolyte salts that lead to low resistivity do usually favor active corrosion. Conversely, high resistivity of the concrete does appear to limit the rate of corrosion. It has been proposed that significant corrosion is not likely when the resistivity of the concrete exceeds 8500 to 12,000 ohm-cm.[39]

Enevoldsen, et al., found a strong dependence of the corrosion rate with the electrical resistivity of the concrete surrounding the steel (and they cite other studies supporting this conclusion).[42] These workers identified the existence of a threshold limit for the internal relative humidity in concrete below which active corrosion does not take place. The value of this corrosion threshold varies with concrete type and ambient conditions; although it is suggested that, below an internal relative humidity of 70 to 80 percent, a corrosion current cannot be maintained. The relationship between internal and external relative humidity is not a simple function and has not been addressed.

In considering the influence of the ionic conductivity of the concrete on the nature and rate of corrosion, it is necessary to consider that corrosion currents can flow, not only short distances on the same rebar surface, but also relatively long distances between two layers of reinforcing steel (macrocell corrosion). It has been shown that, in reinforced concrete structures where the corrosion current is between two different layers of rebar, the corrosion currents through concretes with a high resistivity are less than through concretes with a low electrical resistivity.[43] This effect has been observed in many systems and a decrease in macrocell activity as resistivity increases is well established. Dense concretes, having high electrical resistivities, may also increase the time to corrosion by inhibiting transport processes.

From the studies conducted to date, it can be concluded that the ionic conductivity/resistivity of concrete, at both the micro and macro level, does affect the rate of corrosion. Factors affecting these electrical properties of concrete include:

1. The internal relative humidity of the concrete (degree of dryness).
2. The evaporable water content (controlled primarily by water-cement ratio).
3. The level of connected porosity in the cement paste phase (controlled by water-cement ratio and the presence of mineral admixtures).
4. Ionic strength of the pore water.

It may be expected that an increase in temperature would cause an increase in corrosion rate due to the known effect of temperature on the rate of chemical reactions. It has also been shown that an increase in temperature from 20 °C to 70 °C results in a decrease in hydroxyl ion concentration.[44]

Concrete Microstructure

It is well-known that portland cement concrete has a very heterogenous microstructure at both the micro and macro level. Particles in concrete range from submiccron-size hydrated cement phase crystallites to coarse aggregate particles over 25.4 mm (1 in) in diameter. Total porosity and pore size distribution in the cement paste is strongly influenced by water-cement ratio and the presence of mineral admixtures. Even within a single concrete, large local variations in the nature of the cement paste porosity can occur. The porosity of the cement paste phase of the transition zones between the paste and embedments (including steel and aggregates) is different from cement paste in concrete away from these embedments. Entrained and entrapped air

voids may also show nonuniform distribution and a preference to accumulate around large embedments such as coarse aggregate particles and reinforcing steel.

The heterogeneous nature of the microstructure of portland cement concrete may be a factor controlling the nature of corrosion of embedded reinforcing steel.[45,46] It is known that the corrosion of steel in chloride-contaminated concrete is characterized by localized breakdown of passivity rather than a uniform corrosion over the entire steel surface.[46] Despite the practical interest of this pitting corrosion phenomenon, few systematic studies have been conducted to study it. In one recent study, it was observed that corrosion reactions appear to occur preferentially on the surface of rebar embedded in "denser matrices".[45] This was explained by a depletion of oxygen at the steel-cement paste interface, resulting in the formation of anodic areas. However, others (including this writer) have observed that steel corrosion products grow in abundance within entrapped air voids in contact with the steel. This implies that corrosion rates are higher in less-dense matrices where the availability of oxygen and moisture is higher. In either case, it is the heterogeneous nature of the concrete environment and chloride distribution that results in the localized breakdown of the passive film resulting in localized corrosion (both micro and macro).

FACTORS AFFECTING THE RATE OF CORROSION-INDUCED DAMAGE

With the exception of the depth of concrete cover over the steel reinforcement, there is very little information in the literature dealing with the ability of concrete to eliminate or minimize cracking/spalling damage once corrosion starts. There is some risk in assuming that the higher the concrete's strength, the better it will be able to resist damage resulting from the build-up of steel corrosion products. High strength concretes almost always have a low water-cement ratio, and a relatively high modulus of elasticity. Reflecting the low water-cement ratio, high strength concretes will have a relatively low porosity level, which may mean that their ability to "absorb" steel corrosion products is minimized. A high elastic modulus in these concretes also means that they are less forgiving than a lower elastic modulus/lower strength material. As corrosion-induced stresses arise, the lower modulus concrete can deflect without cracking to relieve the stress. In the higher modulus concretes stresses may build up and cause a fracture"

SUMMARY

Literature concerned with the corrosion of embedded reinforcing steel in chloride-contaminated concrete has been reviewed. This review was made recognizing the fact that there are three main rate processes that control the time of onset of corrosion, as well as the deterioration of the concrete to the point that the structure requires repair or is no longer serviceable. These rate processes include (1) the chloride diffusion rate, (2) the corrosion rate, and (3) the rate of corrosion-induced damage.

The review of the literature, in this context, leads to the following conclusions and significant observations:

1. Historically, the greatest research effort has been expended on a study of factors affecting the chloride diffusion rate.

2. Within the last 10 to 15 years, there has been a significant increase in studies focused on factors affecting the rate of corrosion once chloride reaches the level of the reinforcing steel. This is due in large part to the fact that techniques to measure corrosion rates of embedded steel in concrete have been only recently available. Even at that, there are questions regarding the reliability, accuracy, and meaning of such measurements when applied to concrete structures.

3. The rate of corrosion-induced damage in reinforced concrete has been largely neglected in the literature. This is due, in part, to the difficulty in reproducing field conditions in laboratory environments, and to the long times required for damage to occur and progress.

4. Concrete compositional variable that influence the diffusion rate of chloride ion into concrete have been well-studied and well-defined. Concretes showing high levels of resistance to chloride ion penetration have been prepared using low water-cement ratios and mineral admixtures. Low water-cement ratios are achieved through the use of high-range water reducers (superplasticizers). Of the mineral admixture that are available, silica fume provides the greatest and most consistent reduction in chloride ion penetration rates into concrete.

5. Factors that have been shown to affect the corrosion of embedded reinforcing steel in concrete, once chloride ions reach the steel, include (1) pore water chemistry, (2) concrete ionic conductivity, (3) concrete microstructure, and (4) temperature and relative humidity. A primary variable controlling rate of corrosion is the Cl^-/OH^- ratio of the pore water solution.

6. For most reinforced concrete structures that are exposed to extraneous sources of chloride (deicing salts, sea water), the chloride source may be viewed as inexhaustible. It has been well-established that the Cl^-/ OH^- ratio of the pore water in the concrete surrounding the steel controls the rate of corrosion. The higher this ratio, the higher the rate of corrosion. However, with an inexhaustible supply of chloride ion, it appears useless to control concrete compositional variables that maximize the hydroxyl concentration in the pore water.

7. With an inexhaustible supply of chloride ion, it is necessary to concentrate concrete compositional studies on factors that effect the rate of oxygen diffusion to the steel reinforcement, and on the ionic conductivity of the concrete surrounding the reinforcement.

8. The phenomenon of pitting corrosion of reinforcing steel in chloride-contaminated concrete is a well-known but little-studied phenomenon. A systematic study of the influence of local concrete microstructure relative to this phenomenon should be fruitful. Even in the limited studies conducted to date in this area,

there is disagreement as to what microstructural features promote this pitting corrosion.

9. It is a well-known fact that many State highway agencies are aware of individual bridge structures that have performed satisfactorily for many years in environments in which other nearby structures have shown damage to the point of requiring repair or replacement. While this result may simply be a result of depth of concrete cover, it is possible that some other feature of the concrete has mitigated the rate of damage resulting from corrosion of the steel. Despite the experimental difficulties associated with such an endeavor, it is obvious that research to study the effect of concrete composition and microstructure on the rate of corrosion-induced damage is very important.

CHAPTER 3. TASK A - CORROSIVE ENVIRONMENT STUDIES

The experimental phase of this project had as its goals to (1) quantify the effects of environmental variables on the corrosion of reinforcing steel in concrete and (2) quantify the effects of concrete mix variables on the corrosion induced deterioration of concrete. To accomplish this, the experimental program is divided into three tasks:

Task A - Corrosive Environment Studies
Task B - Concrete Chemical And Physical Properties
Task C - Long-Term Corrosion Performance.

This interim report contains the results of tasks A and B and recommendations for task C. In this section, the experimental approach and results of task A are presented.

EXPERIMENTAL APPROACH: TASK A - CORROSIVE ENVIRONMENT STUDIES

The purpose of task A was to establish boundary conditions for the environmental parameters moisture, chlorides, and temperature on the corrosion rate on the reinforcing steel embedded in concrete.

Specimen Design

Figure 2 shows the type of specimen configuration used in task A. This specimen design is rather novel but it facilitates evaluation of both corrosion product phases and interfacial chemistry of the concrete/cement phase.

For a majority of the task A tests, it was decided that a mortar paste would be used. A normal concrete mix contains cement, water, coarse and fine aggregates. A mortar paste is essentially the same but without the coarse aggregates. In all reinforced concreted materials, the interface surface of the concrete in contact with the reinforcing steel is composed principally of the fine particulates materials in the concrete (100 mesh material). This includes the hydrated portland cement phases, any finely divided particulate additives such as silica fume, slag, or flyash, and a small contribution of fine particulate material from the fine aggregate or the coarse aggregate phase. Only rarely does actual fine or coarse aggregate particles greater than 0.15 mm (0.006 in) come in contact with the reinforcing steel. This situation is illustrated in figure 3 which shows a section view through the reinforcing steel in a concrete specimen. Although aggregate particles can come close to the reinforcing steel, the actual material in contact with the steel is the fine particulates just described. It is appropriate then to conduct the corrosion rate screening tests using a mortar (cementitious material plus fine aggregate) rather than a concrete. The proportion of cementitious material to fine aggregate and water-cement ratio has to be the same in the mortars as it is in the corresponding concretes. Concrete was used in one series of tests for comparison to the mortars.

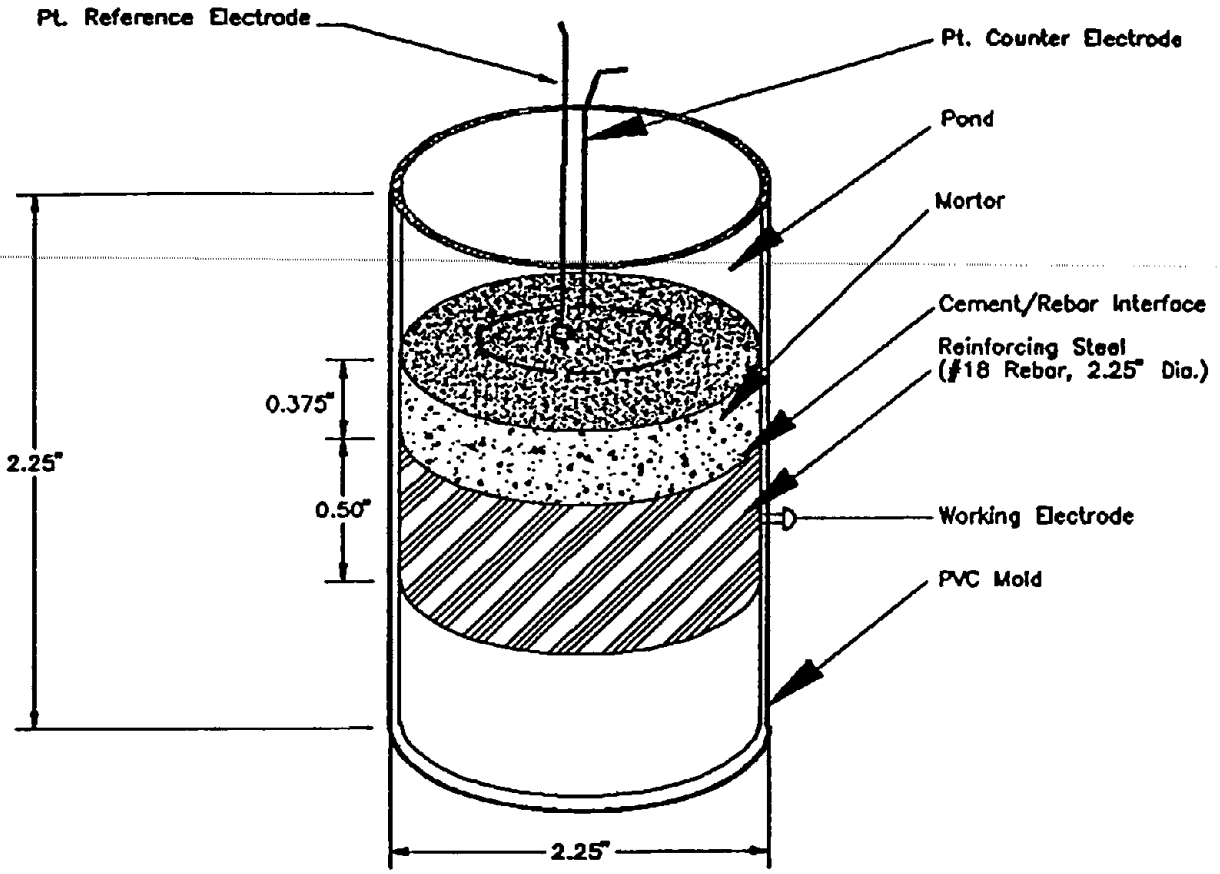

Figure 2. Specimen design for short-term corrosion tests using # 18 normal rebar.

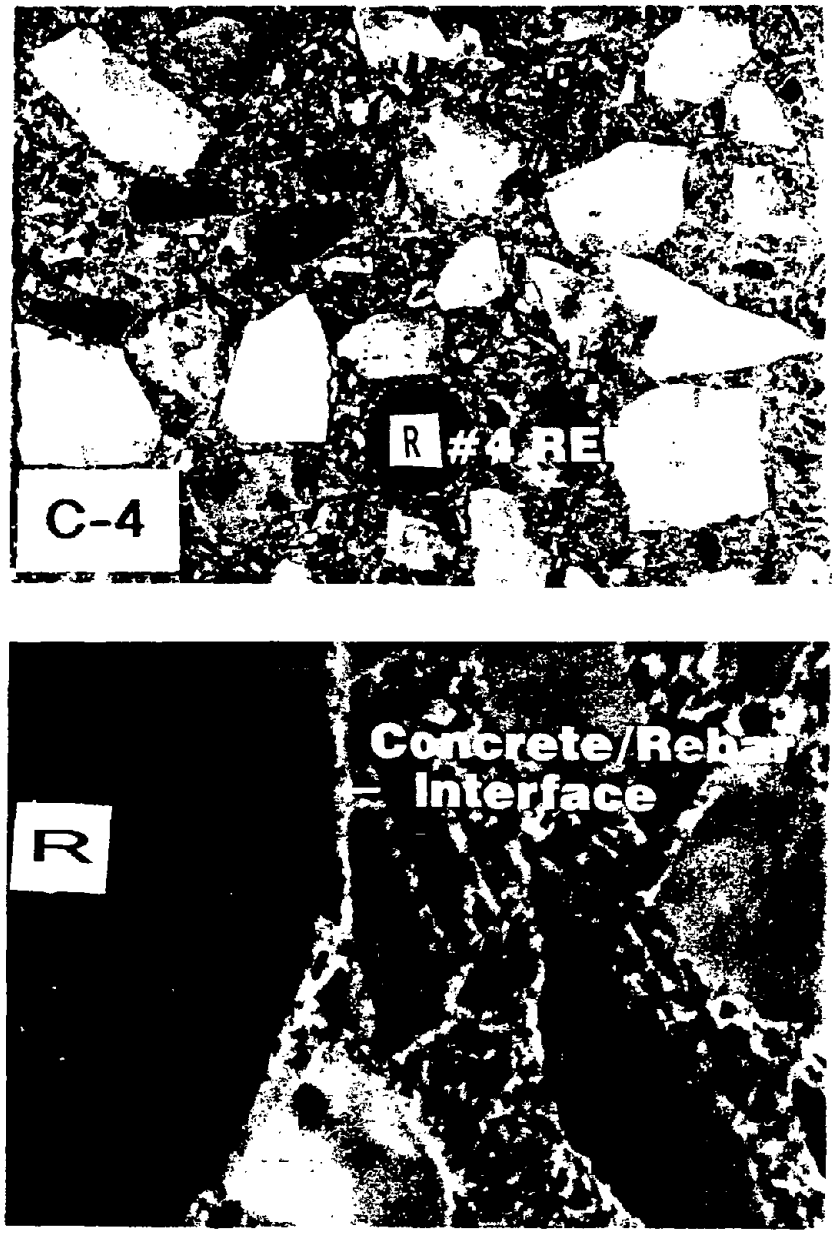

Figure 1-6. Section Views Through A Reinforced Concrete Specimen Perpendicular To The Rebar (R).

As apparent from figure 2, the specimen design is such that the concrete (mortar) environment is in contact with the cross-sectional face of the rebar rather than the circumferential area. The steel specimen is a #18 (57 mm, 2.25 in diameter) rebar about 25.4 mm (1 in) long. Except the cross-sectional interface, which is in contact with the mortar and has a uniform surface finish, all other areas of the steel are sealed with an epoxy compound. The steel specimen is snugly fitted into a plastic mold (a PVC pipe fitting) and 9.5 mm (0.375 in) layer of mortar is poured onto the cross-sectional area. For the concrete specimens, a 19 mm (0.75 in) concrete thickness was used. A reference electrode and a counter electrode, both made of platinized niobium wire, are incorporated into the mortar so that they are isolated from each other and the steel.

The specimen design for the prestressing steel is slightly different since unlike conventional rebars, large diameter prestressing steel rebars are not available so that strand tendons have to be used. The cross-sectional area consists of a bundle of seven strand tendons tied together. Again, as in the case of the conventional rebar specimens, 9.5 mm (0.37 in) layer of mortar is poured onto the cross-sectional surface incorporating the wire electrodes. A schematic drawing of the prestressing steel test specimen is shown in figure 4.

Preliminary Tests

Using the specimen design discussed above, preliminary tests were performed to examine certain aspects of the design and subsequent test procedures.

Optimum Mortar Thickness

The purpose of these tests was to determine what would be the optimum thickness of the mortar layer which would be free of cracks and also allow easy incorporation of the test electrodes for monitoring corrosion. A total of 42 test specimens using the #18 rebar were fabricated as per the design in figure 2. The mortar was cast in three thicknesses: 6.4 mm (0.25 in), 12.7 mm (0.50 in), and 19 mm (0.75 in). Curing was carried out at room temperature for 28-days with the mortar being ponded with saturated $Ca(OH)_2$ solution. During the curing period the specimens were kept covered with Parafilm (a clear plastic film) to prevent loss of moisture. After the curing period, the two sets of the specimens of three different thicknesses were oven dried at 40 °C (104 °F) and 55 °C (131 °F) respectively. The loss of moisture from the specimens was monitored at different time intervals for about 48 h. The specimens were also observed periodically under the stereo-microscope for the development of cracks. A set of three specimens was also dried at room temperature under controlled relative humidity of about 20 percent.

The preliminary tests indicated that a mortar thickness of 6.4 mm (0.25 in) would be suitable since no defects developed. However, because it was more difficult to incorporate the test electrodes in the specimen, it was decided to use a thickness of

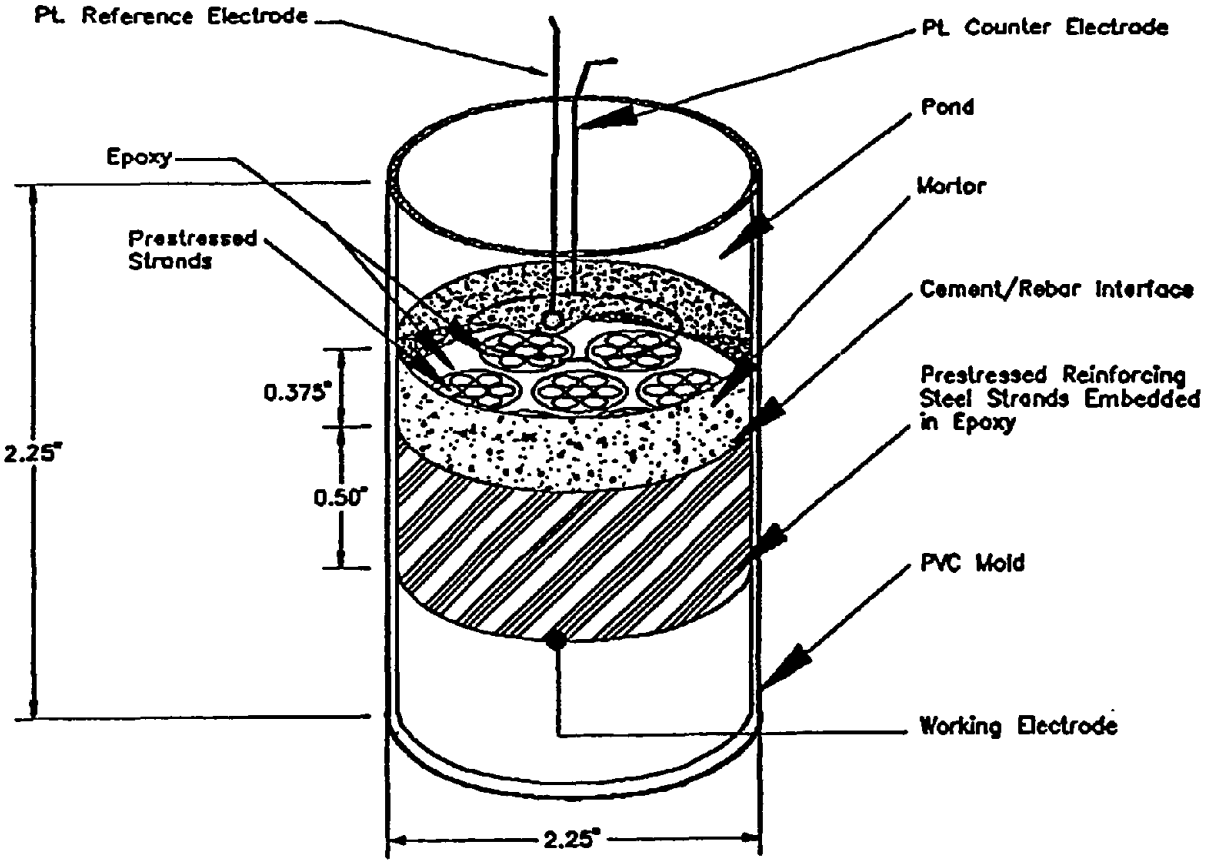

a. Assembled specimen.

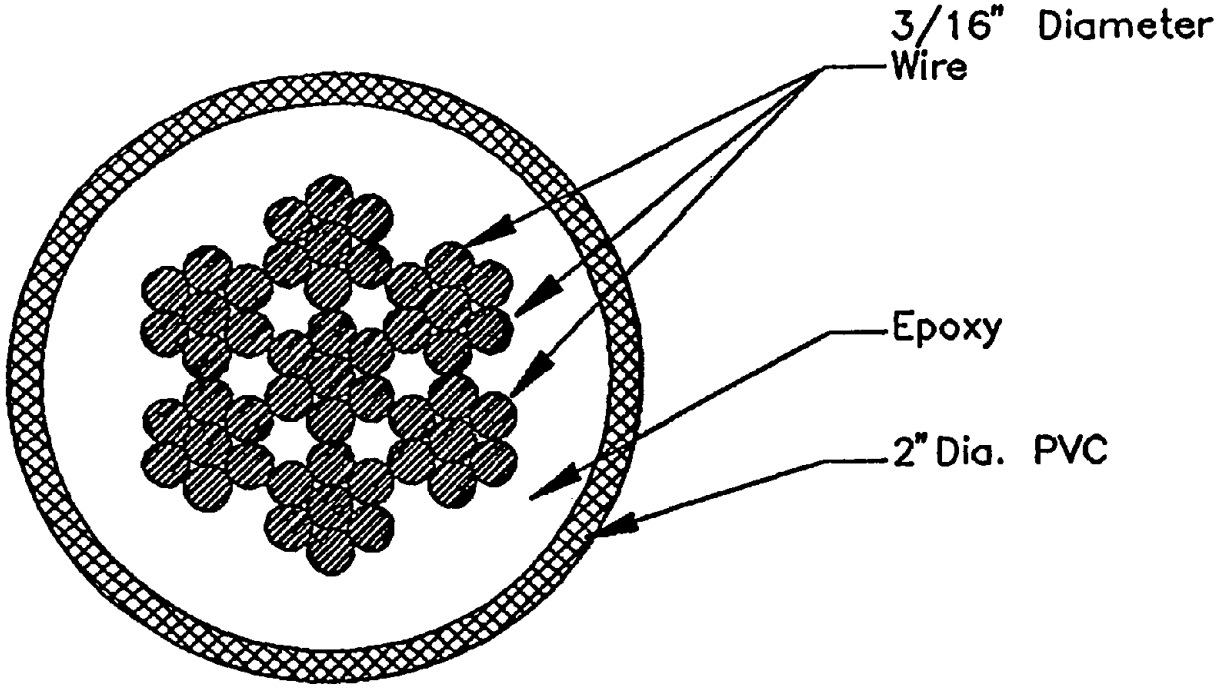

b. Sectional view.

Figure 4. Specimen design for short-term corrosion tests using prestressed strands.

9.5 mm (0.375 in). From an experimental standpoint (i.e. electrochemical tests, diffusion of chlorides, etc.) it is better to have the mortar thickness as small as possible. For specimens with a concrete cover (instead of mortar), the size of the coarse aggregates dictates the minimum thickness which is 19 mm (0.75 in) or twice the diameter of the largest aggregate size.

Loss Of Moisture From Mortar

The specimens used for moisture loss were the same specimens used for the "Optimum Mortar Thickness" tests.

The non-evaporable water in the concrete (or mortar) is considered as being 20 percent of the cement weight. Thus the evaporable water is simply calculated as the total water added minus the non-evaporable water.

The moisture loss tests indicated that the evaporable water in the mortar is not easily removed at ambient temperature particularly for the thicker samples. At a higher temperature (38 °C, 100 °F) and with the application of simultaneous vacuum the moisture removal was markedly improved. For the 6.4 mm (0.25 in) sample, about 90 percent of the evaporable could be removed under heat and vacuum. An even higher temperature of 60 °C (140 °F) resulted in further moisture loss (100 percent for the 6.4 mm (0.25 in) and >90 percent for the 12.7-mm (0.50-in) specimen). However, the specimens developed a few cracks at this higher temperature. Hence the treatment for removal of the evaporable water from the mortar was decided to be 38 °C (100 °F) with simultaneous vacuum.

Rate Of Chloride Ingress In Mortar

To incorporate chloride into the mortar specimens, it was decided to use chloride solution ponding on the cured and dried specimens instead of initially mixing the chloride with the mortar. With ponding, the chloride is introduced into the mortar matrix by a process of diffusion which simulates a real life situation. Theoretical calculations were made to estimate the solution concentration that would be required to achieve a certain level of chloride in the mortar (based on weight percent mortar). These calculations were based on replacing the evaporable water in the mortar specimens with the chloride ponding solution.

Chloride concentrations in the test samples were determined with a portable test kit manufactured by Germann Instruments. The portable kit was chosen because it is very convenient to use and is much less time consuming than the standard AASHTO/ASTM laboratory test method. The accuracy of the test kit is well established and was further confirmed during this project by conducting parallel analysis using the method developed by SHRP. The comparative results given in table 2 for eight different mortar samples, clearly show that there is very good correlation between the Germann and the SHRP methods.

Table 2. Comparison of SHRP and Germann methods of chloride analysis.

Sample No.	% Chloride	
	SHRP Method*	Germann Method
1	0.23	0.19
2	0.11	0.12
3	0.28	0.34
4	0.77	0.88
5	0.82	0.91
6	0.74	0.78
7	0.00	0.00
8	0.74	0.80

* Standard solutions of 1.25, 0.60, 0.30, 0.03, and 0.01 percent were used to calibrate probe.

A series of tests were conducted to determine the rate of chloride ingress in the mortar samples by ponding for different lengths of time using 12.7-mm (0.50-in) thick samples and a 20 percent NaCl solution. Some tests were also conducted with lower chloride concentrations for a fixed time period. The mortar samples were first dried at 38 °C (100 °F) under vacuum for about 48 h prior to ponding with the chloride solutions. Ponding was carried out at 38 °C (100 °F) to facilitate the chloride uptake by the samples. At the end of the ponding time, chloride concentrations were determined at a depth of 6.4 mm and 12.7 mm (mortar/steel interface) for each of the samples. Table 3 shows the data obtained. Some anomalous readings were obtained which are indicated in the table and were due to the leakage of ponding solution. Following 14-days of ponding, 90 percent of the theoretically chloride concentration was achieved at the 6.4-mm (0.25-in) depth.

Test Specimen Fabrication

A total of 198 samples were fabricated for the short-term tests which were all instrumented for corrosion potential and corrosion rate measurements under the different experimental conditions (see test matrix section). It was decided to make additional specimens for chloride analysis under each set of test conditions at the beginning and during the progress of the tests. It was estimated that 102 additional specimens would be required. Thus a total of 300 specimens were made using two types of mortar, one type of concrete, and two types of reinforcing steel.

Both the reference and counter electrode were fabricated from platinized niobium wire (niobium wire with a 100-micron platinum coating). The specimen surface in contact with the mortar was given a 80-grit finish. Except for the face in contact with the mortar (or concrete), the exposed parts of the steel were covered with a thin coating of coal tar epoxy. Recall that # 18 rebar (with a diameter of 57.2 mm (2.25 in) was used as the conventional reinforcing steel and that it is the cross-sectional surface of the rebar which is in contact with the mortar. The total surface area of the steel in contact with the mortar was 2 548-mm^2 (3.98 in^2).

The prestressed strands consist of seven high tensile steel wires twisted together in a bundle. The steel wires used in this study had a diameter of 4.8 mm (0.187 in). The prestressed strand was first cut into 30.5 mm (12 in) long pieces. Seven of these long pieces were then tightly bundled together with steel wires ties and then encapsulated in epoxy resin using a 5.1 mm (2 in) diameter PVC pipe as the mold. After curing, the encapsulated composite strand bundle was sliced into 1.3 mm (0.5 in) thick cross-sections as shown in figure 4. To ensure that there was electrical continuity between the individual wires and throughout the composite bundle, a conductive coating was painted on the back side of the specimen. A small screw with a soldered wire was then installed into the bundle for subsequent electrical connection to the specimen. Finally this surface was coated with coal tar epoxy. The cross-section surface which received the mortar was given a 80-grit finish. There are altogether 49 wires in the composite bundle. The total surface area of the prestressed steel in contact with the mortar was 871 mm^2 (1.35 in^2).

Table 3. Rate of chloride ingress in 12.7-mm (0.50-in) thick mortar samples.

Ponding Time (days)	NaCl Ponding Soln (%)	Theoretical Cl in Mortar*		Actual Cl in Mortar At 6.4 mm Depth		Actual Cl in Mortar at 12.7 mm (Interface)	
		(%)	lb/yd³ ***	(%)	lb/yd³ ***	(%)	lb/yd³ ***
2	20	0.51	19.9	0.18	7.0	0.03	1.2
5	20	0.65	25.4	0.26	10.1	0.12	4.7
11	20	0.67	26.1	0.42	16.4	0.64	24.9**
13	20	0.62	24.2	0.60	23.4	0.42	16.4**
14	10	0.29	11.3	0.26	10.1	0.24	9.4
14	5	0.16	6.2	0.15	5.9	0.07	2.7
14	1	0.04	1.6	0.033	1.3	0.026	1.0

*Based on moisture uptake after drying samples at 38 °C (100 °F) under vacuum for 48 h and then ponding with NaCl solution.
**Ponding solution leaked to interface due to bad sealing.
***1 lb/yd^3 = 0.594 Kg/m^3

The specimens were made up in batches of 35 to 40 samples per-day. The mortar specimens were cast to a thickness of 9.5 mm (0.375 in) and the concrete specimens to a thickness of 19 mm (0.75 in). All specimens were given a 28-day cure at room temperature by ponding with saturated calcium hydroxide solution.

Test Matrix

The variables included in the task A test matrix were:

- Mortar/concrete mix.
- Reinforcing steel type.
- Environment.

The mortar/concrete variables tested included two mortars (A-2 and B-2) and one concrete (A-5). Table 4 presents the mortar and concrete compositions. The only difference in mortar A-2 and concrete A-5 is that concrete A-5 contains coarse aggregate. The two types of reinforcing steel included conventional and prestressed tendons (7-wire).

The environmental variables that have been shown to have an effect on the corrosion of reinforcing steel in concrete include:

- Chloride concentration.
- Relative Humidity.
- Temperature.

The levels of the environmental variables were selected to provide a realistic range to which bridge structures are exposed. Three levels were selected for each of the environmental variables. The levels were designed to provide low, moderate, and high conditions for each variable.

The levels selected were:

- Chloride concentration at 0.6, 1.8, and 6 Kg/m^3 (1, 3, and 10 lb/yd^3).
- External humidity at 43, 75, and 98 percent.
- Temperature at 4, 21, and 38 °C (40, 70, and 100 °F).

A full factorial matrix of these three variables, each at three levels gives a matrix of 27 test conditions. Triplicate specimens were tested for each environmental condition.

A full matrix of tests was performed for two mortars (A-2 and B-2) using conventional reinforcing steel specimens. For the concrete (A-5), tests were performed in triplicate for a single temperature (21 °C, 70 °F), two humidities (75 percent and 98 percent), and three chlorides (0.6, 1,8, and 6 Kg/m^3 (1,3, and 10 lb/yd^3)). For the prestressing steel tendons, tests were performed for the same conditions as concrete

Table 4. Mortar and concrete compositions for Task A tests.

Composition ID	Cement	Sand	Coarse Aggregate	Water/Cement Ratio
Mortar (A-2)	Medusa Type-I Portland Cement	Sidley Quartz	None	0.45
Mortar (B-2)	Lumnite Calcium Aluminate	Sidley Quartz	None	0.45
Concrete (A-5)	Medusa Type-I Portland Cement	Sidley Quartz	Sidley Quartz # 8	0.45

A-5. Appendix A gives the test matrices for the four series of tests performed in task A.

Chloride Incorporation

As described previously, the specimens have to be thoroughly dried after the 28-day curing cycle to facilitate chloride uptake. The following sequence was followed to prepare the samples before exposing them to the various environmental conditions:

(1) Dry samples at 38 °C (100 °F) in a controlled temperature room for 7-days.
(2) Apply epoxy concrete sealant (Sikagard) to joint between mortar and plastic mold.
(3) Dry under vacuum at 38 °C (100 °F) for two additional-days.
(4) Pond with 6 ml of the desired chloride solution for 14-days at 38 °C (100 °F). Ponding was carried out within an hour after completing step 3.
(5) Rinse off any excess chloride solution from the specimen surface after the 14-day ponding period, pat dry with tissue and place them in the various environmental chambers to be hooked up to the data acquisition system.

Weight checks after the drying cycle indicated that samples lost approximately 90 to 95 percent of the theoretical evaporable water. Control samples pulled down at intermediate times during and following ponding indicated that the desired chloride levels at the steel surface were achieved.

Humidity Control In Environmental Test Chambers

Humidity control in the environmental test chambers was achieved with the help of a layer of saturated salt solution placed at the bottom of the chamber. This method of humidity control is well established and referenced in the literature. The relative humidity (RH) - temperature combinations for the different salt solutions are shown in table 5.

Each of the test chambers (444 mm by 356 mm by 165 mm; 17.5 in by 14 in by 6.5 in) was filled up with 1 L of the required salt solution which gave an approximate 19 mm (0.75 in) layer of the solution at the bottom. The samples (24 in each chamber) were supported on a plastic grid above the surface of the solution. The actual humidities and temperatures were measured with the help of a Cole-Parmer Brand Thermo-hygrometer and were found to be within 2 to 3 units (percent in case of RH and degrees in case of temperature) of the desired values.

Table 5. Humidity control using saturated salt solutions.

Humidity Control		
Temp, C	**RH (%)**	**Satd Salt Solution***
4	43	Potassium Carbonate
4	76	Sodium Chloride
4	98	Potassium Sulfate
21	43	Potassium Carbonate
21	75	Sodium Chloride
21	98	Potassium Sulfate
38	48	Magnesium Nitrate
38	75	Sodium Chloride
38	96	Potassium Sulfate

* Standard solutions from ASTM E104 - "Maintaining Constant Relative Humidity By Means Of Aqueous Solutions."

Measured Dependent Variables

The measured dependent variables in task A included:

- Corrosion potential.
- Corrosion rate.
- Chloride concentration at the steel surface.

A data acquisition system (a Multiplexer) was built for automatic monitoring of the corrosion rate of the 198 specimens under different environmental conditions. The computerized system consisted of 32 control boards each capable of monitoring the corrosion potential and polarization resistance (and hence the corrosion rates) of eight different specimens in sequence. The system performed a solution resistance calculation to correct the polarization resistance. In several of these specimens, the solution resistance was quite high compared to the polarization resistance making accurate determination of the polarization resistance difficult. The following two measurement systems were used to more accurately determine the polarization resistance: Model 4500 PR Monitor by Cortest Instrument Systems and Solartron Models 1255 and 1286 electrochemical impedance spectroscopy (EIS) measurement system.

The automated data acquisition system measured corrosion potential of the steel specimen with respect to the permanent platinum reference embedded into the mortar/concrete. Final measurements of the potential with respect to a copper/copper sulfate electrode (CSE) were made prior to final removal of the specimens at the end of the exposure period.

RESULTS: TASK A - CORROSIVE ENVIRONMENT STUDIES

Task A was divided into four subtasks corresponding to the mortars (or concrete) and/or type of reinforcing steel evaluated.

These were as follows:

Subtask A.1 - Mortar A2 and Conventional Reinforcing Steel.
Subtask A.2 - Mortar A2 and Prestressed Steel Tendons.
Subtask A.3 - Concrete A5 and Conventional Reinforcing Steel.
Subtask A.4 - Mortar B2 and Conventional Reinforcing Steel.

Subtasks A.1 and A.4 utilized the full factorial matrix of independent variables with triplicate specimens:

Temperature - 4, 21, and 38C (40, 70, and 100 °F.)
Relative Humidity - 43, 75, and 98 percent.
Chlorides - 0.6, 1.8, and 6 Kg/m^3 (1, 3, and 10 lb/yd^3.)

Subtasks A.2 and A.3 utilized a full factorial matrix but with the following independent variables with triplicate specimens:

Temperature - 38 °C (70 °F).
Relative Humidity - 75 and 98 percent.
Chlorides - 0.6, 1.8, and 6 Kg/m^3 (1, 3, and 10 lb/yd^3.)

Subtask A.1 - Mortar A2 and Conventional Reinforcing Steel

Individual Independent Variable Analysis

Table 6 presents the average (triplicates) for each set of independent variables tested for mortar A2 and conventional reinforcing steel. There is a significant amount of information represented in table 6. One means of examining this data is to average all data for a single level of a particular independent variable and to compare the three different levels. Figure 5 shows the effect of temperature on corrosion rate and corrosion potential for mortar A2. Figure 5a shows that as temperature increases, corrosion rate increases. The average of 1.4 mpy (35.6 μm/yr) corrosion rate at the high temperature includes data for all three relative humidities and all three chloride concentrations tested. It is interesting to note that an increase in temperature makes the corrosion potential more positive (figure 5b plots negative potential). This is seen in table 6 in which low temperature at high humidities produces a negative potential even for the low chloride concentration (-412mV, CSE (copper/copper sulfate electrode)).

Figure 6 shows the effect of relative humidity on corrosion rate and corrosion potential. Figure 6a shows that corrosion rate increases with increasing relative humidity, with a large increase from 75 to 98 percent. Figure 6b shows that there is not a large effect of relative humidity on corrosion potential.

Figure 7 shows the effect of chloride concentration on corrosion rate and corrosion potential. Figure 7a shows that at 0.6 Kg/m^3 (1 lb/yd^3) corrosion rate is negligible, at 1.8 Kg/m^3 (3 lb/yd^3) corrosion can occur (although the average for all

Table 6. Data for mortar A2 and conventional reinforcing steel.

Concrete	Temp		Relative Humidity	Chlorides Target		Average Corrosion Rate [A]		Average Potential [A]
	(C)	(F)	(%)	(Kg/m^3)	(lb/yd^3)	(µm/yr)	(mpy)	(mV, CSE)
A2	4	40	43	0.6	1	0.0	0.00	-52
A2	21	70	43	0.6	1	0.5	0.02	-127
A2	38	100	43	0.6	1	0.1	0.00	-22
A2	4	40	75	0.6	1	0.3	0.01	-97
A2	21	70	75	0.6	1	0.8	0.03	-26
A2	38	100	75	0.6	1	1.4	0.06	-24
A2	4	40	98	0.6	1	0.5	0.02	-412
A2	21	70	98	0.6	1	2.3	0.09	-156
A2	38	100	98	0.6	1	0.8	0.03	-41
A2	4	40	43	1.8	3	0.5	0.02	-122
A2	21	70	43	1.8	3	3.0	0.12	-190
A2	38	100	43	1.8	3	0.3	0.01	39
A2	4	40	75	1.8	3	2.1	0.08	-95
A2	21	70	75	1.8	3	1.2	0.05	-72
A2	38	100	75	1.8	3	4.4	0.17	-136
A2	4	40	98	1.8	3	0.6	0.02	-445
A2	21	70	98	1.8	3	2.0	0.08	-201
A2	38	100	98	1.8	3	14.1	0.56	-192
A2	4	40	43	6	10	1.4	0.05	-334
A2	21	70	43	6	10	10.8	0.42	-428
A2	38	100	43	6	10	9.3	0.37	-204
A2	4	40	75	6	10	15.6	0.61	-426
A2	21	70	75	6	10	21.6	0.85	-359
A2	38	100	75	6	10	20.3	0.80	-251
A2	4	40	98	6	10	0.8	0.03	-489
A2	21	70	98	6	10	54.7	2.2	-477
A2	38	100	98	6	10	271	11	-251

A: Average of triplicate specimens.

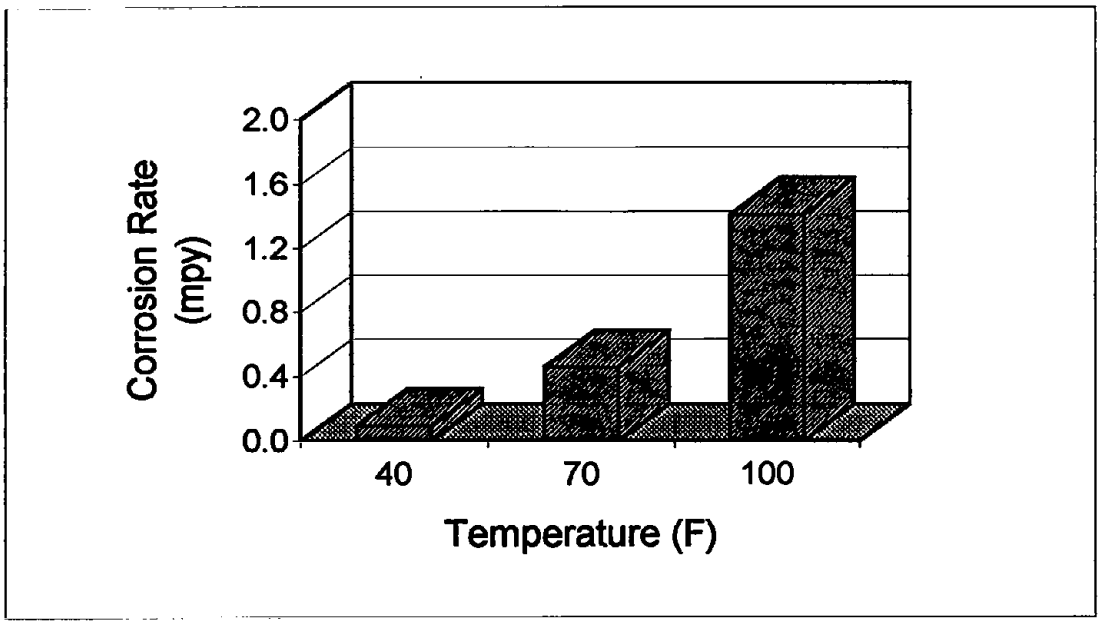

Figure 5a. Corrosion rate.

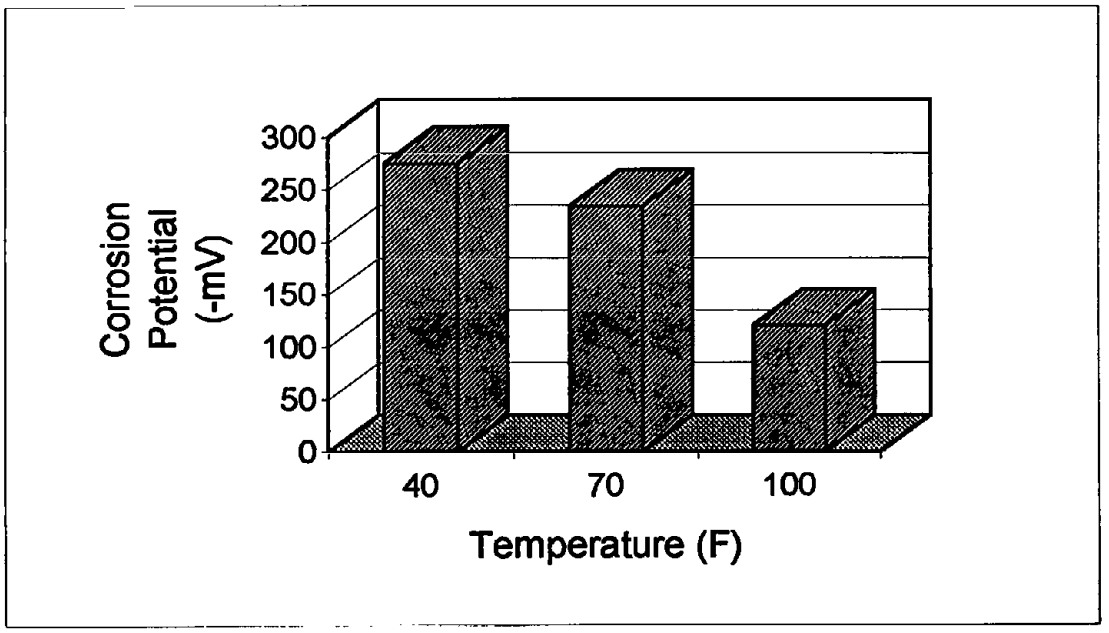

Figure 5b. Corrosion potential.

Figure 5. Effect of temperature on corrosion rate and corrosion potential for mortar A2.

Note: 1mpy = 25.4μm/yr

Note: 40 °F = 4 °C, 70 °F = 21 °C, and 100 °F = 38 °C

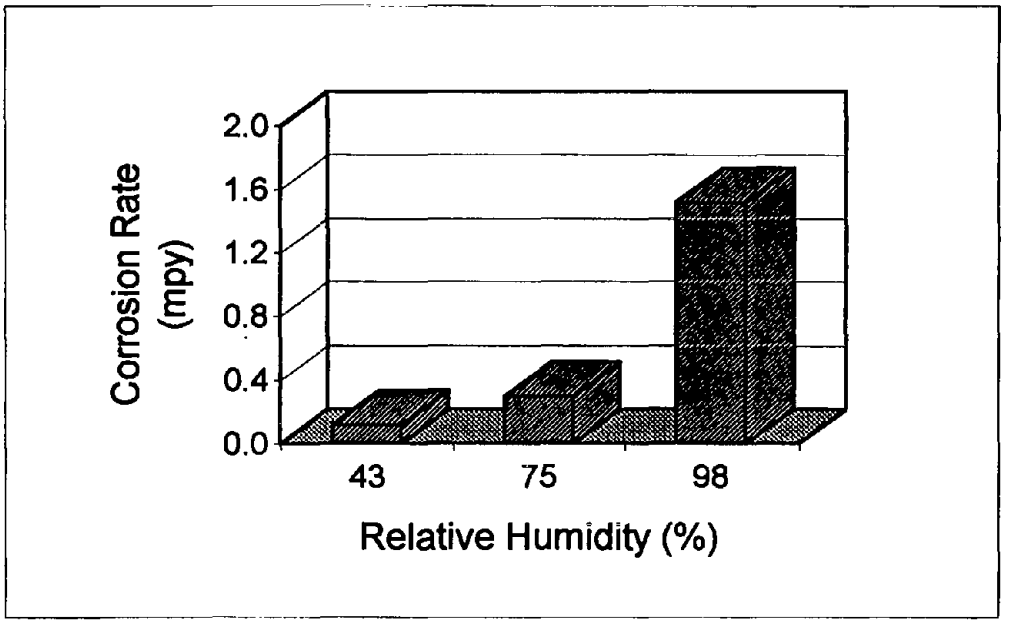

Figure 6a. Corrosion rate.

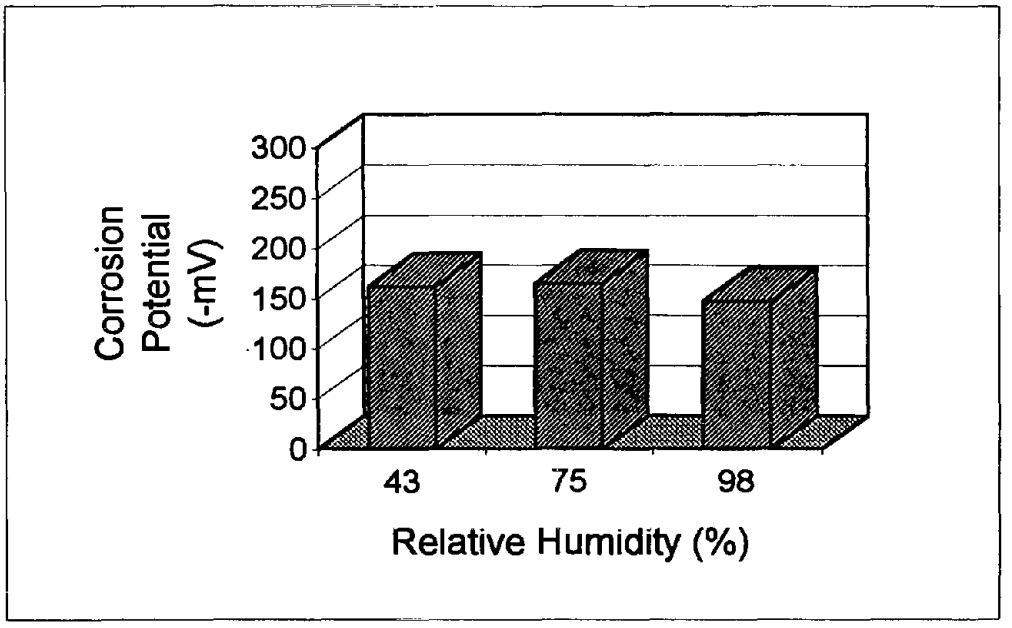

Figure 6b. Corrosion potential.

Figure 6. Effect of relative humidity on corrosion rate and corrosion potential for mortar A2.
Note: 1 mpy = 25.4 μm/yr

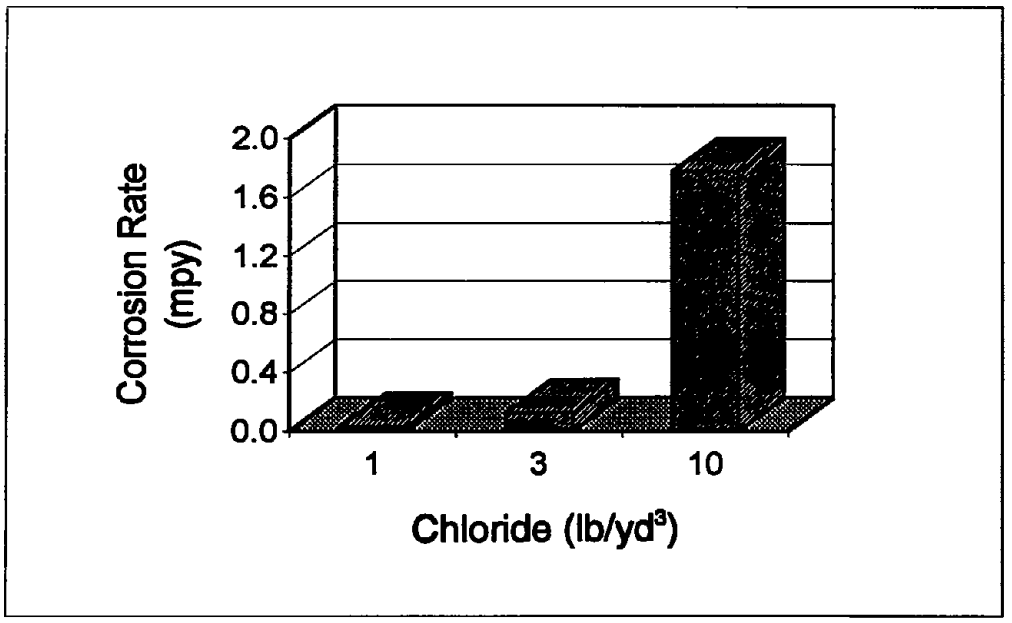

Figure 7a. Corrosion rate.

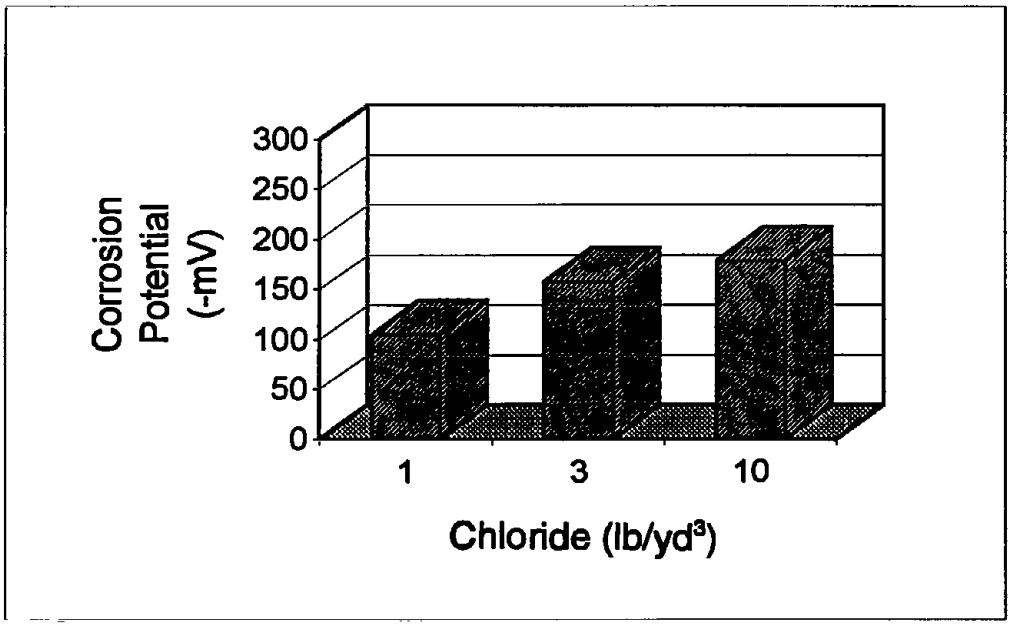

Figure 7b. Corrosion potential.

Figure 7. Effect of chloride concentration on corrosion rate and corrosion potential for mortar A2.
Note: 1 mpy = 25.4 μm/yr
Note: 1 lb/yd^3 = 0.6 Kg/m^3

conditions tested is relatively low), and at 6 Kg/m^3 (10 lb/yd^3) a large increase in the average corrosion rate is observed. At 6 Kg/m^3 (10 lb/yd^3) relatively high corrosion rates were observed in all conditions tested with the exception of low temperature and low humidity. The corrosion potential becomes more negative with increasing chloride concentration.

One of the interesting effects is that for non-saturated conditions, the corrosion rate is a maximum at an intermediate temperature and then decreases at high temperature. This effect was previously reported in the literature by Lopez et al. and observed in the present tests as well.[7] Figure 8 shows a graph of corrosion rate versus temperature at 1.8 Kg/m^3 (3 lb/yd^3) and 6 Kg/m^3 (10 lb/yd^3) chloride and 43 percent relative humidity. This effect of maximum corrosion rate at an intermediate temperature is likely due to a decrease in available pore water solution at the higher temperature even though the humidity remains constant. Although the root cause was not determined, the finding could be significant in understanding and predicting corrosion rate in a variety of environmental conditions. Also, the data clearly show that corrosion can occur in a relatively low (43 percent) humidity environment.

General Linear Model

A statistical regression model was developed to permit prediction of the corrosion rate and potential as a function of temperature, relative humidity, and chloride concentration based on the data presented above. The model included the main-effect terms for temperature, relative humidity, and chloride concentration, quadratic terms for each of the main effects, and interaction terms of the main effects. Table 7 gives the estimate of the coefficient for each parameter predicted and the probability that the parameter is significant. Regardless of the significance of the parameter, all parameters were included in the model. Table 7a gives the results for the corrosion rate model and table 7b gives the results for corrosion potential model. The general linear model equation for predicting corrosion rate (CR) in mpy (1 mpy = 25.4 μm/yr) or the potential (Ecor) in mV versus CSE is given below.

$$CR = \underbrace{a}_{\text{intercept}} + \underbrace{b \cdot T + b \cdot R + b \cdot C}_{\text{main effect terms}} + \underbrace{b \cdot T^2 + b \cdot R^2 + b \cdot C^2}_{\text{quadratic terms}} + \underbrace{b \cdot C \cdot R + b \cdot C \cdot T + b \cdot R \cdot T}_{\text{interaction terms}} \qquad (1)$$

Where,

a is the intercept.
b_i are the estimates of the coefficients.
T is the temperature in degrees F.
C is the chloride concentration in lb/yd^3.
R is the percent relative humidity.

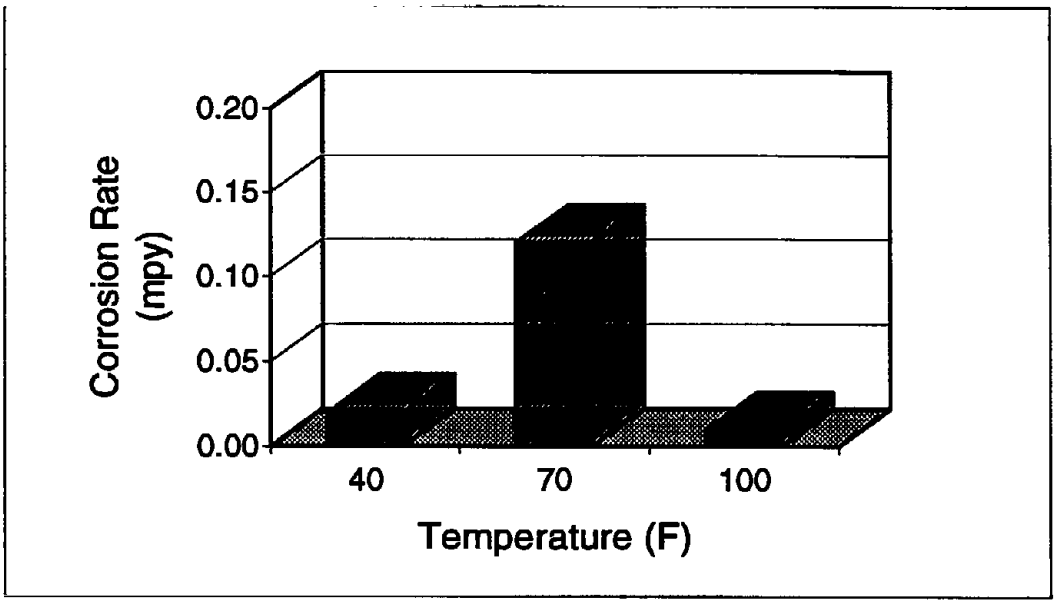

Figure 8a. 1.8 Kg/m^3 (3 lb/yd^3) chloride concentration.

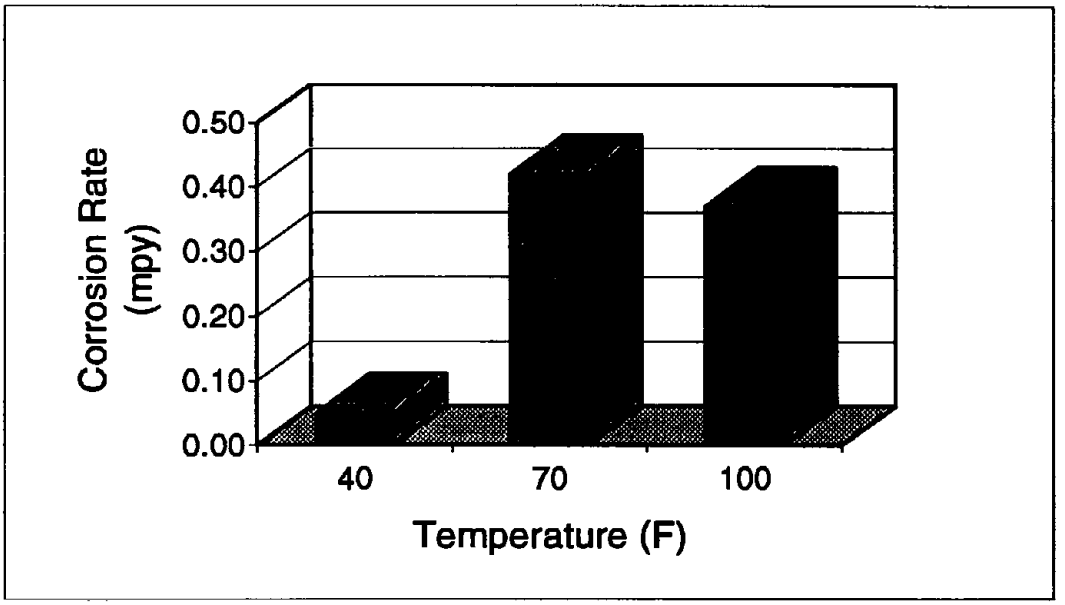

Figure 8b. 6 Kg/m^3 (10 lb/yd^3) chloride concentration.

Figure 8. Effect of temperature on corrosion rate at 43 percent relative humidity.

Note: 1 mpy = 25.4 μm/yr

Note: 40 °F = 4 °C, 70 °F = 21 °C, and 100 °F = 38 °C

Note: 1 lb/yd^3 = 0.6 Kg/m^3

Table 7. Statistical regression analysis results for mortar A2.

7a. Corrosion rate (mpy).

Parameter		Estimate of Coefficient	Probability of Significance
Intercept	I	12.37275	99.99%
Temperature (F)	T	-0.13520	98.1%
Relative Humidity (%)	R	-0.20701	99.7%
Chloride (lb/yd^3)	C	-1.13678	99.9%
	T^2	0.00035	65.3%
	R^2	0.00087	94.5%
	C^2	0.02157	61.4%
	C x T	0.00723	99.99%
	C x R	0.00814	99.99%
	R x T	0.00103	99.96%

R-square	61.9%

7b. Corrosion Potential (mV, CSE).

Parameter		Estimate of Coefficient	Probability of Significance
Intercept	I	-63.5700	22.6%
Temperature (F)	T	-4.9081	76.7%
Relative Humidity (%)	R	6.9026	84.7%
Chloride (lb/yd^3)	C	-44.3689	92.5%
	T^2	0.0255	65.6%
	R^2	-0.0973	99.7%
	C^2	-0.0365	1.6%
	C x T	0.0676	43.6%
	C x R	0.1592	77.7%
	R x T	0.0499	98.5%

R-square	71.3%

Note: 1 mpy = 25.4 μm/yr
Note: °F = (°F - 32)x0.555 °C
Note: 1 lb/yd^3 = 0.6 Kg/m^3

For corrosion rate, all parameters were significant at a 90 percent or greater confidence level except the quadratic terms of temperature and chloride concentration. An R-square value of 62 percent indicates that the model developed is capable of predicting approximately 62 percent of the experimental variation observed. For corrosion potential, only the main-effect term for chloride concentration, the quadratic term for relative humidity, and the interaction term of relative humidity - temperature were significant at a 90 percent or greater confidence level. An R-square value of 71 percent indicates that the model developed is capable of predicting approximately 71 percent of the experimental variation observed. The development of these data and equations provides the necessary tools to begin to develop a prediction model for determining corrosion rate and potential as a function of environment. When related to the long-term experiments designed for task C, corrosion rate and potential predictions will be made.

Subtask A.2 - Mortar A2 and Prestressed Steel Tendons

Table 8 presents the average (triplicates) for each set of independent variables tested for mortar A2 and post tensioned reinforcing steel. In these tests, only a single temperature (21 °C, 70 °F), two humidities (75 and 98 percent), and all three chloride concentrations (0.6, 1.8, and 6 Kg/m^3 (1, 3, and 10 lb/yd^3)) were tested. In comparison to table 6, it can be seen that the rates for each condition are lower than for those of conventional steel. This is shown graphically in figure 9. In this figure, all of the comparable data are averaged for the two types of reinforcing steel. It is seen that the prestressed reinforcing strands have a lower corrosion rate under similar conditions than conventional reinforcing steel. However, the prestressed steel exhibited the same corrosion trends as the conventional reinforcing steel. It should be noted that due to the high strength of the prestressed steel, it is expected that structural damage from hydrogen embrittlement would occur from a lower corrosion rate for the prestressed steel than the conventional reinforcing steel. The corrosion potential data show that the prestressed steel and the conventional steel have similar corrosion potentials (tables 6 and 8 and figure 9).

Subtask A.3 - Concrete A5 and Conventional Reinforcing Steel

Table 9 presents the average (triplicates) for each set of independent variables tested for concrete A5 and conventional reinforcing steel. The same matrix of tests were performed as for the prestressed steel tests discussed above. In comparison to table 6 it can be seen that the rates for each condition are significantly lower than for those of the mortar of similar chemistry. This is shown graphically in figure 9. In this figure, all of the comparable data are averaged for the concrete and mortar.

Table 8. Data for mortar A2-PST and prestressing steel tendons.

Concrete	Temp		Relative Humidity	Chlorides Target		Average Corrosion Rate [A]		Average Potential [A]
	(C)	(F)	(%)	(Kg/m^3)	(lb/yd^3)	(µm/yr)	(mpy)	(mV, CSE)
A2-PST	21	70	75	0.6	1	0.0	0.00	-34
A2-PST	21	70	98	0.6	1	0.4	0.02	-122
A2-PST	21	70	75	1.8	3	0.5	0.02	-57
A2-PST	21	70	98	1.8	3	1.0	0.04	-295
A2-PST	21	70	75	6	10	2.7	0.11	-316
A2-PST	21	70	98	6	10	28	1.1	-450

A: Average of triplicate specimens.

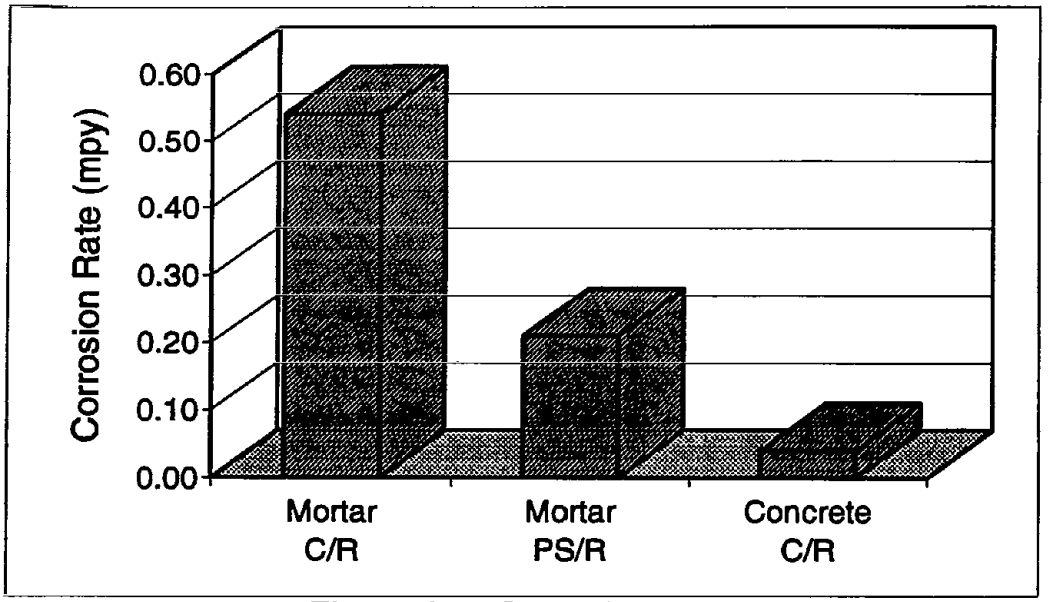

Figure 9a. Corrosion rate.

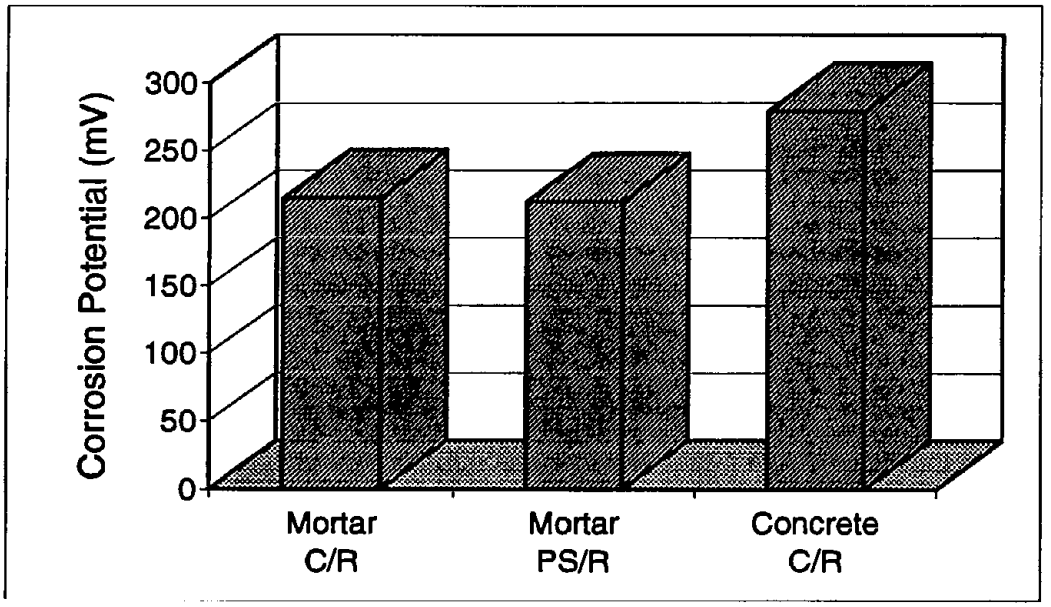

Figure 9b. Corrosion potential.

Figure 9. Effect of mortar versus concrete and conventional reinforcement (C/R) versus prestressing steel reinforcement (PS/R) on corrosion rate and corrosion potential for all data averaged (21 °C, 70 °F).
Note: 1mpy = 25.4 μm/yr

Table 9. Data for concrete A5 and conventional reinforcing steel.

Concrete	Temp		Relative Humidity	Chlorides Target		Average Corrosion Rate [A]		Average Potential [A]
	(C)	(F)	(%)	(Kg/m^3)	(lb/yd^3)	(µm/yr)	(mpy)	(mV, CSE)
A5	21	70	75	0.6	1	0.3	0.01	-107
A5	21	70	98	0.6	1	1.3	0.05	-207
A5	21	70	75	1.8	3	0.4	0.02	-117
A5	21	70	98	1.8	3	0.6	0.02	-273
A5	21	70	75	6	10	1.1	0.04	-384
A5	21	70	98	6	10	3	0.1	-587

A: Average of triplicate specimens.

It is seen that the conventional steel in the concrete has a much lower corrosion rate under similar conditions than the mortar. The reason for this is not immediately apparent. The conductivity of the mortar is greater than the concrete but this is not a completely satisfactory cause for the large effect observed. In addition, for a concrete, the cement paste containing most of the chloride has a smaller surface area in contact with the steel.

Figure 10 compares the actual measured values of chloride concentration to the desired target values for the three series of tests performed using the same cement A. The values shown are for the average of all comparative conditions. There is no reason for a difference in the A2 and A2-PST data since the only difference was the type of steel. However, the measured chloride concentration for A2-PST is consistently lower than A2. The A5 data is a concrete (A2 and A2-PST are mortars) with a greater cover thickness. The A5 data for the 0.6 Kg/m^3 (1 lb/yd^3) and 1.8 Kg/m^3 (3 lb/yd^3) targeted chloride concentrations are lower than the A2 and A2-PST data, but the A5 data for the 6 Kg/m^3 (10 lb/yd^3) targeted chloride concentration is greater than the A2 and A2-PST data. Therefore, the chloride concentration does not explain the difference in the corrosion rate data observed.

The corrosion potential data show that the concrete has a somewhat more negative corrosion potential than for the mortar conditions (tables 6 and 9 and figure 9).

Subtask A.4 - Mortar B2 and Conventional Reinforcing Steel

A similar full factorial matrix of experiments was performed for mortar B2 as discussed above for mortar A2 (three levels each of temperature. relative humidity, and chloride concentration). Table 10 presents the average (triplicates) for each set of independent variables tested for mortar B2 and conventional reinforcing steel. One means of examining this data is to average all data for a single level of a particular independent variable and to compare the three different levels. Figure 11 shows the effect of temperature on corrosion rate and corrosion potential for mortar B2. Figure 11a shows the same trend discussed for mortar A2 for non-saturated moisture levels. That is, at intermediate temperatures, corrosion rate is a maximum and decreases at high temperatures. A closer examination of table 10 shows that this trend is not the case for the high chloride level at 75 or 98 percent relative humidity, but is the case for most other conditions. The effect of temperature on corrosion potential is that a higher temperature tends to make the corrosion potential more positive (figure 11b plots negative potential). This is the same effect observed for mortar A2.

Figure 12 shows the effect of relative humidity on corrosion rate and corrosion potential. Figure 12a shows that corrosion rate increases with increasing relative humidity. Figure 12b shows that the most negative value of potential occurs at an intermediate relative humidity. At 98 percent relative humidity, the average corrosion

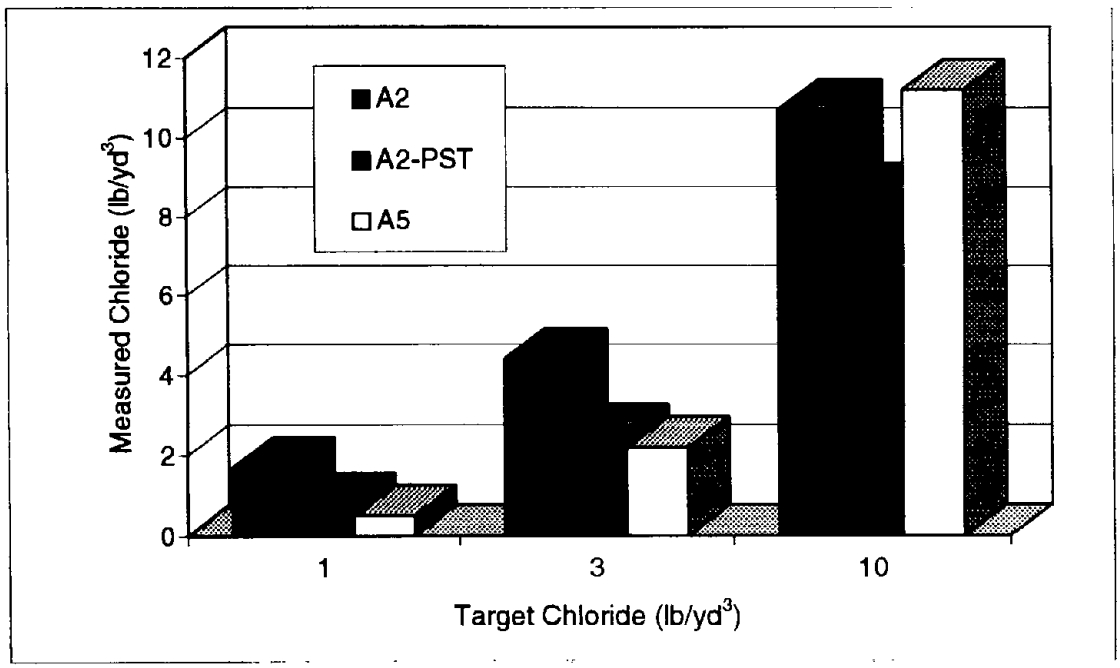

Figure 10. Comparison of actual chloride concentrations measured at the steel-cement interface for tests in mortar A2 (conventional reinforcing steel), mortar A2-PST (post-tensioning reinforcing steel), and concrete A5 (conventional reinforcing steel).

Table 10. Data for mortar B2 and conventional reinforcing steel.

Concrete	Temp		Relative Humidity	Chlorides Target		Average Corrosion Rate [A]		Average Potential [A]
	(C)	(F)	(%)	(Kg/m^3)	(lb/yd^3)	(µm/yr)	(mpy)	(mV, CSE)
B2	4	40	43	0.6	1	0.3	0.01	-221
B2	21	70	43	0.6	1	5.8	0.23	-281
B2	38	100	43	0.6	1	0.4	0.02	-102
B2	4	40	75	0.6	1	1.1	0.04	-251
B2	21	70	75	0.6	1	1.9	0.07	-236
B2	38	100	75	0.6	1	5.8	0.23	-348
B2	4	40	98	0.6	1	1.4	0.06	-720
B2	21	70	98	0.6	1	11.9	0.47	-252
B2	38	100	98	0.6	1	3.0	0.12	-31
B2	4	40	43	1.8	3	2.0	0.08	-199
B2	21	70	43	1.8	3	14.2	0.56	-364
B2	38	100	43	1.8	3	2.5	0.10	-217
B2	4	40	75	1.8	3	12.7	0.50	-461
B2	21	70	75	1.8	3	83.0	3.27	-273
B2	38	100	75	1.8	3	4.0	0.16	-323
B2	4	40	98	1.8	3	3.2	0.13	-332
B2	21	70	98	1.8	3	127.0	5.00	-224
B2	38	100	98	1.8	3	27.1	1.07	-137
B2	4	40	43	6	10	27.1	1.07	-393
B2	21	70	43	6	10	115.1	4.53	-376
B2	38	100	43	6	10	27.9	1.10	-288
B2	4	40	75	6	10	41.9	1.65	-419
B2	21	70	75	6	10	31.3	1.23	-407
B2	38	100	75	6	10	127.0	5.00	-404
B2	4	40	98	6	10	34.7	1.37	-675
B2	21	70	98	6	10	144.8	5.7	-164
B2	38	100	98	6	10	288	11	-185

A: Average of triplicate specimens.

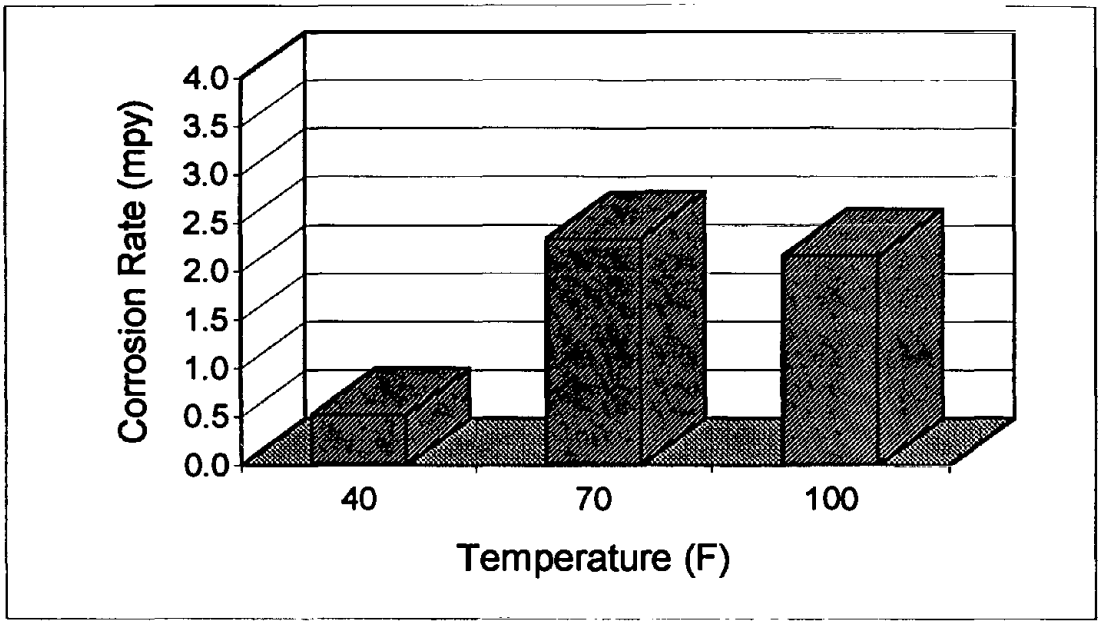

Figure 11a. Corrosion rate.

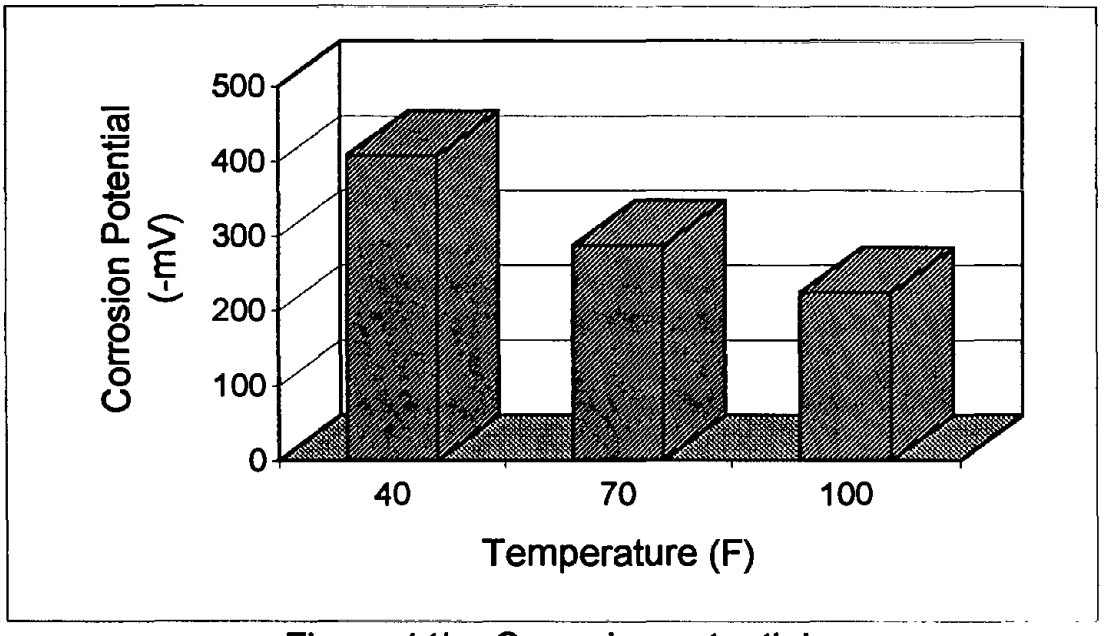

Figure 11b. Corrosion potential.

Figure 11. Effect of temperature on corrosion rate and corrosion potential for mortar B2. Note: 1 mpy - 25.4 μm/yr.

Note: 1 mpy = 25.4 μm/yr

Note: 40 °F = 4 °C, 70 °F = 21 °C, and 100 °F = 38 °C

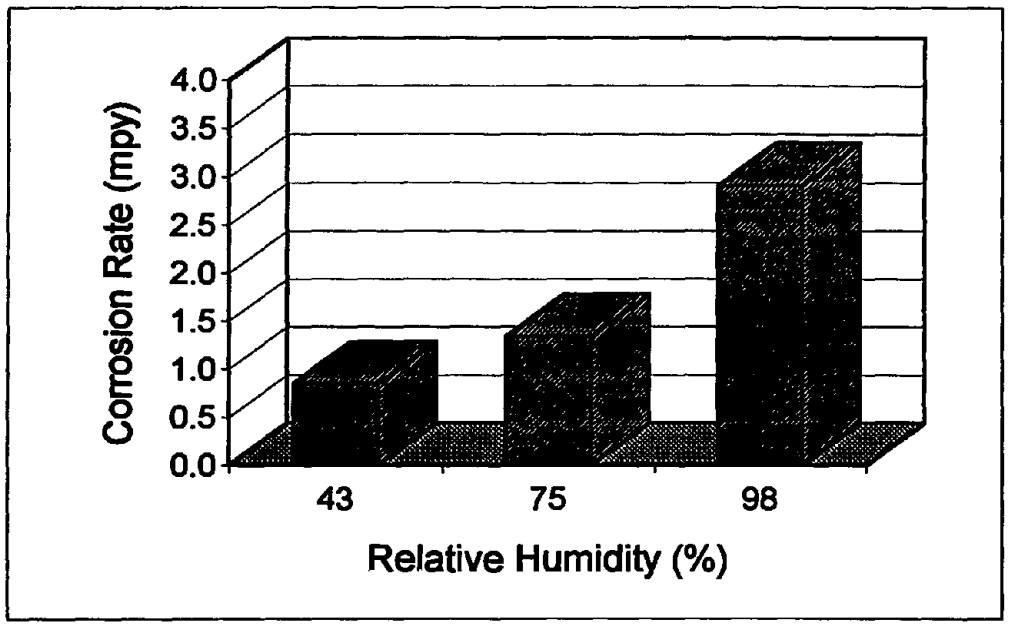

Figure 12a. Corrosion rate.

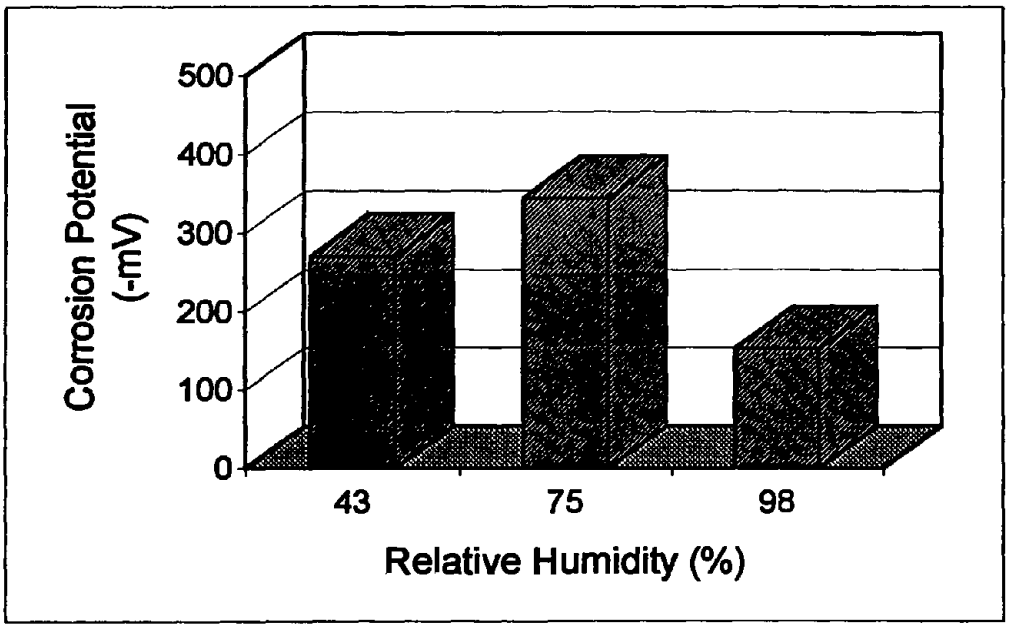

Figure 12b. Corrosion potential.

Figure 12. Effect of relative humidity on corrosion rate and corrosion potential for mortar B2.
Note: 1 mpy = 25.4 μm/yr

potential is significantly more positive than at either 43 or 75 percent. Although similar, this trend is much more pronounced than observed for mortar A2.

Figure 13 shows the effect of chloride concentration on corrosion rate and corrosion potential. Figure 13a shows that at 0.6 Kg/m^3 (1 lb/yd^3) corrosion rate is negligible, at 1.8 Kg/m^3 (3 lb/yd^3) corrosion rate is significant, and at 6 Kg/m^3 (10 lb/yd^3) an extremely high corrosion rate is observed. At 6 Kg/m^3 (10 lb/yd^3) a high corrosion rate (>1 mpy) was observed for all conditions tested. The average corrosion rates observed for mortar B2 are significantly higher than those for mortar A2. In addition, several environmental conditions produced corrosion in mortar B2 that were not corrosive in mortar A2 (tables 6 and 9). The expected trend of corrosion potential becoming more negative with increasing chloride concentration was not observed (figure 13b). This is possibly due to the fact that corrosion occurred at all chloride levels and indicates that a more negative corrosion potential does not translate to a higher corrosion rate. This is well understood since potential is a thermodynamic parameter and not a rate parameter, but it is sometimes forgotten in field application.

A statistical regression model was developed to permit prediction of the corrosion rate and potential as a function of temperature, relative humidity, and chloride concentration based on the data presented above. The model included the main effect terms for temperature, relative humidity, and chloride concentration, quadratic terms for each of the main effects, and two factor interaction terms of the main effects. Table 11 gives the estimate of the coefficient for each parameter predicted and the probability that the parameter is significant. Regardless of the significance of the parameter, all parameters were included in the model. Table 11.a gives the results for the corrosion rate model and table 11.b gives the results for corrosion potential model. The regression equation for predicting corrosion rate (CR) in mpy (1 mpy = 25.4 μm/yr) or the potential (Ecor) in mV versus CSE confidence level was previously given in equation 1.

For corrosion rate, all of the interactions were significant at a 90 percent or greater, along with the quadratic terms of temperature and relative humidity, and the main effect term for relative humidity. An R-square value of 69.5 percent indicates that the model developed is capable of predicting approximately 69 percent of the experimental variation observed. For corrosion potential, only the main effect term of relative humidity, the quadratic term of relative humidity, and the interactive term of relative humidity versus temperature were significant at a 90 percent or greater confidence level. An R-square value of 48 percent indicates that the model developed is capable of predicting approximately 48 percent of the experimental variation observed. The development of these data and equations provides the necessary tools to begin to develop a prediction model for determining corrosion rate and potential. When related to the long term experiments designed for task C, corrosion rate and potential predictions will be possible.

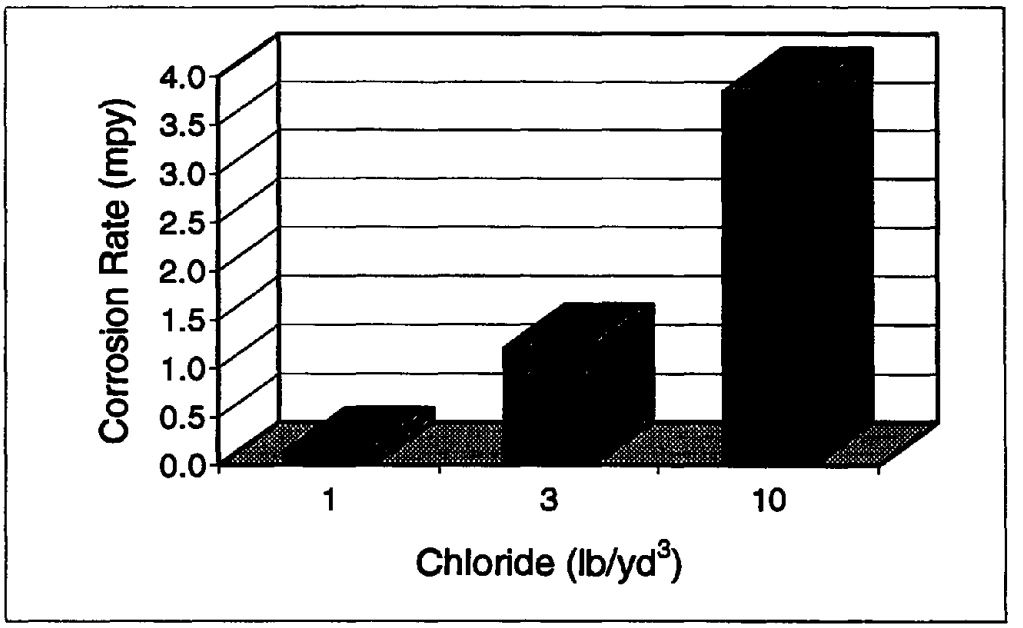

Figure 13a. Corrosion rate.

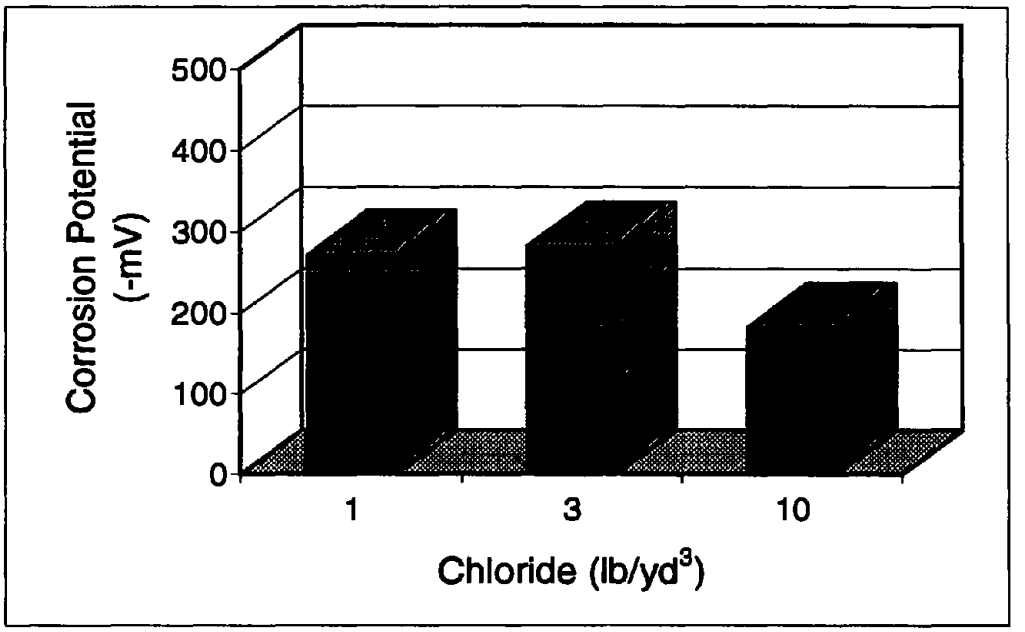

Figure 13b. Corrosion potential.

Figure 13. Effect of choloride concentration on corrosion rate and corrosion potential for mortar B2.
Note: 1 mpy = 25.4 μm/yr
Note: 1 lb/yd^3 = 0.6 Kg/m^3

Table 11. Statistical regression analysis results for mortar B2.

11a. Corrosion rate (mpy).

Parameter		Estimate of Coefficient	Probability of Significance
Intercept	I	4.75169	81.3%
Temperature (F)	T	0.06699	70.0%
Relative Humidity (%)	R	-0.19923	98.8%
Chloride (lb/yd^3)	C	-0.46424	76.7%
	T^2	-0.00110	98.9%
	R^2	0.00095	92.5%
	C^2	-0.02044	52.5%
	C x T	0.00922	99.99%
	C x R	0.00613	99.5%
	R x T	0.00101	99.7%

R-square	69.5%

11b. Corrosion Potential (mV, CSE).

Parameter		Estimate of Coefficient	Probability of Significance
Intercept	I	401.0200	84.1%
Temperature (F)	T	0.2007	3.2%
Relative Humidity (%)	R	-20.9246	99.9%
Chloride (lb/yd^3)	C	-18.0334	44.6%
	T^2	-0.0385	74.8%
	R^2	0.0815	94.8%
	C^2	-0.9565	33.0%
	C x T	0.0171	8.8%
	C x R	0.2189	81.1%
	R x T	0.1131	99.99%

R-square	48.1%

Note: 1 mpy = 25.4 μm/yr
Note: °F = (°F - 32)x0.555 °C
Note: 1 lb/yd^3 = 0.6 Kg/m^3

CHAPTER 4. TASK B - CONCRETE CHEMICAL AND PHYSICAL PROPERTIES

The experimental phase of this project had as its goals to (1) quantify the effects of environmental variables on the corrosion of reinforcing steel in concrete and (2) quantify the effects of concrete mix variables on the corrosion induced deterioration of concrete. To accomplish this, the experimental program is divided into three tasks:

Task A - Corrosive Environment Studies
Task B - Concrete Chemical And Physical Properties
Task C - Long-Term Corrosion Performance.

This interim report contains the results of tasks A and B and recommendations for task C. In this section, the experimental approach and results of task B are presented.

EXPERIMENTAL APPROACH: TASK B- CONCRETE CHEMICAL AND PHYSICAL PROPERTIES

The purpose of task B is to characterize the chemical and the physical characteristics of concretes as they relate to the corrosion behavior of embedded reinforcing steel.

Independent variables examined in task B can be classified into the following:

- Environmental variables.
- Material variables.
- Mix variables.

Environmental Variables

The environmental variables that have been shown to have an effect on the corrosion of reinforcing steel in concrete include:

- Chloride concentration.
- Relative Humidity.
- Temperature.

Based on the results of the task A work, two environments were selected to be used in the task B tests. The environments were selected to provide (1) moderately

aggressive corrosive conditions (moderate environment) and (2) highly aggressive corrosive conditions (aggressive environment). These environments were:

Moderate environment: 21 °C (70 °F) - 75 percent RH - 1.8 Kg/m^3 (3 lb/yd^3) chloride.
Aggressive environment: 38 °C (100 °F) - 98 percent RH - 6 Kg/m^3 (10 lb/yd^3) chloride.

As in task A, chlorides were diffused into the concrete following curing of the specimens. Relative humidity was maintained through the use of selected salt solutions maintained at the bottom of test chambers. Therefore, the relative humidity was that of the outside air surrounding the concrete (or mortar) specimens. Temperature was maintained plus or minus 2 °C (4 °F) during the exposure period.

Material Variables

The selection of materials and mixture proportions for the concretes was guided by the results of previous studies and by experience with concretes used for the repair and construction of bridges. Although both mortars and concretes were used in task A, only concretes were used in task B (and will be used in task C).

Material variables considered include:

1. Cement type.
2. Mineral admixture type.
3. Fine aggregate type.
4. Coarse aggregate type.

A summary of the material variables considered in the research is presented in table 12.

Cements

Six different cements were selected for use in the research, which are identified in table 13. They include four portland cements, a calcium aluminate cement, and a magnesium phosphate cement. The cements were chosen to provide a wide but realistic range in tricalcium aluminate (C_3A) content, alkali (Na_2O, K_2O) content, and pH.

The variation in C_3A content of the portland cements provides variation in the amount of chloride ion that is chemically bound. The calcium aluminate cement is expected to bind large quantities of chlorides, while magnesium phosphate cement may exhibit no chloride binding qualities at all.

Table 12. Summary of material variables considered in the research.

Variable	**Range of Variables**	**Number**
Cement Type	A. Type I portland cement - high alkali B. Calcium aluminate cement - intermediate pH C. Type I portland cement - low alkali D. Type I portland cement - high C_3A E. Oil Well Cement - 0 C_3A F. Magnesium phosphate cement - low pH	6
Mineral Admixture Type	1. Silica fume 2. Class F fly ash 3. Class C fly ash 4. Granulated blast furnace slag 5. None	5
Fine Aggregate	1. Pure quartz (SiO_2) sand 2. Natural sand with high levels of carbonate rock types (limestone/dolomitic limestone)	2
Coarse Aggregate	1. A dense, inert, impermeable quartz 2. A permeable limestone	2

Table 13. Cements used in the research.

Cememt Identification Letter for the Investigation	Cement Description	C_3A Content,	Alkali as Na_2O,
A	Type I portland cement containing a high level of alkali (Medusa Cement Company, Type I portland cement from the Charlevoix, MI, Plant)	9.8	1.03
B	Calcium aluminate cement (Lumnite cement from the Lehigh portland Cement Company, Buffington Plant, Gary, IN)	N.A.	N.A.
C	Type I portland cement with a low alkali content (Holnam Type I portland cement, Holly Hill, SC, plant)	7.0	0.10
D	Type I portland cement with a high C_3A content (Holnam Type I portland cement from the Artesia, MS, plant)	12.3	0.40
E	Portland cement with a low C_3A level (Lone Star Industries, Oilwell cement from Maryneal, TX, plant)	0	0.23
F	Magnesium phosphate cement	N.A.	N.A

An increase in alkali content in the portland cements is expected to exert an influence on the corrosion events. This includes (1) an increase in the conductivity of the electrolyte phase in the saturated concrete, and (2) an increase in the OH^- levels in the electrolyte phase (pore water phase).

The two non-portland cements provide two significantly lower levels of pH values in the concrete matrix phase. With the calcium aluminate cement, the pH value is 8 to 9, while in the magnesium phosphate cement the value is 5 to 6.

Mineral Admixtures

Mineral admixtures that were selected to be used as partial replacements for the cements include:

1. Silica fume.
2. Class F fly ash.
3. Class C fly ash.
4. Granulated blast furnace slag.

The silica fume and Class F fly ash function principally as pozzolonic materials, while the Class C fly ash and granulated blast furnace slag function as cementitious materials in addition to participating in pozzolonic reactions. Depending upon the level of pozzolonic activity, the availability of OH^- is expected to decrease in concretes containing the pozzolonic additives.

For all of the additives, the in situ creation of additional calcium silicate hydrate (CSH) and other cement hydrates will reduce the porosity and permeability of the matrix phase in the concretes. This has the effect of reducing the diffusion rate of chloride ion in the concrete. The additional cementitious material also is expected to provide an increase in strength and elastic modulus in the concrete.

Fine Aggregate Type

Typically, the fine aggregate used in concretes for bridge structures can be thought of as inert material when contained in a concrete having a pH of 12.5 to 13.8 (the "normal" range). However, as the pH of the matrix phase surrounding a corroding rebar changes, the solubility of some fine aggregate constituents may change. This is an important consideration since the finest particle size materials in the fine aggregate phase may end up in the interface material that is actually in contact with the reinforcing steel.

Two fine aggregates were obtained to represent reasonable extremes in porosity and chemical activity. Both aggregates are natural sands, obtained from Ohio sources. They include (table 14) a quartz sand, and a mixed siliceous/calcareous sand derived from glacial deposits. The silica sand is a pure quartz sand (SiO_2 >99.0 percent) derived from a quartz conglomerate source. The glacial deposit-derived sand contains about 50 percent carbonate rock types (dolo

Table 14. Fine aggregates used in the research.

Fine Aggre-gate Source	Type Of Sand	Source Location	SSD Specific Gravity	Water Ab-sorption %	Fineness Modulus
Sidley	Quartz Conglomer-ate	Painesville Ohio	2.65	0.33	2.78
Frank Road	Glacial Deposit	Columbus Ohio	2.70	2.18	2.86

mitic limestones/limestones), with the bulk of the remaining sample dominated by sedimentary and igneous rock types. Both meet the gradation requirements of ASTM C 33-90, the Standard Specification for Concrete Aggregates.

Coarse Aggregate

The coarse aggregate also is typically considered to be inert in a portland cement concrete with a pH in the 12.4 to 13.5 range. The coarse aggregate is not expected to exert a significant influence on the overall chemistry at the interface between the concrete and the rebar. However, it is known that the permeability of many concrete aggregates is greater than that of good quality hydrated cement paste. Aggregate permeability may be an important factor influencing the migration rate of chloride ions into the concrete and the ionic conductivity of the concrete.

Two coarse aggregates were obtained including a quartz aggregate from an Ohio source (same source as the quartz sand), and a limestone from a Florida source. Both coarse aggregates meet the gradation requirements of ASTM C 33-90, no 8 gradation (3/8 in maximum size). The coarse aggregates, described in table 15, were chosen to represent meaningful extremes in porosity and water absorption values.

Concrete Mix Proportion Variables

Because of the relatively large number of material variables evaluated in the research, it was necessary to limit the concrete mix proportion variables. At the same time, it was necessary to provide reasonable variations in the cement content of the concretes to reflect both past and expected future practice. This was handled in the present research by varying water-cement ratio, while maintaining the volume of cementitious phase at a constant value (30 volume percent). Water-cement ratios of 0.3, 0.4, and 0.5 were used in these concretes. In addition, air contents were adjusted at 2 percent, 5 percent, and 8 percent.

An example of concrete mix design is shown in table 16. In this example, the water-cement ratio is 0.40, and the entrained air content is 7 percent. The cementitious phase in this example comprises the portland cement, ground granulated blast furnace slag, and the water. When summed these components represent 30 percent by volume.

In this project, the variation in water-cement ratio over a relatively wide but realistic range provided variations in the porosity and permeability of the cementitious matrix phase of the concretes. By maintaining the cementitious phase at a constant level (30 volume percent) and varying the water-cement ratio, it was possible to provide a large (but realistic) range in cement content. In the concretes, the proportion of fine and coarse aggregate was maintained at 1.0:1.0. Variations in air content were achieved at the expense of the combined aggregate phases.

Table 15. Coarse aggregates (ASTM C 33 no 8 gradation) used in the research.

Coarse Aggregate Source	Aggregate Type	Source Location	SSD Specific Gravity	Water Absorption, %
Sidley	Quartz (Gravel)	Painesville, OH	2.62	0.59
Harper Brothers	Limestone (Crushed)	Ft Myers, FL (Alico Pit)	2.38	9.79

Table 16. Example of concrete mix design for the research.

Concrete Constituents	Batch Weights		Density		Volume Ratio Component to Concrete	
	Kg/m^3	lb/yd^3	Kg/m^3	lb/ft^3	m^3/m^3	ft^3/yd^3
Portland Cement (D)	268	452	3152	196.6	0.085	2.30
GranCem GCBF Slag	144	243	2881	179.7	0.050	1.35
Sidley Quartz Sand	835	1406	2652	165.4	0.315	8.50
Sidley Quartz Aggregate	825	1390	2621	163.5	0.315	8.50
Water	165	278	1000	62.4	0.165	4.46
Air (AEA 15 - 7 v/o)[a]					0.070	1.89
Totals	2238	3769			1.00	27.00

Cement Paste Content = 30 volume percent
Unit Weight = 2238 Kg/m^3 (139.6 lb/ft^3)
Water Cement Ratio = 0.40
Air Content (Entrained) = 7.0 volume percent
[a] 3.75 oz/Cwt; Cwt includes cement + slag

Experimental Design

The experimental design for the task B Investigation is shown in table 17. Thirty trial concrete mix designs were identified which incorporate all the material and concrete proportion variables previously discussed. The concretes for the task B Investigation have the following features in common:

(1) A cement paste content of 30 volume percent.
(2) The proportion of coarse aggregate to fine aggregate is 1.0:1.0.
(3) Entrained air is added at the expense of the aggregate phases.

The cement past content was maintained close to the desired value of 30 percent. The average value for 29 concretes was 30.2 percent, with a minimum of 29.4 percent (Concrete no 1) and a maximum of 32.10 percent (Concrete no 8). The greatest difficulty in maintaining the desired design levels of the independent variables was for entrained air. Most of this difficulty was for magnesium phosphate cements. The primary reason for this is the fact that air-entraining admixtures used in the present investigation were developed for portland cement concretes, and do not perform the same function in magnesium phosphate cements.

Because of an incompatibility between constituents of the cementitious phase, it was not possible to prepare concrete no 14. A rapid reaction between the magnesium phosphate cement and sulfides present in the slag additive produced a large exotherm and a flash set. Therefore, 29 concretes were examined instead of the originally planned 30. Appendix B gives unit weight, air content, and cement paste contents for the 29 task B concretes.

The statistical experimental design was developed using the software package ECHIP for the independent variables below:

1. Water to Cement (W/C) ratio - 3 levels: 0.3, 0.4, 0.5.
2. Air Entrainment - 3 levels: 2 percent, 5 percent, 8 percent.
3. Fine Aggregates (Fine-Agg) - 2 levels: Glacial Deposit (G), Quartz (Q).
4. Coarse Aggregates (Coar-Agg) - 2 levels: Quartz (Q), Limestone (LS).
5. Minerals - 5 levels: None, Flyash-F (FA-F), Micro-silica (MS), Slag, Flay-ash-C (FA-C).
6. Cement type - (6 levels: A, B,C,D,E,F as per table 12).

In task A, a full factorial matrix of tests were performed and a model was developed that included terms related to the linear effects of the individual independent variables (main effect terms), interactions between these main effects (interaction terms), and non-linear main effects (quadratic terms). In task B, there are too many independent variables (6) with too many levels (6 for cement type) to perform sufficient tests to either (1) perform a full factorial matrix of tests or (2) determine a model containing interaction and quadratic terms. Therefore, a main effect terms only statistical design was generated. The design given below allows estimation of the six main effect terms listed above (Water to Cement ratio, Air, etc.)

Table 17. Experimental design for the task B investigation.

Concrete Mix Design No.	Water-Cement Ratio	Air Content, %	Fine Aggregate	Coarse Aggregate	Mineral Additive	Cement Identification[e]	Admixture Dosage, oz/cwt[a]		
							Superplasticizer[b]	Air-Entraining Admixture[c]	Set Retarder[d]
1	0.3	2	Q	Q	FA - C	A	18.0	None	4.0
2	0.3	8	Q	LS	FA - F	A	18.0	2.0	6.0
3	0.3	8	G	Q	FA - C	C	10.0	2.5	3.0
4	0.5	5	Q	Q	Slag	B	None	0.75	None
5R	0.5	2	Q	Q	MS	D	15.0	None	None
6	0.3	5	Q	Q	None	E	16.0	0.75	None
7	0.4	5	Q	Q	MS	F	None	0.5	Boric Acid
8	0.5	8	Q	Q	None	F	None	1.0	Boric Acid
9	0.4	8	Q	Q	Slag	D	None	3.75	None
10	0.4	8	Q	Q	FA - C	B	None	1.5	6.0
11	0.5	2	Q	Q	FA - F	E	None	None	None
12	0.4	8	G	LS	MS	E	18.0	7.0	None
13	0.4	5	Q	Q	None	C	None	1.5	None
14*	0.3	5	G	Q	Slag	F	—	—	—
15R	0.5	8	G	Q	MS	C	10.0	8.0	None
16	0.3	2	G	Q	None	B	36.0**	None	Citric Acid
17	0.5	5	G	LS	FA - C	D	None	0.3	None
18	0.3	5	Q	LS	MS	B	18.0	1.0	6.0
19	0.5	2	Q	LS	Slag	C	None	None	None
20	0.5	2	G	LS	FA - F	F	None	None	Boric Acid
21	0.4	5	G	Q	FA - F	B	None	2.5	None
22	0.4	2	G	LS	None	D	None	None	None
23	0.4	5	G	Q	Slag	A	13.0	2.5	None
24	0.3	8	Q	LS	Slag	E	13.0	0.75	None
25	0.4	2	Q	LS	FA - C	F	None	None	Boric Acid
26	0.5	5	G	Q	FA - C	E	None	0.6	None
27	0.4	5	Q	LS	FA - F	C	None	0.75	None
28	0.4	2	G	Q	MS	A	18.0	None	3.0
29	0.5	8	Q	LS	None	A	6.0	2.0	None
30	0.3	5	Q	Q	FA - F	D	18.0	1.0	4.0

[a] oz/100 lb of cement + mineral additive.
[b] Boremco Company's Might 150 superplasticizer.
[c] Sika Corporation's AEA-15 air-entraining agent.
[d] Sika Corporation's Plastiment set-retarding admixture.
[e] See table 1 for cement descriptions.

Q = Sidley quartz coarse (3/8 in.)/fine aggregate.
LS = Limestone (Florida - 3/8 in.)
FA - C = Class C fly ash
FA - F = Class F fly ash
Slag = Koch Mineral ground granulated blast furnace slag
MS = Elkem Materials EMS960 microsilica
* = Concrete 14 was not be prepared because of an incompatibility between constituents of the cementitious phase
** = MISO and Darvan 811D
G = Glacial sand

but does not provide estimates of the interaction of any of theses effects (e.g., interaction of Water to Cement ratio with Air Entrainment) or the non-linear quadratic terms.

ECHIP was used to find an optimal design for the experimental matrix, subject to using a base design limited to 30 samples (concrete mix designs). Supplied with the information of the number of independent variables and the levels of each, ECHIP designed an experimental matrix that maximizes the information to be captured for a main effects only model. This matrix is given in table 17.

The experimental matrix of 30 concrete mix designs has good balance between the various levels of the independent variables. The design included duplicates for the concrete property testing and triplicates for the corrosion rate testing. Each row in table 17 represents a different experimental combination of the independent variables (concrete mix design) for which the dependent variables will be measured.

Measured Dependent Variables

The dependent variables to be measured for each of the concrete mix designs given in table 17 are:

1. Rapid Chloride Permeability.
2. Compressive Strength.
3. Electrical Resistivity.
4. Corrosion Rate.
5. Corrosion Potential.
6. Final Chloride at the Steel Surface.

Rapid Chloride Permeability

The test procedure used here is the rapid chloride ion permeability test identified as AASHTO Designation T277-83, The Standard Method Of Test For Rapid Determination Of The Chloride Permeability Of Concrete. For this test, 102-mm (4-in) diameter by 203-mm (8-in) long cylinders are being cast from the experimental concretes. The specimen for the test is a 51-mm (2-in) thick slice sawcut from the cylinders. Duplicate specimens were run following a 28-day curing period and following a 90-day curing period. The longer curing periods refer to maintaining the concretes in the same 100 percent humidity room as was used for the initial 28-day cure.

Compressive Strength Measurements

The test procedure used here is the compressive strength test identified as ASTM C109-92, The Standard Test Method For Compressive Strength Of Hydraulic Cement Mortars [using 51-mm (2-in) cube specimens]. For this test, 51-mm (2-in) cubes are being cast from the experimental concretes. Triplicate specimens are tested following a 7-day, 28-day, 90-day, and 365-day curing period.

Electrical Resistivity Measurements

The electrical resistivity of the concretes is measured using a Nilsson Electric laboratory model 4-PIN soil resistance meter. For this test, the concrete is cast in a 100-mm polypropylene beaker (Nalgene 1201-0100). The cups are fitted with two 1.6-mm (0.062-in) diameter platinum clad, niobium coated copper core wires. The distance between the wires is 1.0. The beakers are sealed to prevent moisture loss from the concrete. This condition is verified by periodic measurements of the specimen weight. Electrical resistivity is measured immediately after casting the specimen and at 1, 7, 28, 90, 189, and 365-days.

Corrosion Rate and Potential Measurements

The same specimen design and fabrication procedures were used in the task B investigation as were used in task A (see figure 2). In task B, all of the tests were performed with concrete and the concrete cover was maintained at 19 mm (0.75 in). This gave a concrete cover that was a factor of two greater than the largest aggregate size. Conventional reinforcing steel was the only steel tested in task B. As in task A, triplicate specimens were tested in the corrosion tests.

Although the primary independent variables of interest in task B are concrete mix variables, it is of interest to evaluate these variables in different environmental conditions. Based on the task A results, a moderate and an aggressive environment were selected. The moderate environment was 21 °C (70 °F), 75 percent relative humidity, and 1.8 Kg/m^3 (3 lb/yd^3) of chloride. The aggressive environment was 38 °C (100 °F), 98 percent relative humidity, and 6 Kg/m^3 (10 lb/yd^3) of chloride. The full matrix of 29 concretes were tested in each of the two environments. Triplicate samples were tested in each condition.

The test procedures used in task B were the same as developed and used in task A. Following curing of a minimum of 28-days, the specimens were (1) dried, (2) ponded to diffuse in chlorides, and (3) exposed to one of the two environmental conditions listed above. Corrosion rate and potential measurements were made as described in task A.

Final Chloride At The Steel Surface

At the completion of the corrosion tests, the chloride concentration in the 1.6 mm (0.062 in) of concrete in contact with the steel surface was measured. Although severe drying followed by ponding was used to drive chlorides into the concrete specimens, the amount of chloride achieved at the steel surface is a measure of the ability of chloride to diffuse into the concrete matrix.

RESULTS: TASK B - CONCRETE CHEMICAL AND PHYSICAL PROPERTIES

Task B work was divided into two subtasks: (1) Concrete Property Data and (2) Corrosion Performance Data. For presentation purposes, these data are combined and presented for each independent variable in the test matrix.

The following concrete property data (dependent variables) was obtained on the 29 concretes listed in table 17:

- Rapid chloride permeability at 28 and 90-days.
- Compressive strength at 7, 28, 90, 365-days.
- Electrical resistivity at 1, 7, 28, 90, 180, and 365-days.

The following corrosion performance variables (dependent variables) were obtained on the 29 concretes.

- Corrosion rate.
- Corrosion potential.

The full matrix of 29 concretes were evaluated in each of two environments selected from the task A work:

- Aggressive environment: 38 °C (100 °F) - 98 percent RH - 6 Kg/m^3 (10 lb/yd^3) chloride.
- Moderate environment: 21 °C (70 °F) - 75 percent RH - 1.8 Kg/m^3 (3 lb/yd^3) chloride.

In addition, data was obtained on the actual chloride levels at the steel surface following exposure. The method of diffusing chloride into the concrete specimens was well controlled, such that any observed variation in chloride concentration from the designed concentrations of 1.8 Kg/m^3 (3 lb/yd^3) (Moderate Environment) or 6 Kg/m^3 (10 lb/yd^3) (Aggressive Environment) is most likely dependent on the concrete s property controlling diffusion of chlorides.

The 29 concretes were experimentally designed to optimize statistical analysis (see Approach Section). Appendixes A and B give the full matrices of concrete property data and corrosion performance data, respectively, for each dependent variable. In the following sections, the effects are presented of each independent variable on the measured dependent variables: rapid chloride permeability, electrical resistivity, compressive strength, corrosion rate, corrosion potential, and final chloride at the steel surface. The independent variables studied in task B were:

- Water-cement ratio.
- Air content.
- Coarse aggregate type.

- Fine aggregate type.
- Mineral admixture.
- Cement type.

Water-Cement Ratio

Figure 14 shows the mean values of rapid chloride permeability, electrical resistivity, and compressive strength at 28 and 90-day exposures for concretes prepared with water-cement ratios of 0.3, 0.4, and 0.5. The mean values presented in the graphs are the mean of all the concretes (from the matrix of 29 concretes) that had a water-cement ratio set at the particular level given.

Rapid chloride permeability decreases as a function of decreasing water-cement ratio. This is an expected result, inasmuch as the total porosity in the cement paste phase decreases as a function of decreasing water-cement ratio. In the test procedure used here (ASTM C 1202), it is the ionic conductivity of the concrete that is being measured. A reduction in total pore volume results in a corresponding reduction in the current carrying medium (i.e., pore water containing dissolved ions). Also, the 90-day rapid chloride permeability is consistently less than the 28-day data.

The effect of water-cement ratio on concrete electrical resistivity at 28-days and 90-days is shown in figure 14b. It is expected that the higher the water-cement ratio, the lower the electrical resistivity. This effect is not established until 90-days, where the electrical resistivity decreases from a water-cement ratio of 0.3 (67,000 ohm-cm) to 0.5 (30,000 ohm-cm). Since both the rapid chloride permeability and the resistivity measure ionic activity within the concrete, an inverse relationship is expected and illustrated in figures 14a and 14b.

Mean values of 28-day and 90-day compressive strength are shown graphically in figure 14c. Compressive strength increases as a function of decreasing water-cement ratio. This is a well-known and expected result.

Figure 15 shows the mean values of corrosion rate, potential, and chloride concentration for the aggressive and moderate environments for concretes prepared with water-cement ratios of 0.3, 0.4, and 0.5. (Note the difference in scales for the moderate and aggressive environments.) Although statistically significant, the magnitude of the effect of water-cement ratio on the moderate environment is not large for corrosion rate or chloride concentration. For the water-cement ratio, the chloride concentration shows the same trend as the corrosion rate, but this is not the case for all sets of data. For the aggressive environment, the higher the water-cement ratio the higher the corrosion rate. The relative magnitude of the effect on corrosion rate was greater for the aggressive environment than the moderate environment. There were similar trends in corrosion potential for the two environments, but the variations were not statistically significant at 90 percent or greater confidence level.

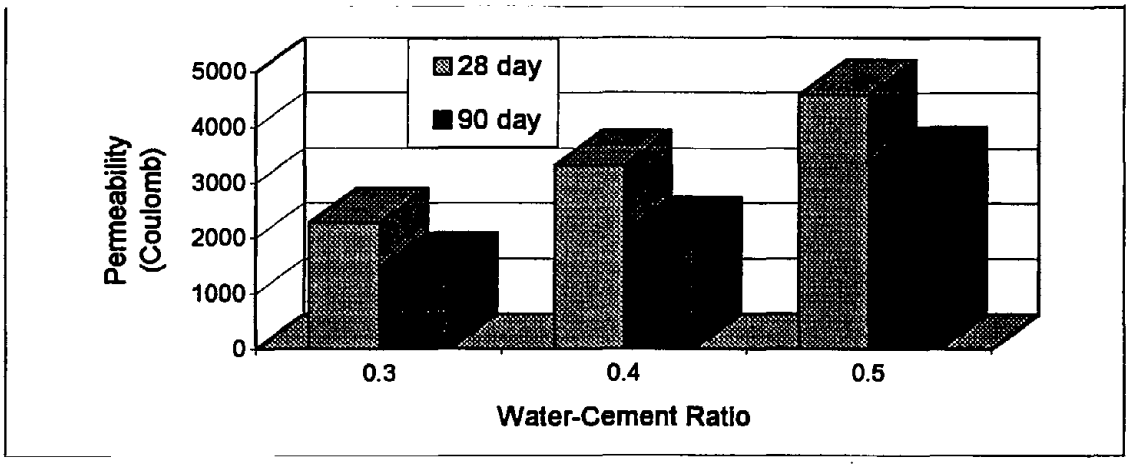

Figure 14a. Rapid chloride permeability.

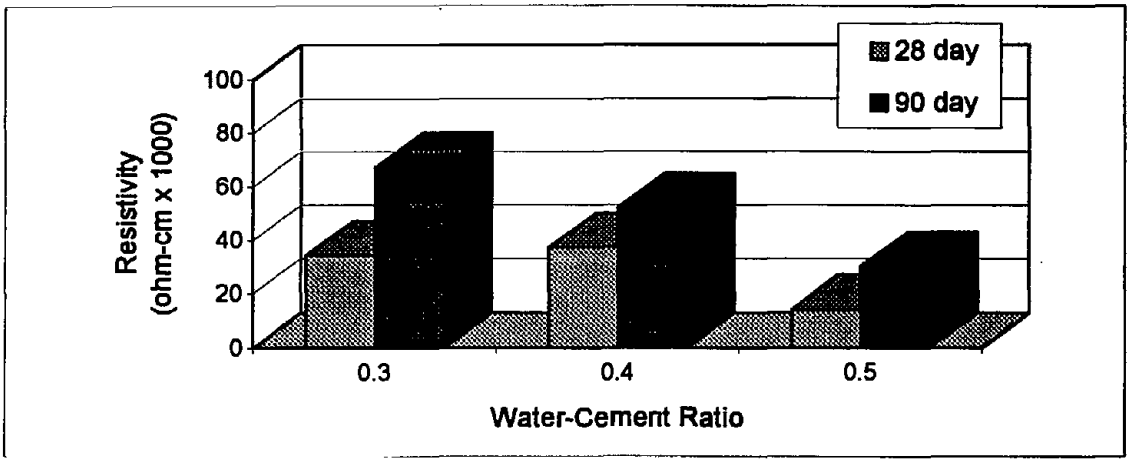

Figure 14b. Electrical resistivity.

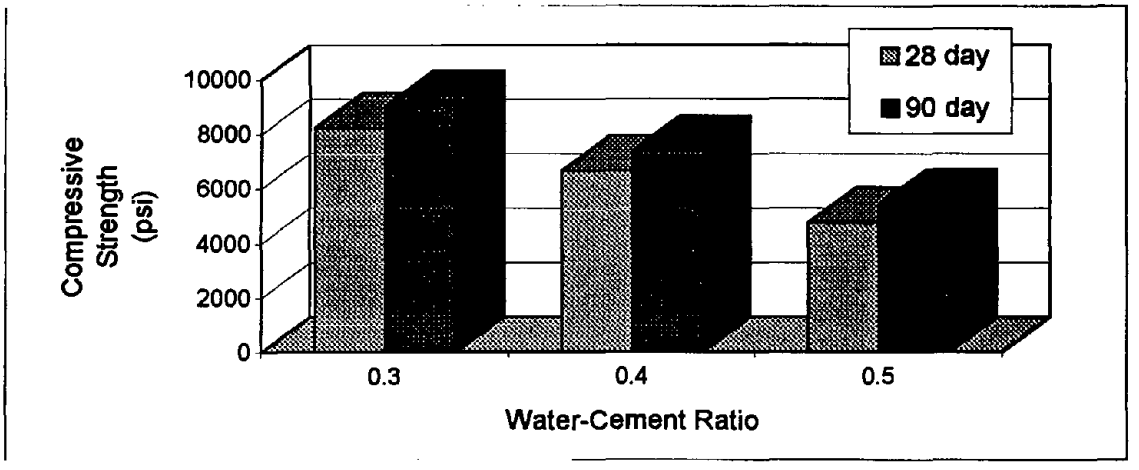

Figure 14c. Compressive strength.

Figure 14. Summary of mean data for independent variable, water-cement ratio, for the concrete property variables of chloride permeability, resistivity, and compressive strength.
Note: 1 psi = 6.895 KPa

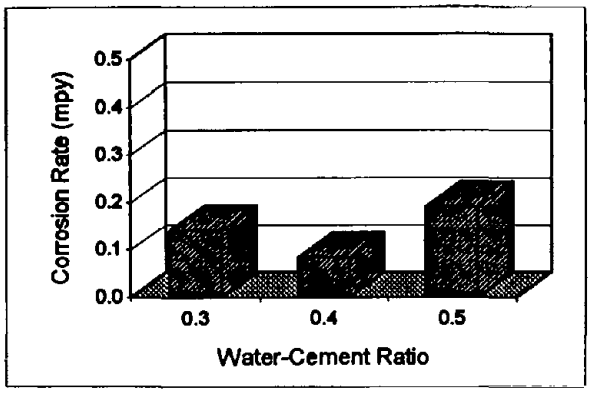

Figure 15a. Corrosion rate for moderate environment.

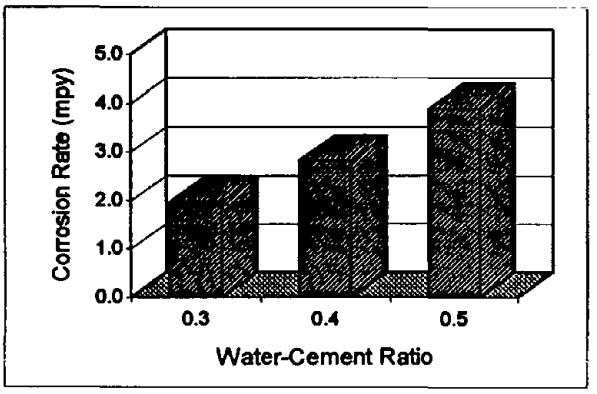

Figure 15d. Corrosion rate for aggressive environment.

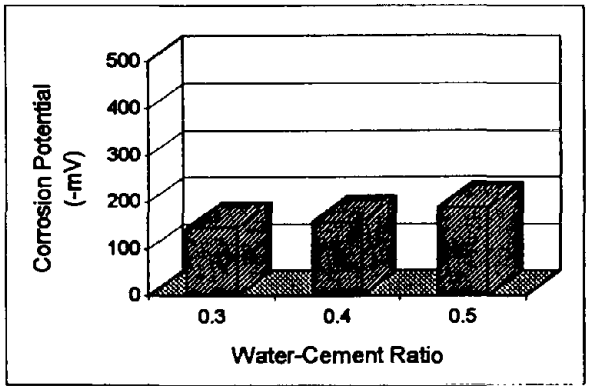

Figure 15b. Corrosion potential for moderate environment.

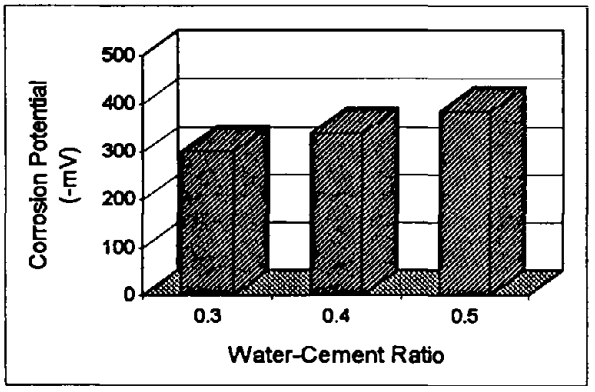

Figure 15e. Corrosion potential for aggressive environment.

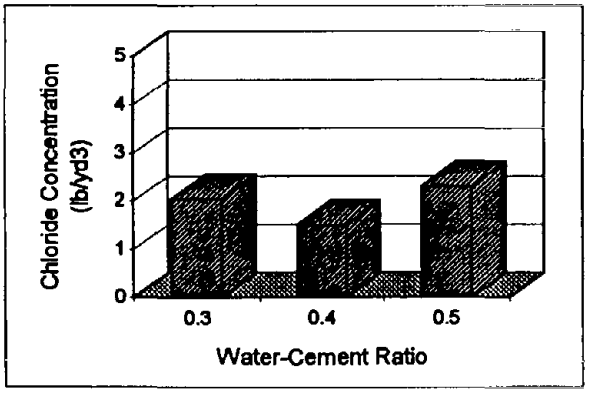

Figure 15c. Chloride concentration for moderate environment.

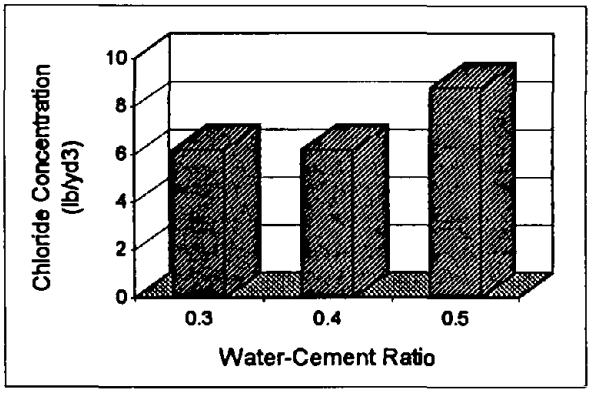

Figure 15f. Chloride concentration for aggressive environment.

Figure 15. Summary of mean data for independent variable, water-cement ratio, for the moderate (a,b, and c) and aggressive environments (d,e, and f).

Note: 1 mpy = 25.4 μm/yr

Note: 1 lb/yd3 = 0.6 Kg/m3

Air Content

Figure 16 shows the mean values of rapid chloride permeability, electrical resistivity, and compressive strength at 28 and 90-day exposures for concretes prepared with air contents of 2, 5, and 8 percent. The effect of air content on the 28-day and 90-day rapid chloride permeability is shown graphically in figure 16a. At 28-days, the highest rapid chloride permeability value is shown by concretes containing 5 percent air, and the lowest value by concretes containing the highest air content. At 90-days, there is virtually no difference in the rapid chloride permeability values as affected by air content in the 2-to 8-percent range.

The expected contribution of air void content to the chloride permeability (as measured in this test) depends upon whether or not the air voids are filled with water during the test. If the air voids become water-filled during the specimen preparation step, it is expected that they would act as conduits for increased chloride permeability and, hence would provide a higher charge passed. If the air voids are not water-filled at the time of testing, the air voids would not contribute to increased chloride permeability.

Since the cement paste content was held constant in these concretes (at 30 volume percent), the results obtained at 90-days indicate that air content, within the range studied here, has no significant effect on rapid chloride permeability. The anomalous result at 28-days may relate to the fact that, during this early age, ionic conductivity values are changing rapidly in the concretes.

The effect of air content on concrete electrical resistivity at 28-days and 90-days is shown in figure 16b. Although there is no established pattern at 28-days, at 90-days there is no significant difference in electrical resistivity as affected by air content (within the range 2 percent to 8 percent), with electrical resistivity values ranging between 45,000 ohm-cm and 53,000 ohm-cm.

The effect of air content on the 28-day and 90-day compressive strength is shown graphically in figure 16c. The highest values of compressive strength were shown for the concretes with air contents of 2 and 5 percent, with the 8 percent air content condition slightly lower. In general, air content had only minimal effect on the concrete properties measured.

Figure 17 shows the mean values of corrosion rate, potential, and chloride concentration for the aggressive and moderate environments for concretes prepared with air contents of 2, 5, and 8 percent. For the moderate environment, the only statistically significant effect is at 8 percent air, a lower chloride concentration is observed. For the aggressive environment, no effect on chloride concentration was observed, although a decrease in corrosion rate and corrosion potential (more negative) with an increase in air content was observed. These observations are in conflict with conventional understanding. Typically, the more negative potential means that there is a greater probability for corrosion. However, a decrease in corrosion rate was also noted. One possible explanation is that in these tests where

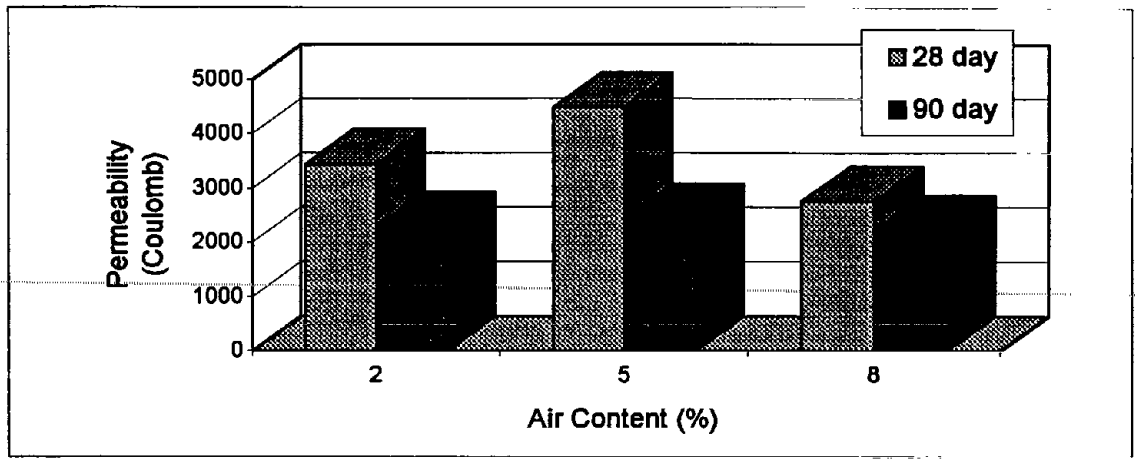

Figure 16a. Rapid chloride permeability.

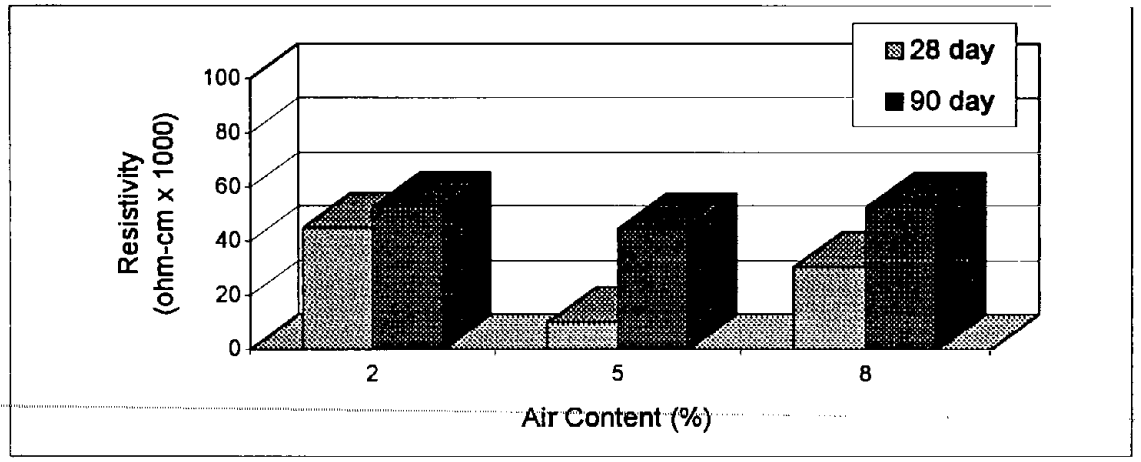

Figure 16b. Electrical resistivity.

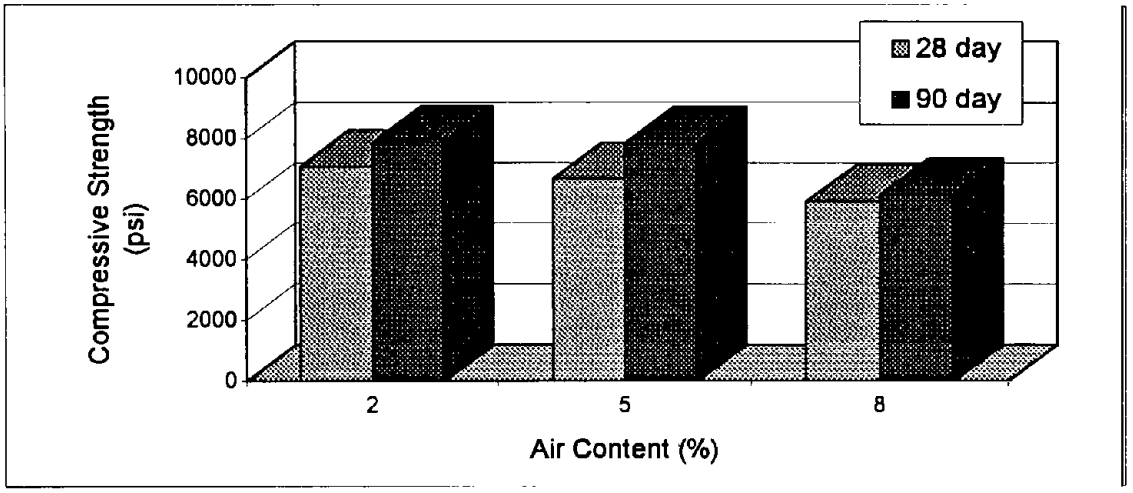

Figure 16c. Compressive strength.

Figure 16. Summary of mean data for independent variable, air content, for the concrete property variables of chloride permeability, resistivity, and compressive strength.
Note: 1 psi = 6.895 KPa

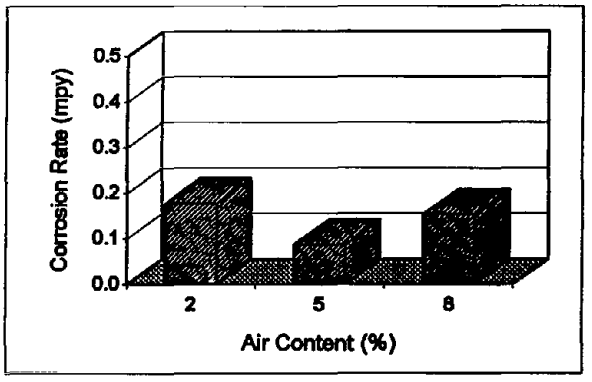

Figure 17a. Corrosion rate for moderate environment.

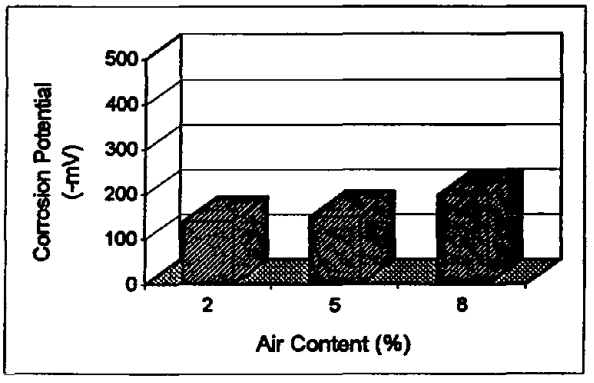

Figure 17b. Corrosion potential for moderate environment.

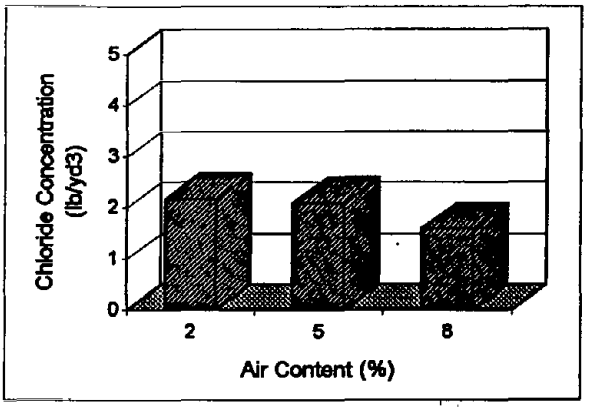

Figure 17c. Chloride concentration for moderate environment.

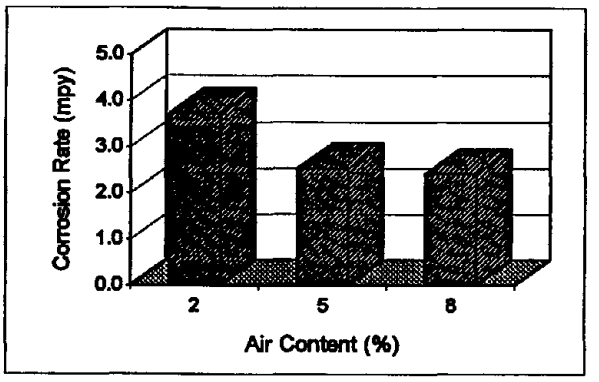

Figure 17d. Corrosion rate for aggressive environment.

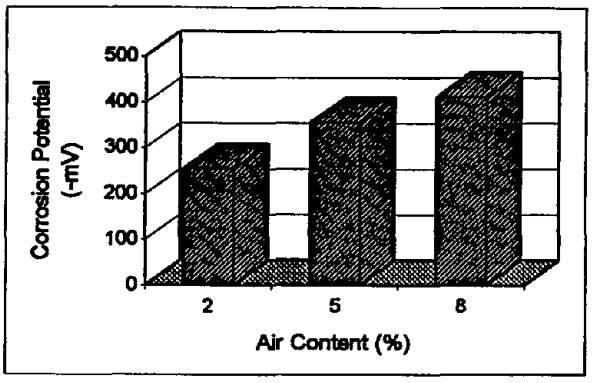

Figure 17e. Corrosion potential for aggressive environment.

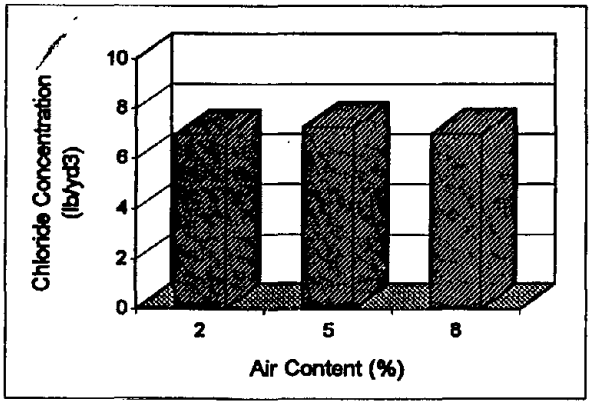

Figure 17f. Chloride concentration for aggressive environment.

Figure 17. Summary of mean data for independent variable, air content, for the moderate (a,b, and c) and aggressive environments (d,e, and f).

Note: 1 mpy = 25.4 μm/yr

Note: 1 lb/yd^3 = 0.6 Kg/m^3

macrocell corrosion is not present, the highly active steel surface behaves in a manner that is typical for activation polarization systems (decrease in corrosion rate with more negative potentials). For the typical concrete exposure with macrocells present, the more standard behavior of a more negative potential (larger macrocell) being related to higher corrosion is observed.

Coarse Aggregate Type

Figure 18 shows the mean values of rapid chloride permeability, electrical resistivity, and compressive strength at 28 and 90-day exposures for concretes prepared with two different coarse aggregates. One is a relatively impermeable quartz aggregate with an absorption value under 1 percent. The other is a relatively permeable limestone with an absorption value over 9 percent. Both aggregates are 9.5-mm (0.375-in) maximum size (ASTM C 33 no 8 Gradation).

The effect of coarse aggregate type on 28-day and 90-day rapid chloride permeability is shown graphically in figure 18a. The high-absorption limestone aggregate results in a significantly higher rapid chloride permeability at both 28-days and 90-days than the quartz aggregate. This is an expected result if it is assumed that the aggregates are saturated during the rapid chloride permeability test. The highly absorptive limestone aggregate contains a significantly higher level of the medium responsible for the ionic conductivity of the concretes (i.e., water-containing dissolved ions). If this is the case, it is expected that the effect of aggregate absorption (porosity) on rapid chloride permeability will remain constant throughout the concrete's curing history, as long as the concrete is in a saturated condition.

The effect of coarse aggregate type on concrete electrical resistivity at 28-days and 90-days is shown graphically in figure 18b. Concretes containing the quartz aggregate show slightly to moderately higher values of electrical resistivity as both ages.

The effect of coarse aggregate type on the 28-day and 90-day compressive strength of the concretes is shown in figure 18c. The highest values of compressive strength were provided by the quartz aggregate at both curing ages. At 90-days, concretes containing the quartz coarse aggregate showed a mean compressive strength of 56.1MPa (8145 psi), compared to 44.MPa (6445 psi) for concretes containing the limestone coarse aggregate. The greater porosity and lower intrinsic strength of the limestone aggregate is responsible for this result.

Figure 19 shows the mean values of corrosion rate, potential, and chloride concentration for the aggressive and moderate environments for concretes prepared with coarse aggregate types of limestone and quartz. For the moderate environment, no effect of coarse aggregate was observed. For the aggressive environment, No

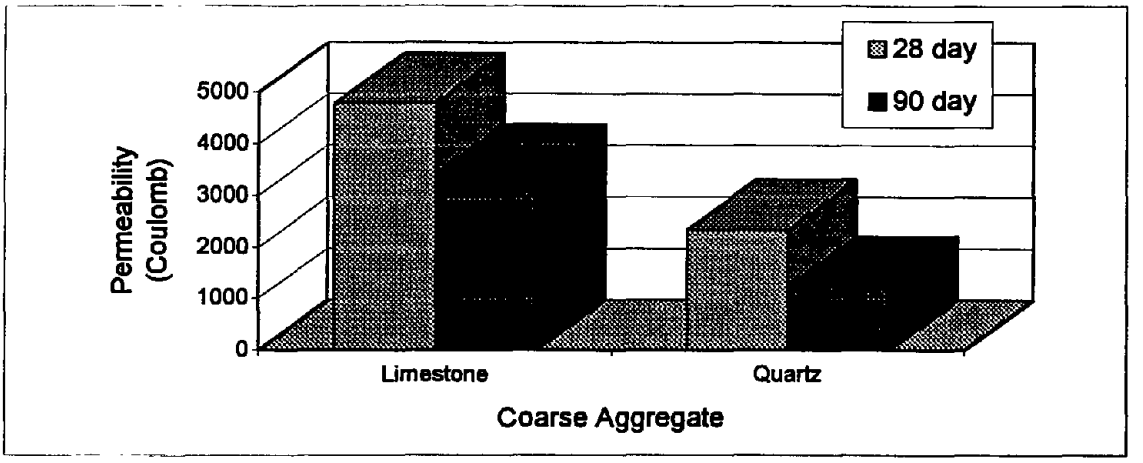

Figure 18a. Rapid chloride permeability.

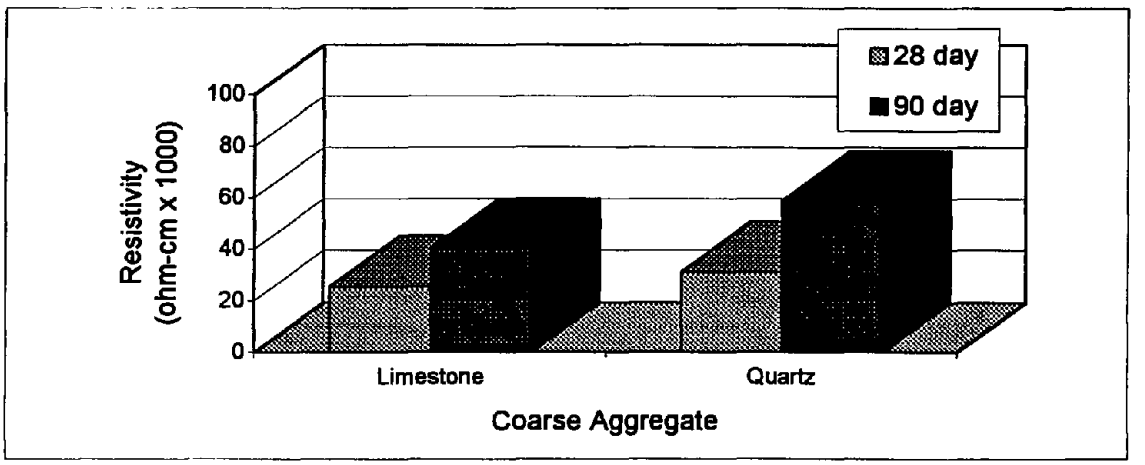

Figure 18b. Electrical resistivity.

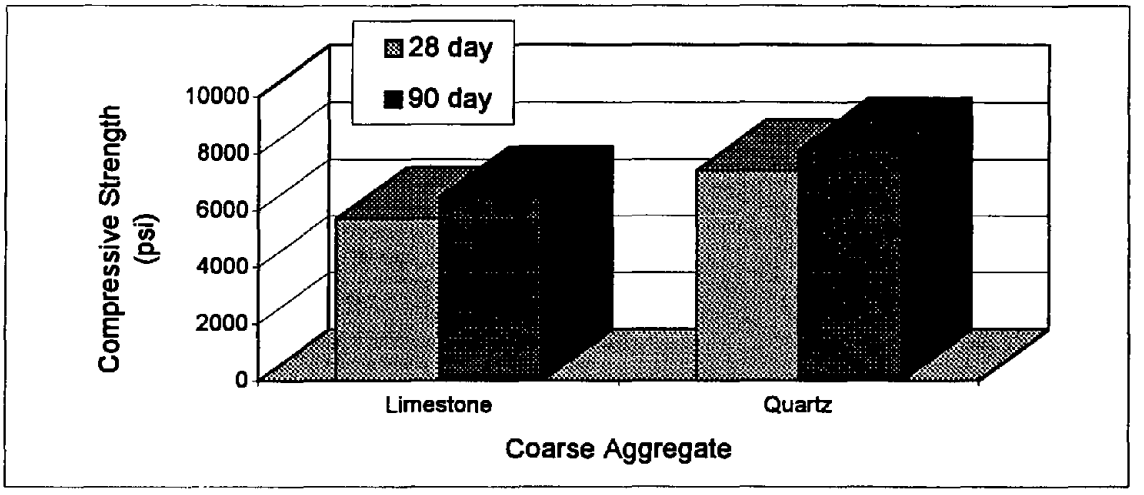

Figure 18c. Compressive strength.

Figure 18. Summary of mean data for independent variable, coarse aggregate, for the concrete property variables of chloride permeability, resistivity, and compressive strength.
Note: 1 psi = 6.895 KPa

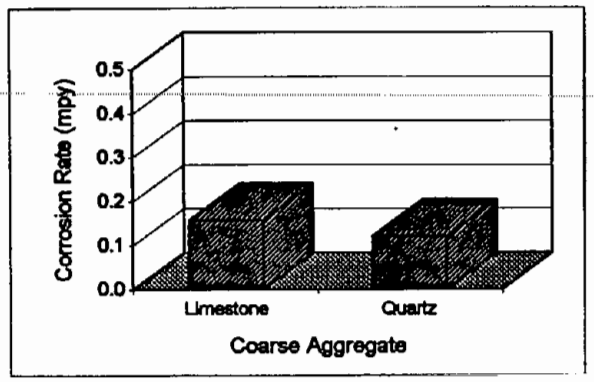

Figure 19a. Corrosion rate for moderate environment.

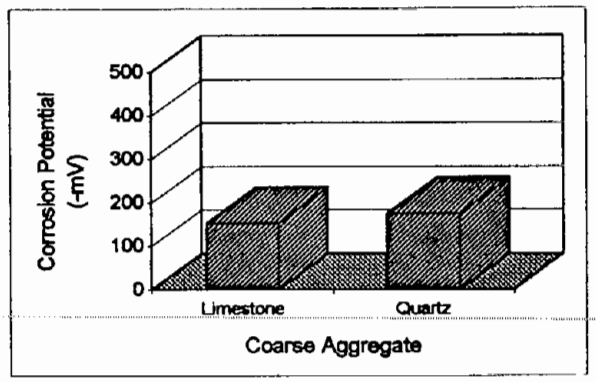

Figure 19b. Corrosion potential for moderate environment.

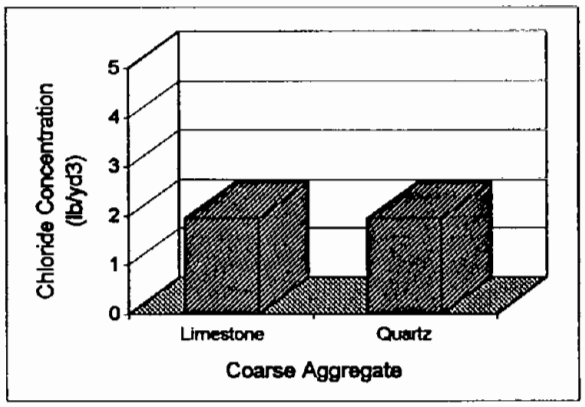

Figure 19c. Chloride concentration for moderate environment.

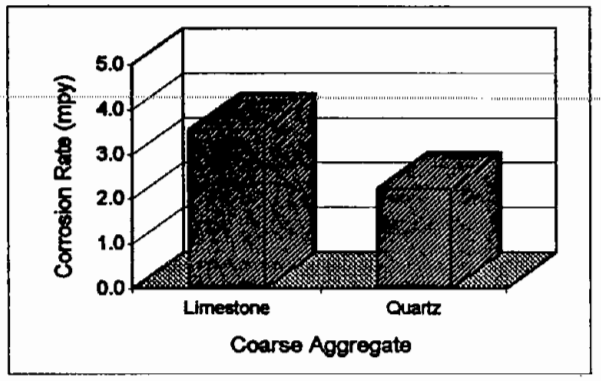

Figure 19d. Corrosion rate for aggressive environment.

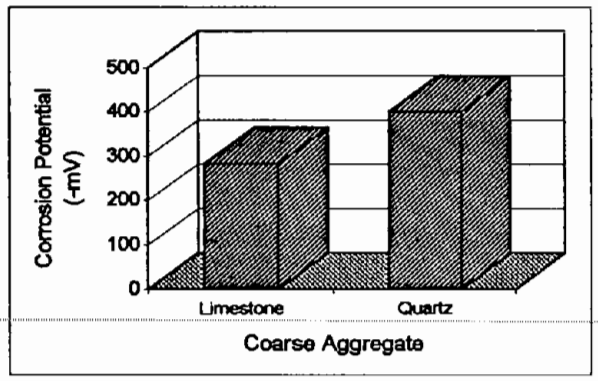

Figure 19e. Corrosion potential for aggressive environment.

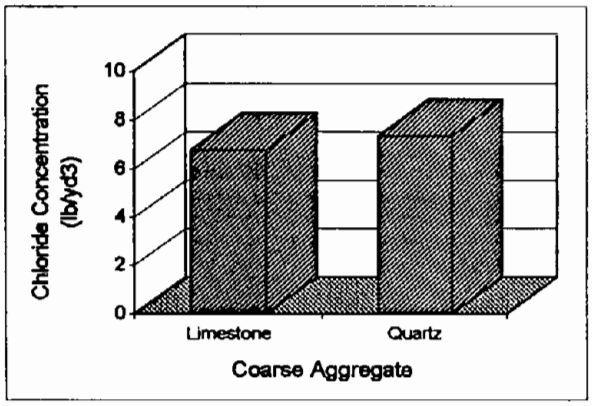

Figure 19f. Chloride concentration for aggressive environment.

Figure 19. Summary of mean data for independent variable, coarse aggregate, for the moderate (a,b, and c) and aggressive environments (d,e, and f).

Note: 1 mpy = 25.4 μm/yr

Note: 1 lb/yd3 = 0.6 Kg/m3

effect of chloride concentration was observed, but a lower corrosion rate was measured for the quartz aggregate. A more negative corrosion potential was also observed for the quartz aggregate. This is similar behavior as discussed above for air content .

Fine Aggregate Type

Figure 20 shows the mean values of rapid chloride permeability, electrical resistivity, and compressive strength at 28 and 90-day exposures for concretes prepared with two different fine aggregates. They include the same, relatively impermeable quartz aggregate used the coarse aggregate. The other fine aggregate is a glacial sand composed of a variety of rock types including limestones, dolomitic limestones, quartz, and siltstones. The porosity of the glacial sand, as indicated by water absorption, is moderately higher than that of the quartz sand (2.2 vs. 0.3 percent).

The mean rapid chloride permeability values are show graphically in figure 20a. As with the coarse aggregates, the mean values of rapid chloride permeability (coulombs) are lower for concretes containing the quartz fine aggregate, relative to those containing the glacial sand (mixed carbonate/siliceous rock types). The effect of fine aggregate type is less significant than the effect of coarse aggregate type on rapid chloride permeability. This result is not unexpected since the difference in porosity (absorption) is not nearly as great for the fine aggregate as it is for the coarse aggregate.

The effect of fine aggregate type on concrete electrical resistivity at 28-days and 90-days is shown graphically in figure 20b. Concretes containing the quartz aggregate show slightly to moderately higher values of electrical resistivity as both ages. This data is very similar to for the coarse aggregate.

The effect of fine aggregate type on the 28-day and 90-day compressive strength of the concretes is shown in figure 20c. The highest value of compressive strength was provided by the quartz fine aggregate at both curing ages. The data for the fine aggregate is similar as observed for the coarse aggregate. The glacial sand has a higher porosity and a lower intrinsic strength than the quartz sand.

Figure 21 shows the mean values of corrosion rate, potential, and chloride concentration for the aggressive and moderate environments for concretes prepared with fine aggregate types of glacial sand and quartz sand. The effects of fine aggregate on the corrosion rate were more pronounced than for the coarse aggregate. The quartz sand had the lower corrosion rate in both of the environments. The effects on corrosion potential and chloride concentration were minimal.

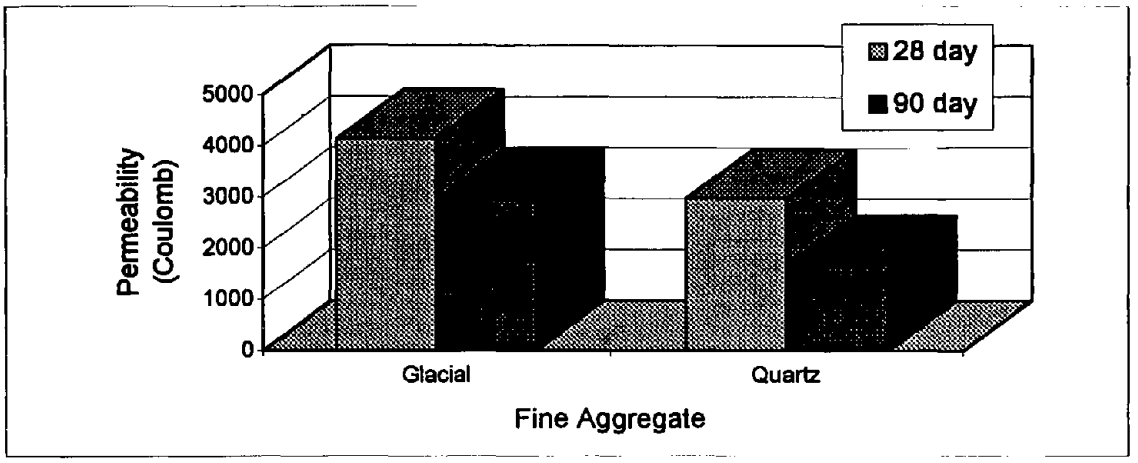

Figure 20a. Rapid chloride permeability.

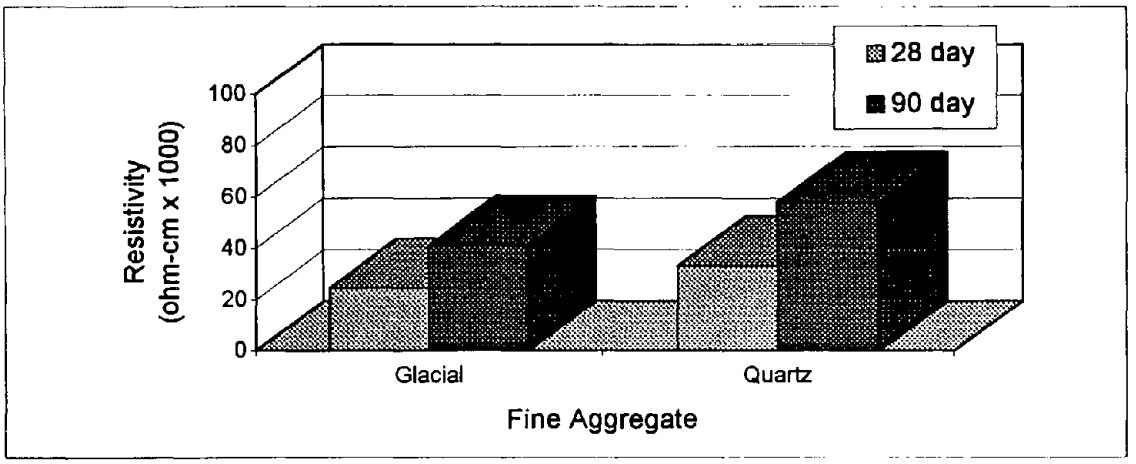

Figure 20b. Electrical resistivity.

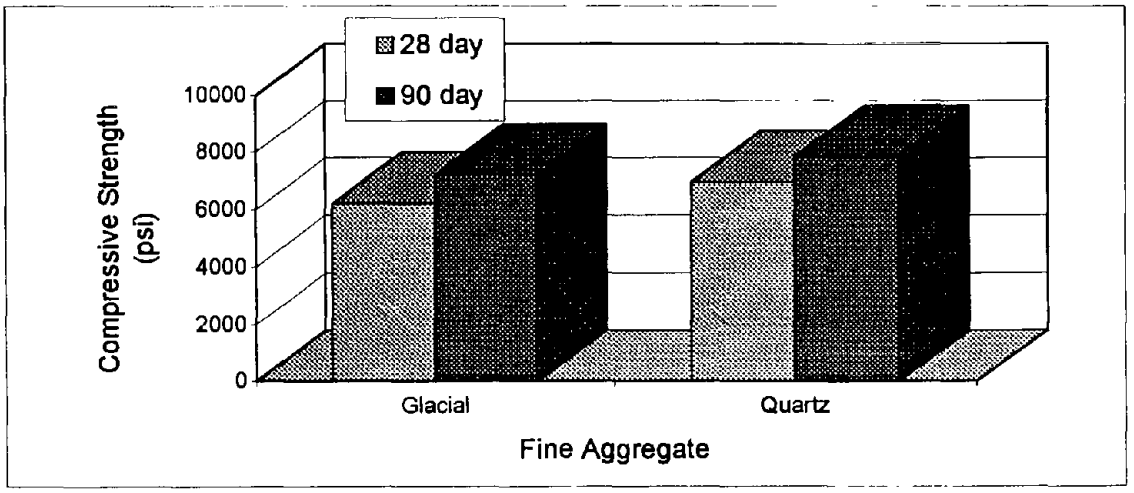

Figure 20c. Compressive strength.

Figure 20. Summary of mean data for independent variable, fine aggregate, for the concrete property variables of chloride permeability, resistivity, and compressive strength.
Note: 1 psi = 6.895 KPa

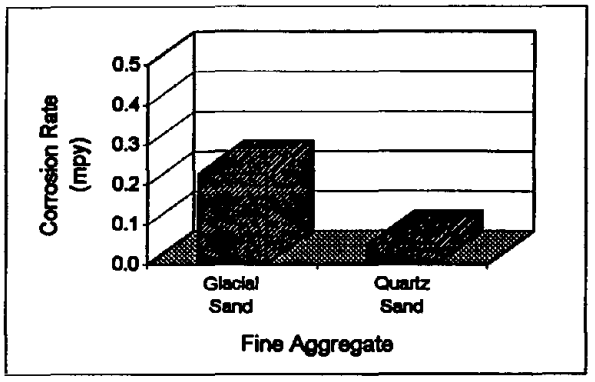

Figure 21a. Corrosion rate for moderate environment.

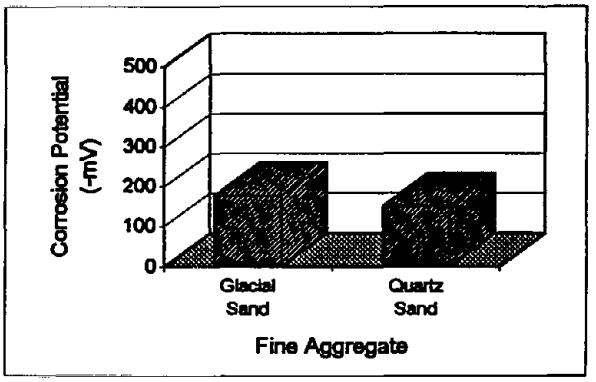

Figure 21b. Corrosion potential for moderate environment.

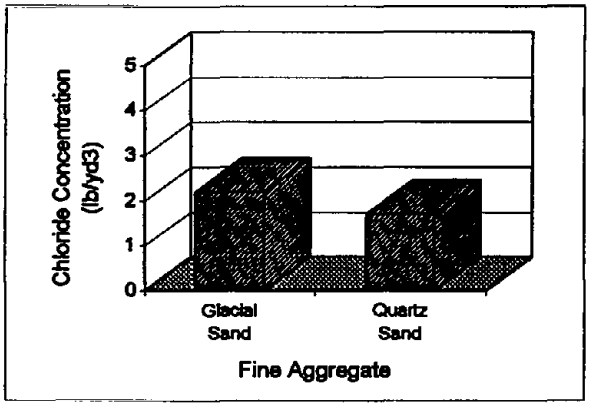

Figure 21c. Chloride concentration for moderate environment.

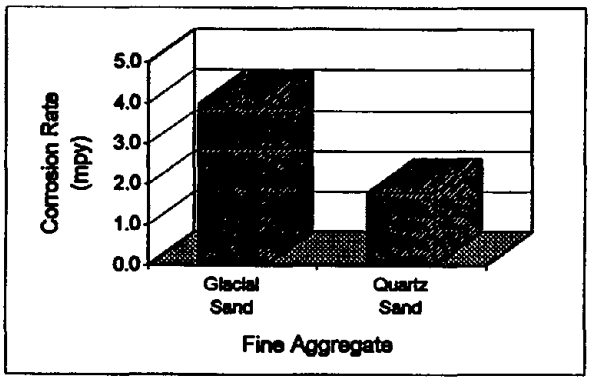

Figure 21d. Corrosion rate for aggressive environment.

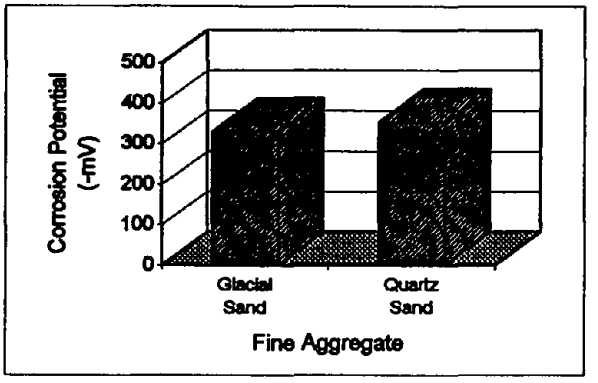

Figure 21e. Corrosion potential for aggressive environment.

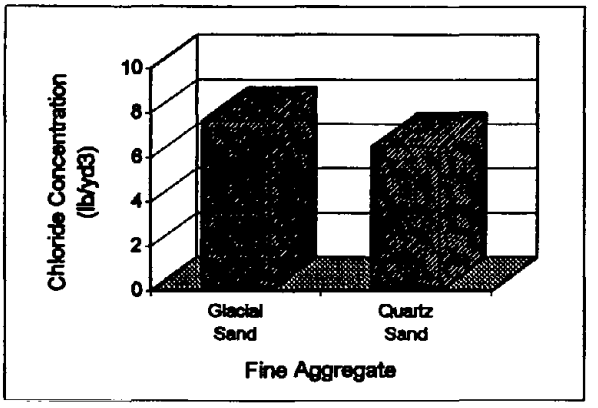

Figure 21f. Chloride concentration for aggressive environment.

Figure 21. Summary of mean data for independent variable, fine aggregate, for the moderate (a,b, and c) and aggressive environments (d,e, and f).

Note: 1 mpy = 25.4 μm/yr

Note: 1 lb/yd3 = 0.6 Kg/m3

Mineral Admixture

Figure 22 shows the mean values of rapid chloride permeability, electrical resistivity, and compressive strength for concretes prepared with mineral admixtures of silica fume, Class C fly ash, Class F fly ash, ground granulated blast furnace slag (GGBF) slag, and no admixture. The microsilica was used at a constant rate of 10 percent (by weight) of total cementitious material. Both the Class C and Class F fly ash were used at a constant rate of 25 percent (by weight) of cementitious material. The GGBF slag was used at a constant rate of 35 percent (by weight) of cementitious material.

Mean rapid chloride permeability values at 28-days and 90-days, as a function of mineral admixture type, are shown graphically in figure 22a. The most significant influence of mineral admixture on rapid chloride permeability is shown in the 90-day value where concretes prepared with silica fume, Class C fly ash, and slag all have a mean rapid chloride permeability value of less than 2000 coulombs. The mean 90-day rapid chloride permeability value of the concretes containing no mineral admixture is 3992 coulombs. The use of Class F fly ash provided only a slight reduction in rapid chloride permeability at 90-days (3143 coulombs). At 28-days, concretes containing silica fume also provided the lowest concrete rapid chloride permeability value (1966 coulombs). At 28-days, the concretes containing the Class F fly ash actually showed the highest rapid chloride permeability values (5183 coulombs).

The contribution of the mineral admixture to reductions in rapid chloride permeability are related to either its pozzolonic activity, or to its ability to contribute additional cementitious material. Silica fume provided the most dramatic reduction in rapid chloride permeability at both 28-days and 90-days, despite the fact that it was used at only a 10 percent cement-replacement level. The small particle size (submicron) and expected high pozzolonic activity of silica fume are thought to be responsible for this result.

Both GGBF slag and Class C fly ash also provide significant reductions in concrete rapid chloride permeability, although the effect is considerably more significant at 90-days, relative to 28-days. Both of these mineral admixtures provide some material that participates in the pozzolonic reaction, and material that itself is capable of hydrating to form additional cementitious phases.

Class F fly ash provided the least significant reduction in rapid chloride permeability, relative to the other mineral admixtures evaluated here. This result is also not unexpected inasmuch as Class F fly ash participates primarily in the pozzolonic reactions, but it is not as reactive as the other mineral admixture in this category (silica fume). The larger mean particle size of the Class F fly ash, along with its expected lower pozzolonic activity, account for the fact that its effect on rapid chloride permeability is less significant and, in fact, is not seen until the advanced curing age of 90-days.

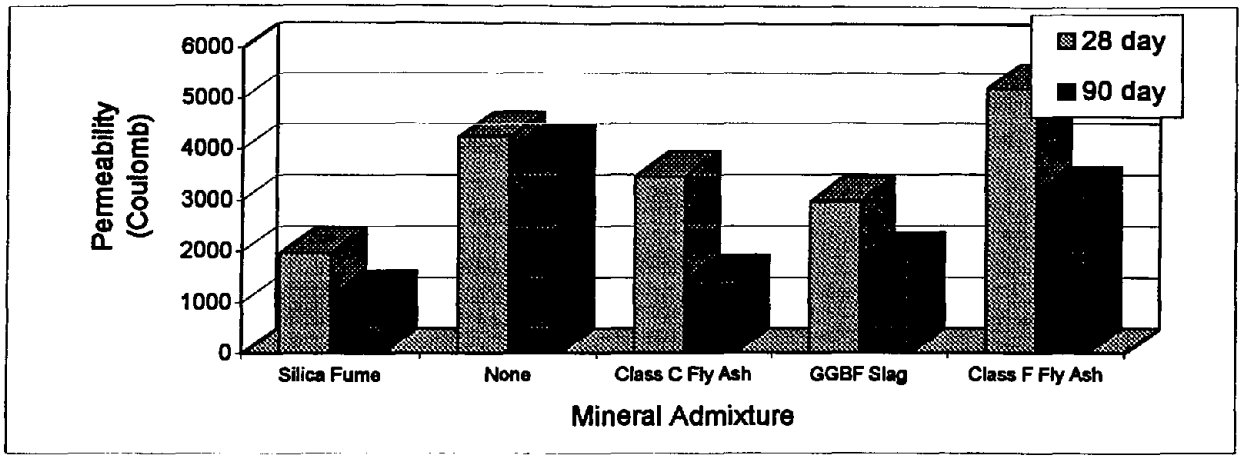

Figure 22a. Rapid chloride permeability.

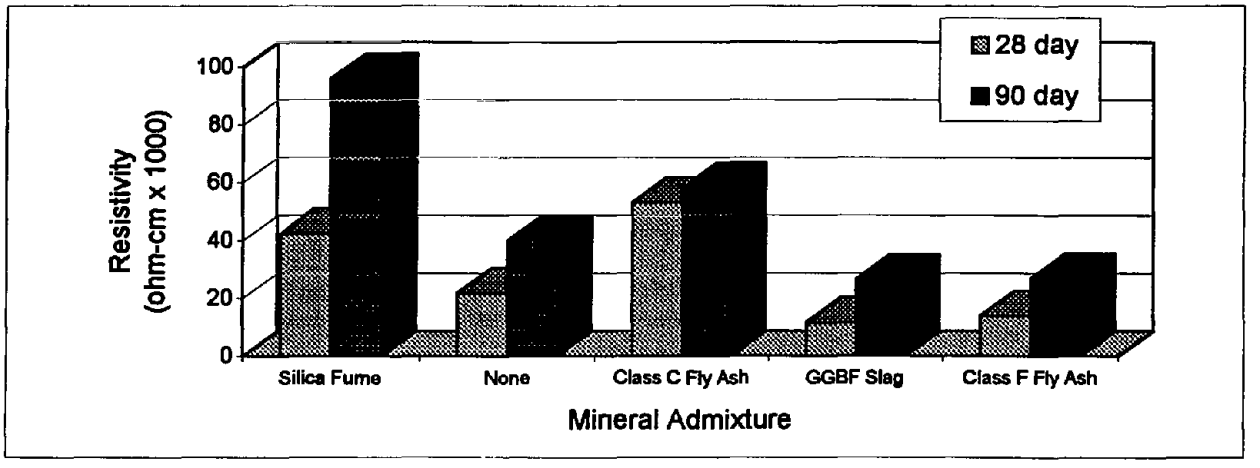

Figure 22b. Electrical resistivity.

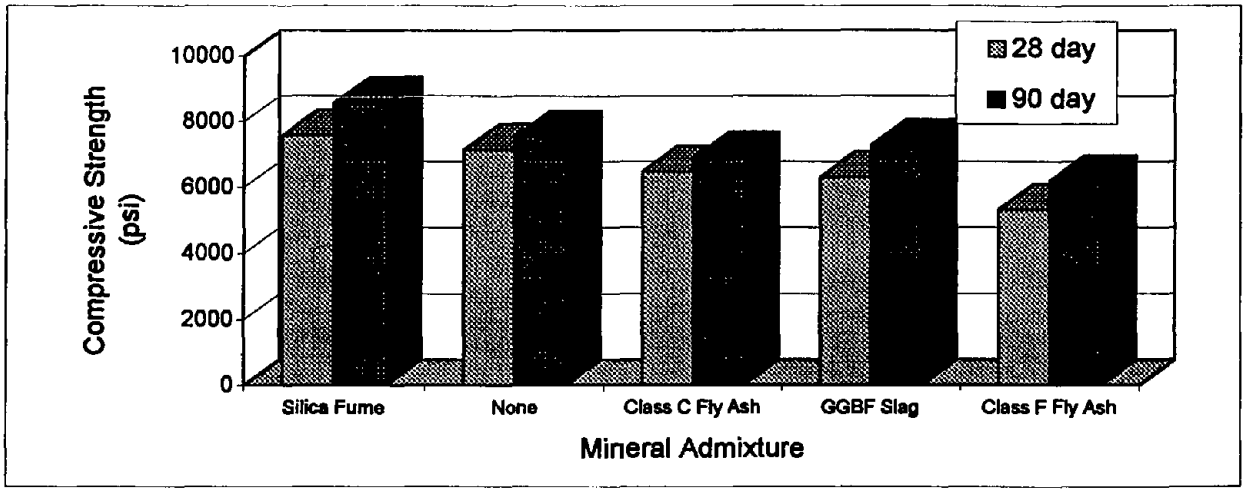

Figure 22c. Compressive strength.

Figure 22. Summary of mean data for independent variable, mineral admixture, for the concrete property variables of chloride permeability, resistivity, and compressive strength.
Note: 1 psi = 6.895 KPa

The effect of mineral admixture type on concrete electrical resistivity at 28-days and 90-days is shown graphically in figure 22b. Relative to the concretes containing no mineral admixture, the use of silica fume or Class C fly ash produced increases in electrical resistivity at both 28-days and 90-days. Concretes containing 10 percent silica fume showed the highest 90-day value of electrical resistivity (95,000 ohm-cm). Concretes containing the Class F fly ash or the GGBF slag showed both 28-day and 90-day electrical resistivity values slightly lower than the concretes that contained no mineral admixture.

The effect of mineral admixture type on compressive strength at 28-days and 90-days is shown in figure 22c. At both curing ages, concretes in which the total cementitious phase was 10 percent silica fume had the highest level of compressive strength. The next highest level of compressive strength was shown by concretes containing no mineral admixtures. The fact that the concrete containing no mineral admixtures has a somewhat higher compressive strength than concretes containing Class C fly ash and GGBF slag is somewhat surprising. It is generally assumed that compressive strength at later curing ages will be higher when these admixtures are used. However, in the present investigation, the total amount of cementitious material was held constant at 30 volume percent. This may account for the result in the present case. At both curing ages, concretes containing the Class F fly ash had the lowest values of compressive strength.

Figure 23 shows the mean values of corrosion rate, potential, and chloride concentration for the aggressive and moderate environments for concretes prepared with mineral admixtures of silica fume, Class C fly ash, Class F fly ash, GGBF slag, and no admixture. Silica fume exhibited the lowest corrosion rate for both environments. GGBF slag and Class F fly ash exhibited the highest corrosion rates in both the environments. For the moderate environment, the effect of mineral admixture on corrosion potential and chloride concentration are not significant. For the aggressive environment, the mineral admixtures tended to make the corrosion potential more positive to varying degrees. For the aggressive environment, the mineral admixtures tended to decrease the chloride concentration at the steel surface by similar values for all of the admixture types.

Cement Type

Figure 24 shows the mean values of rapid chloride permeability, electrical resistivity, and compressive strength for concretes prepared with six different cements; including four prtland cements, a calcium aluminate cement, and a magnesium phosphate cement. The portland cements include one with a low tricalcium aluminate (C3A) content, one with a high C3A content, one with a low total alkali content, and one with a high total alkali content.

Mean concrete rapid chloride permeability values at 28-days and 90-days, as a function of cement type, are shown graphically in figure 24a. The highest values of 28- and 90-day rapid chloride permeability were shown by concretes containing the magnesium phosphate cement. For the water-cement ratios used in the task B

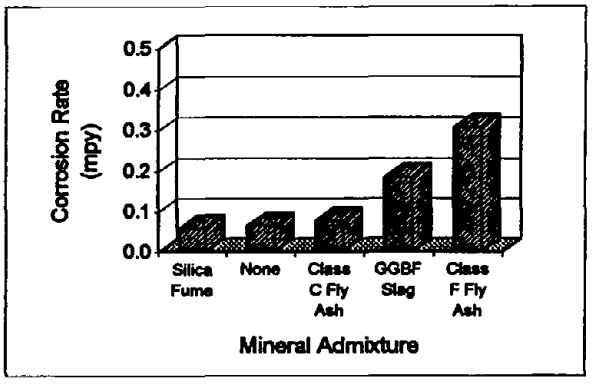

Figure 23a. Corrosion rate for moderate environment.

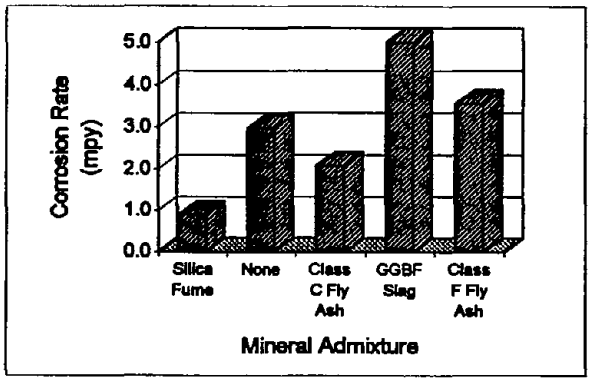

Figure 23d. Corrosion rate for aggressive environment.

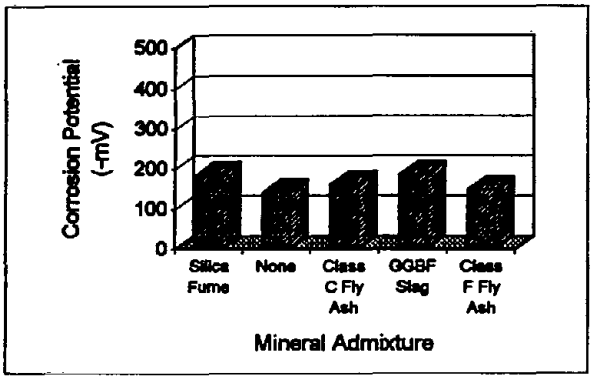

Figure 23b. Corrosion potential for moderate environment.

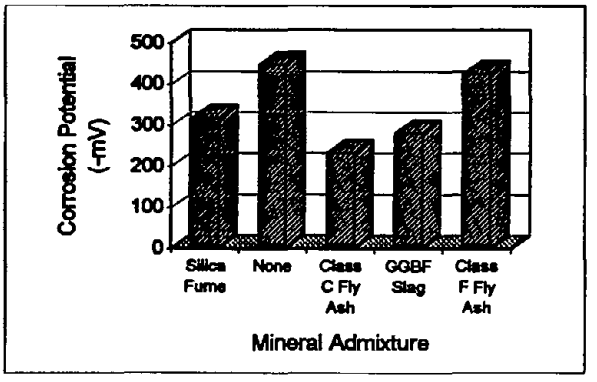

Figure 23e. Corrosion potential for aggressive environment.

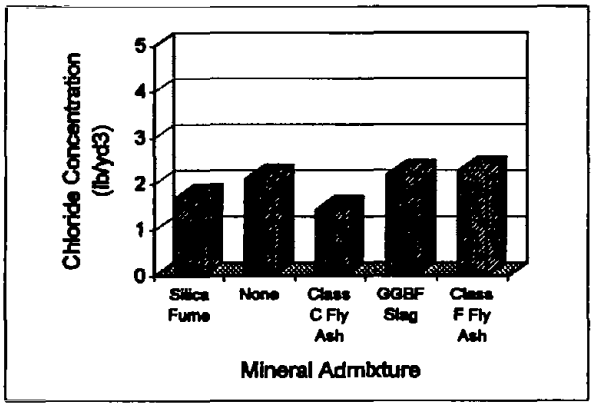

Figure 23c. Chloride concentration for moderate environment.

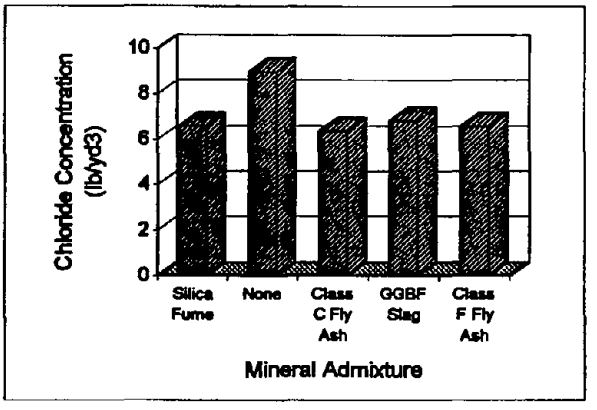

Figure 23f. Chloride concentration for aggressive environment.

Figure 23. Summary of mean data for independent variable, mineral admixture, for the moderate (a,b, and c) and aggressive environments (d,e, and f).

Note: 1 mpy = 25.4 μm/yr

Note: 1 lb/yd3 = 0.6 Kg/m3

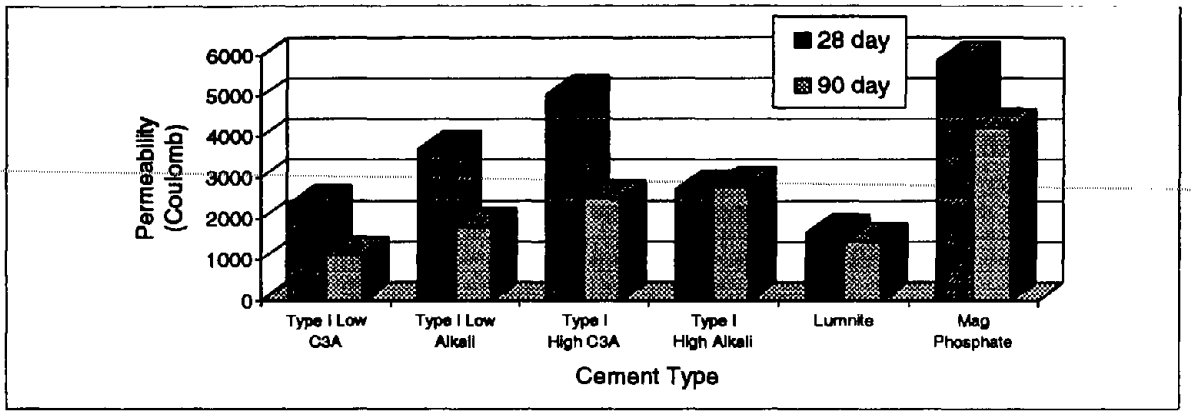

Figure 24a. Rapid Chloride Permeability.

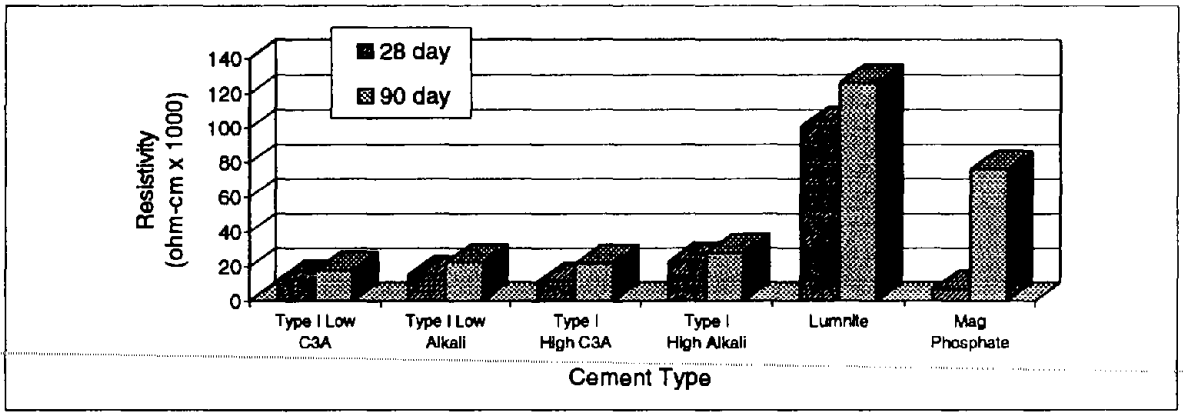

Figure 24b. Electrical Resistivity.

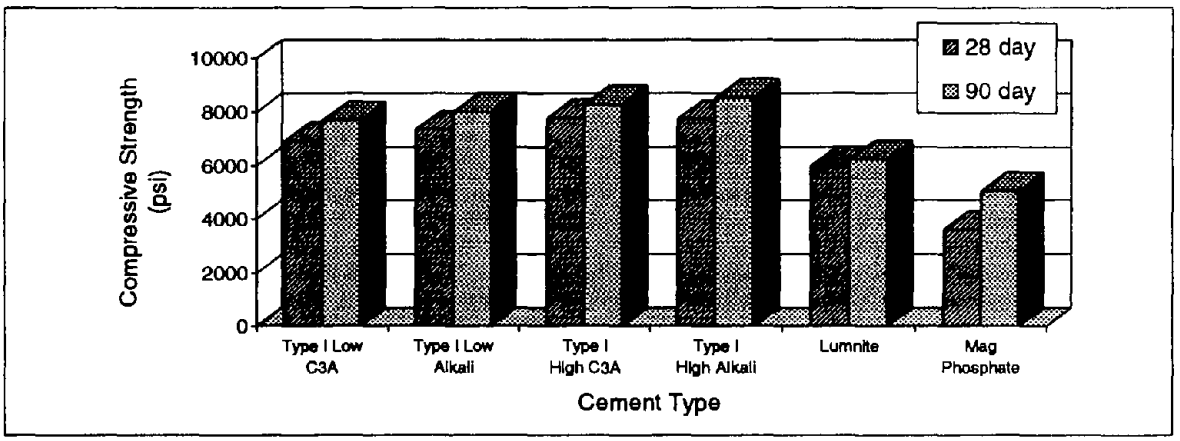

Figure 24c. Compressive Strength.

Figure 24. Summary of mean data for independent variable, cement type, for the concrete property variables of rapid chloride permeability, resistivity, and compressive strength.

investigation, it is expected that the porosity of the cement paste phase may be highest for the magnesium phosphate cements. This expected higher level of open porosity would contribute to an increased rapid chloride permeability. Concretes containing the calcium aluminate cement showed the lowest rapid chloride permeability at 28-days (1664 coulombs), and the next to lowest value at 90-days (1444 coulombs).

There was a surprisingly large variation in 28-day and 90-day rapid chloride permeability values as affected by the portland cement source. Concretes containing the low C3A content cement showed the lowest 28-day and 90-day rapid chloride permeability values (2358 coulombs and 1109 coulombs, respectively). Concretes containing the high C3A content cement showed the highest 28-day rapid chloride permeability value (5051 coulombs). Concretes containing the high alkali portland cement had the highest value of 90-day rapid chloride permeability (2797 coulombs), almost three times greater than the concretes containing the low C3A content cement (1109 coulombs). The high alkali cement showed unique behavior in that the 28-day and 90-days rapid chloride permeability values are virtually identical.

In-depth chemical characterization of the Type I portland cements was not planned for the task B investigation. This work will be done in task C. It is sufficient to note, at this point, that the chemistry of the portland cement (as reflected in the C3A content and alkali content) has a significant effect on rapid chloride permeability.

The effect of cement type on concrete electrical resistivity at 28-days and 90-days is shown graphically in figure 24b. The most dramatic effect of cement type is shown by concretes containing the calcium aluminate (Lumnite) cement. These concretes showed extremely high (greater than 100,000 ohmxcm) at both 28-days and 90-days. For the portland cements, the variability in 28-day and 90-day electrical resistivity is not large. Twenty-eight-day values ranged from around 12,000 to 24,000 ohm-cm. Ninety-day values ranged from around 19,000 to 29,000 ohm-cm. Concretes containing the magnesium phosphate concrete showed somewhat anomalous electrical resistivity results. The 28-day electrical resistivity of these concretes is relatively low (around 6,000 ohm-cm), while the 90-day values are over 75,000 ohm-cm.

Mean concrete compressive strength values at 28-days and 90-days, as a function of cement type, are shown graphically in figure 24c. The lowest values of compressive strength at both 28 and 90-days were shown by concretes containing the magnesium phosphate cement and the calcium aluminate (Lumnite) cement.

For the water-cement ratios used here, 0.3, 0.4, and 0.5, the total water content of the magnesium phosphate concretes is moderately to significantly higher than that which would be used for these types of concretes in the field. This accounts for the fact that these concretes showed the lowest values of compressive strength in the present investigation.

Figure 25 shows the mean values of corrosion rate, potential, and chloride concentration for the aggressive and moderate environments for concretes prepared with cement types of Type I low C3A, Type I high C3A, Type I low alkali, Type I high alkali, Lumnite, and magnesium phosphate. The type of cement had significant effects on all of the dependent variables measured. Type I low C3A and Type I low alkali exhibited the lowest corrosion rates while Lumnite and magnesium phosphate exhibited the highest corrosion rates for both the environments. Magnesium phosphate cement exhibited a very large effect on the corrosion potential; tended to make the corrosion potential very negative relative to the other cements. The effect of cement type on chloride concentration was not the same for the two environments, except that the Type I low alkali and the Type I high C3A exhibited relatively high chloride concentrations for both environments.

Statistical Model

General linear main effect term models were developed to predict rapid chloride permeability, electrical resistivity, compressive strength, corrosion rate (both moderate and aggressive environment), and corrosion potential (both moderate and aggressive environment). Because of the discrete variables, the model is in a different form than that described for the previous task A work. Also, because of the large number of independent variables, only the main effect terms are included in the model and no quadratic or interaction terms are included. Appendix C provides the set-up parameters and a description of the analysis. Table 18 shows the intercept, the estimate for each level of each parameter (independent variable), the R-square value for the model, and the mean value for all of the data for the rapid chloride permeability model. To help clarify the magnitude of the effect of each parameter, a high and low value (range of effect) predicted by the model is shown for each parameter assuming that all of the other parameters are maintained at their zero estimate value. The range of effect data is used only to see the range that a particular parameter has on the value of a dependent variable, the absolute magnitudes are of little general interest.

To calculate the rapid chloride permeability for any combination of independent variables, the intercept is summed along with the estimate of each discrete level for the concrete mix of interest. For example, the predicted chloride estimate for a mix with a water-cement ratio of 0.4 (-1255), air content of 5 percent (199), limestone coarse aggregate (2177), glacial sand fine aggregate (1288), no mineral admixture (2128), and Type I low alkali cement (-2414) is 5124 coulombs (3011-1255+199+2177+1288+2128-2414).

From table 18 it is seen that all of the parameters have a large effect on the rapid chloride permeability with the exception of air content. Mineral admixture and cement type can each vary the rapid chloride permeability by approximately 3000 coulombs depending on the particular level chosen. The R-square value of 65 percent indicates that only 65 percent of the variation observed in the data can be explained by the model presented in table 18. It is likely that quadratic and interaction

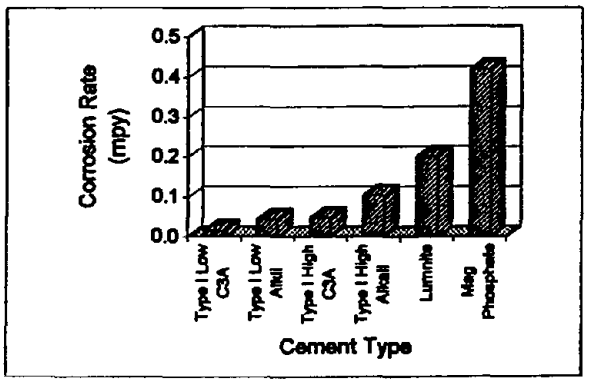

Figure 25a. Corrosion rate for moderate environment.

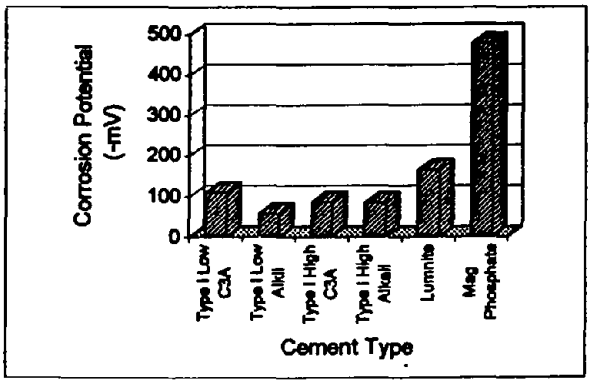

Figure 25b. Corrosion potential for moderate environment.

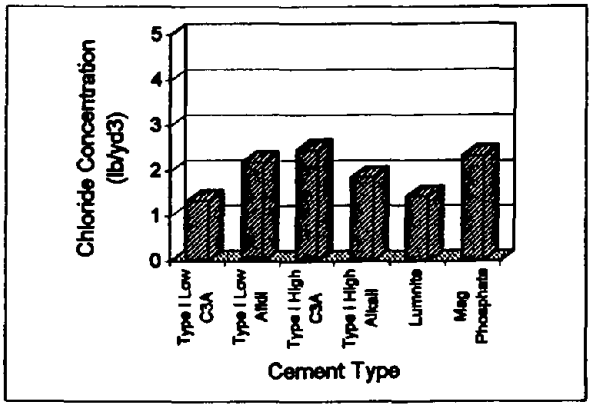

Figure 25c. Chloride concentration for moderate environment.

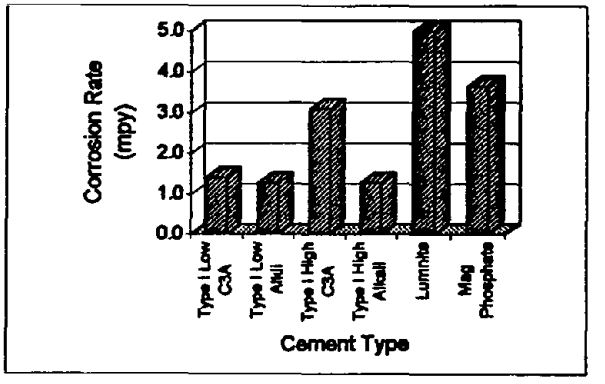

Figure 25d. Corrosion rate for aggressive environment.

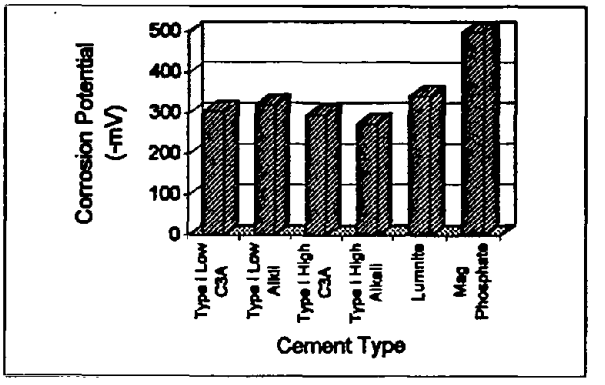

Figure 25e. Corrosion potential for aggressive environment.

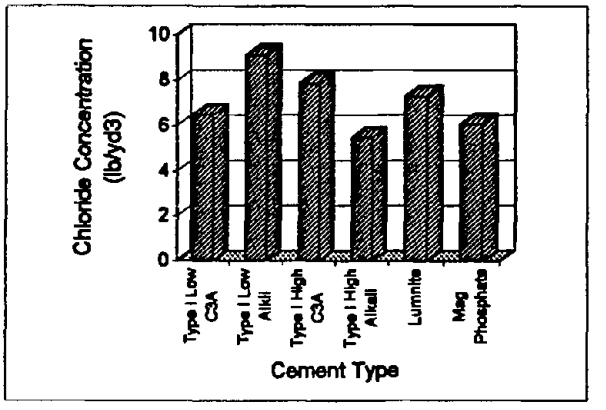

Figure 25f. Chloride concentration for aggressive environment.

Figure 25. Summary of mean data for independent variable, cement type, for the moderate (a,b, and c) and aggressive environments (d,e, and f).

Note: 1 mpy = 25.4 μm/yr

Note: 1 lb/yd3 = 0.6 Kg/m3

Table 18. General linear model for main effect terms for rapid chloride permeability (coulomb) after 90-days.

Parameter	Level		Estimate (Coulomb)	Range of Effect (Coulomb) Low	High
Intercept			3,011		
Water-Cement Ratio	0.3		-1,894	1,117	3,011
	0.4		-1,255		
	0.5		0		
Air Content (%)	2		57	3,011	3,210
	5		199		
	8		0		
Coarse Aggregate	Limestone		2,177	3,011	5,188
	Quartz		0		
Fine Aggregate	Glacial Sand		1,288	3,011	4,299
	Quartz		0		
Mineral Admixture	Silica Fume		-734	2,277	5,139
	None		2,128		
	Class C Fly Ash		-431		
	GGBF Slag		0		
	Class F Fly Ash		1,279		
Cement Type	Type I Low C3A	E	-3,118	-107	3,011
	Type I Low Alkli	C	-2,414		
	Type I High C3A	D	-1,743		
	Type I High Alkali	A	-1,430		
	Lumnite	B	-2,783		
	Mag Phosphate	F	0		

R-Square	65%
Mean (C)	1,902

terms, which were not part of the experimental design, represent a large portion of the variability not explained by the model.

Table 19 shows the intercept, the estimate for each level of each parameter (independent variable), the R-square value for the model, and the mean value for all of the data for the electrical resistivity model. Examining the range of the effect, all parameters can have a large effect on the electrical resistivity. The mineral admixtures, and cement type exhibited the largest effect. The R-square value for this model is 73 percent. This indicates that the model explains a reasonable portion of the variability in the data and should provide a relatively good prediction of resistivity for the range of parameters tested.

Table 20 shows the intercept, the estimate for each level of each parameter (independent variable), the R-square value for the model, and the mean value for all of the data for the compressive strength model. Examining the range of the effects of each parameter on the magnitude of the compressive strength indicates that all parameters tested can have a large effect on the compressive strength. Water-cement ratio and cement type had the largest effect. The R-square value of 90 percent is very high and indicates that the main effect term model presented in table 20 explains the majority of the variation in the data and should provide accurate predictions of compressive strength for the range of parameters tested.

Table 21 shows the intercept, the estimate for each level of each parameter (independent variable), the R-square value for the model, and the mean value for all of the data for corrosion rate in the moderate environment. The parameter with the largest magnitude effect is the cement type. Coarse aggregate has minimal effect on the magnitude of corrosion rate in the moderate environment. The R-square value of 44 percent is relatively low and it indicates that only 44 percent of the variation observed in the data can be explained by the model presented in table 21. It is likely that quadratic and interaction terms represent a large portion of the inability of the model to predict corrosion rates.

Table 22 shows the intercept, the estimate for each level of each parameter (independent variable), the R-square value for the model, and the mean value for all of the data for corrosion potential in the moderate environment. Examining the range of the effects of each parameter on the magnitude of the corrosion potential, cement type has an overwhelming effect compared to the other parameters. The R-square value of 75 percent is much greater than that for the corrosion rate. Therefore, the model for corrosion potential is expected to be much better in predicting values than the model for the corrosion rate.

Table 23 shows the intercept, the estimate for each level of each parameter (independent variable), the R-square value for the model, and the mean value for all of the data for corrosion rate in the aggressive environment. Examining the range of the effect, the mineral admixtures and the cement type have the largest effect on corrosion rate. The R-square value for this model is 40 percent. This is even slightly lower than that for corrosion rate in the moderate environment.

Table 19. General linear model for main effect terms for electrical resistivity (ohm-cm) after 90-days.

Parameter	Level		Estimate (ohm-cm)	Range of Effect (ohm-cm) Low	High
Intercept			33,574		
Water-Cement Ratio	0.3		23,393	33,574	56,967
	0.4		13,817		
	0.5		0		
Air Content (%)	2		-4	28,432	33,574
	5		-5,142		
	8		0		
Coarse Aggregate	Limestone		-11,423	22,151	33,574
	Quartz		0		
Fine Aggregate	Glacial Sand		-11,039	22,535	33,574
	Quartz		0		
Mineral Admixture	Silica Fume		43,119	33,574	76,693
	None		8,182		
	Class C Fly Ash		19,507		
	GGBF Slag		0		
	Class F Fly Ash		415		
Cement Type	Type I Low C3A	E	-35,721	-2,147	64,648
	Type I Low Alkli	C	-33,325		
	Type I High C3A	D	-31,221		
	Type I High Alkali	A	-29,450		
	Lumnite	B	31,074		
	Mag Phosphate	F	0		

R-Square	45%
Mean (ohm-cm)	32,525

Table 20. General linear model for main effect terms for compressive strength (psi) after 90-days.

Parameter	Level		Estimate (psi)	Range of Effect (psi) Low	High
Intercept			3,496		
Water-Cement Ratio	0.3		3,610	3,496	7,106
	0.4		1,958		
	0.5		0		
Air Content (%)	2		1,689	3,496	5,185
	5		1,684		
	8		0		
Coarse Aggregate	Limestone		-1,700	1,796	3,496
	Quartz		0		
Fine Aggregate	Glacial Sand		-1,213	2,283	3,496
	Quartz		0		
Mineral Admixture	Silica Fume		1,306	2,421	4,802
	None		280		
	Class C Fly Ash		-382		
	GGBF Slag		0		
	Class F Fly Ash		-1,075		
Cement Type	Type I Low C3A	E	2,640	3,496	6,966
	Type I Low Alkli	C	2,970		
	Type I High C3A	D	3,247		
	Type I High Alkali	A	3,470		
	Lumnite	B	1,176		
	Mag Phosphate	F	0		

R-Square	90%
Mean (psi)	7,647

Note: 1 psi = 6.895 KPa

Table 21. General linear model for main effect terms for corrosion rate (mpy) in moderate environment.

Parameter	Level		Estimate (mpy)	Range of Effect (mpy) Low	High
Intercept			0.426		
Water-Cement Ratio	0.3		-0.050	0.32	0.43
	0.4		-0.107		
	0.5		0.000		
Air Content (%)	2		0.024	0.36	0.45
	5		-0.066		
	8		0.000		
Coarse Aggregate	Limestone		0.036	0.43	0.46
	Quartz		0.000		
Fine Aggregate	Glacial Sand		0.175	0.43	0.60
	Quartz		0.000		
Mineral Admixture	Silica Fume		-0.127	0.30	0.55
	None		-0.121		
	Class C Fly Ash		-0.108		
	GGBF Slag		0.000		
	Class F Fly Ash		0.123		
Cement Type	Type I Low C3A	E	-0.404	0.02	0.43
	Type I Low Alkli	C	-0.373		
	Type I High C3A	D	-0.371		
	Type I High Alkali	A	-0.314		
	Lumnite	B	-0.218		
	Mag Phosphate	F	0.000		

R-Square	44%
Mean (mpy)	0.09

Note: 1 mpy = 25.4 μm/yr

Table 22. General linear model for main effect terms for corrosion potential (mV) in moderate environment.

Parameter	Level		Estimate (mV)	Range of Effect (mV) Low	Range of Effect (mV) High
Intercept			-555		
Water-Cement Ratio	0.3		42	-555	-513
	0.4		30		
	0.5		0		
Air Content (%)	2		57	-555	-498
	5		46		
	8		0		
Coarse Aggregate	Limestone		23	-555	-532
	Quartz		0		
Fine Aggregate	Glacial Sand		-28	-583	-555
	Quartz		0		
Mineral Admixture	Silica Fume		1	-555	-511
	None		44		
	Class C Fly Ash		25		
	GGBF Slag		0		
	Class F Fly Ash		36		
Cement Type	Type I Low C3A	E	369	-555	-136
	Type I Low Alkli	C	419		
	Type I High C3A	D	391		
	Type I High Alkali	A	393		
	Lumnite	B	313		
	Mag Phosphate	F	0		

R-Square	75%
Mean (mV)	-149

Table 23. General linear model for main effect terms for corrosion rate (mpy) in aggressive environment.

Parameter	Level		Estimate (mpy)	Range of Effect (mpy) Low	High
Intercept			4.523		
Water-Cement Ratio	0.3		-1.919	2.6	4.5
	0.4		-1.067		
	0.5		0.000		
Air Content (%)	2		1.304	4.5	5.8
	5		0.114		
	8		0.000		
Coarse Aggregate	Limestone		1.322	4.5	5.8
	Quartz		0.000		
Fine Aggregate	Glacial Sand		2.186	4.5	6.7
	Quartz		0.000		
Mineral Admixture	Silica Fume		-4.109	0.41	4.5
	None		-2.035		
	Class C Fly Ash		-0.292		
	GGBF Slag		0.000		
	Class F Fly Ash		-1.444		
Cement Type	Type I Low C3A	E	-2.234	2.1	7.5
	Type I Low Alkli	C	-2.378		
	Type I High C3A	D	-0.557		
	Type I High Alkali	A	-2.385		
	Lumnite	B	2.976		
	Mag Phosphate	F	0.000		

R-Square	40%
Mean (mpy)	2.3

Note: 1 mpy = 25.4 μm/yr

Table 24 shows the intercept, the estimate for each level of each parameter (independent variable), the R-square value for the model, and the mean value for all of the data for corrosion potential in the aggressive environment. Examining the range of effect, all of the parameters with the exception of fine aggregate can have a large effect (greater than 50 to 75mV). The R-square value for this model is 64 percent which not to bad for a main effect model but some what lower than that for the model of corrosion potential in the moderate environment.

The models presented here and will be used to begin to optimize mix designs to minimize corrosion damage. These models will be used to select the concretes to be tested in the long-term tests of task C.

Table 24. General linear model for main effect terms for corrosion potential (mV) in aggressive environment.

Parameter	Level		Estimate (mV)	Range of Effect (mV) Low	High
Intercept			-633		
Water-Cement Ratio	0.3		83	-633	-550
	0.4		44		
	0.5		0		
Air Content (%)	2		158	-633	-475
	5		55		
	8		0		
Coarse Aggregate	Limestone		118	-633	-515
	Quartz		0		
Fine Aggregate	Glacial Sand		23		
	Quartz		0		
Mineral Admixture	Silica Fume		-37	-798	-584
	None		-165		
	Class C Fly Ash		49		
	GGBF Slag		0		
	Class F Fly Ash		-144		
Cement Type	Type I Low C3A	E	203	-633	-399
	Type I Low Alkli	C	188		
	Type I High C3A	D	212		
	Type I High Alkali	A	234		
	Lumnite	B	165		
	Mag Phosphate	F	0		

R-Square	64%
Mean (mV)	-372

CHAPTER 5. DISCUSSION

The data presented in the results section provides a significant data base to analyze concrete deterioration and to predict corrosion behavior for a range of environments and a range of concrete compositions. In the following paragraphs, specific aspects of the data are discussed, with special attention given to the selection of concretes for examination in task C.

EFFECTS OF ENVIRONMENTAL VARIABLES

A primary focus of task A was to determine the effect of environmental variables on corrosion and to establish boundary conditions necessary for corrosion. Task A examined two mortars in detail: (1) Type I portland cement (mortar A-2) and (2) calcium aluminate cement (mortar B-2). Figures 26 and 27 show a corrosion rate mapping [minimal (0.00 to 1.3 µm/yr; 0.00 to 0.05 mpy), intermediate (1.4 to 6.4 µm/yr; 0.06 to 0.25 mpy), high (6.5 to 25 µm/yr; 0.26 to 1.0 mpy), and very high (>25 µm/yr; >1.0 mpy)] as a function of environment. It is clear that the lower pH of the calcium aluminate cement produced a profound effect on the range in which corrosion is possible and significantly increased the rate of corrosion for a specific environment (comparison of figure 26 and 27). For the calcium aluminate cement, significant corrosion occurred even for several conditions tested for the 0.6 Kg/m^3 (1 lb/yd^3) chloride concentration. For the portland cement, only two conditions produced any measurable corrosion at 0.6 Kg/m^3 (1 lb/yd^3) chloride concentration. For those two conditions, the corrosion rate was at the very low end of the corrosion range given.

For the portland cement, only minimal corrosion was observed even at 6 Kg/m^3 (10 lb/yd^3) chloride concentration, for the low temperature (4 °C: 40 °F) condition at the low (43 percent) and high (98 percent) relative humidity. Higher corrosion rates were observed at the low temperature - intermediate (75 percent) humidity for both the 1.8 Kg/m^3 (3 lb/yd^3) and 6 Kg/24m^3 (10 lb/yd^3) chloride concentration. A possible explanation is that the rate of corrosion is controlled by the competing effects between moisture content and available oxygen (corrosion rate in soils is known to have a maximum at an intermediate moisture content). Corrosion rate increases with increasing moisture, but oxygen migration decreases with increasing moisture as pores are filled. This effect is observed at the low temperature only. The reason for this is not clear, but may have to do with the relationship between temperature and internal concrete relative humidity.

EFFECTS OF INDEPENDENT VARIABLES

A primary focus of task B was to characterize the effects of the independent variables (water-cement ratio, air content, coarse aggregate, fine aggregate, mineral admixture, and cement type) on the measured dependent variables. These effects are summarized in table 25. Table 25 uses arrows to indicate whether there is an effect and the direction of the effect. For example, an increase in the water-cement ratio increases the rapid chloride permeability, therefore, a low water-cement ratio is

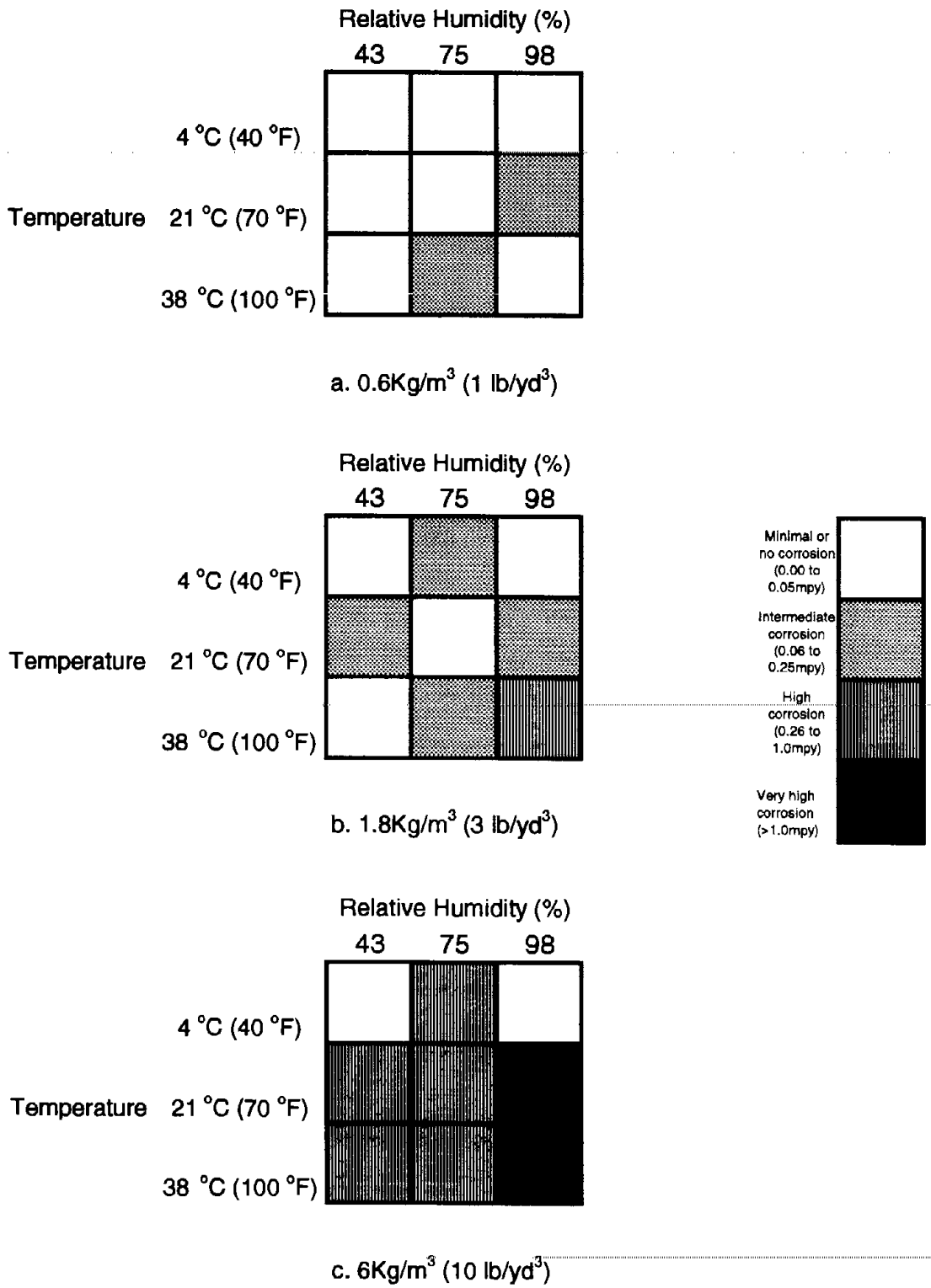

Figure 26. Corrosion rate map as a function of environment for conventional steel in mortar A-2 (Type I portland cement). Note: 1.0 mpy = 25.4 µm/yr.

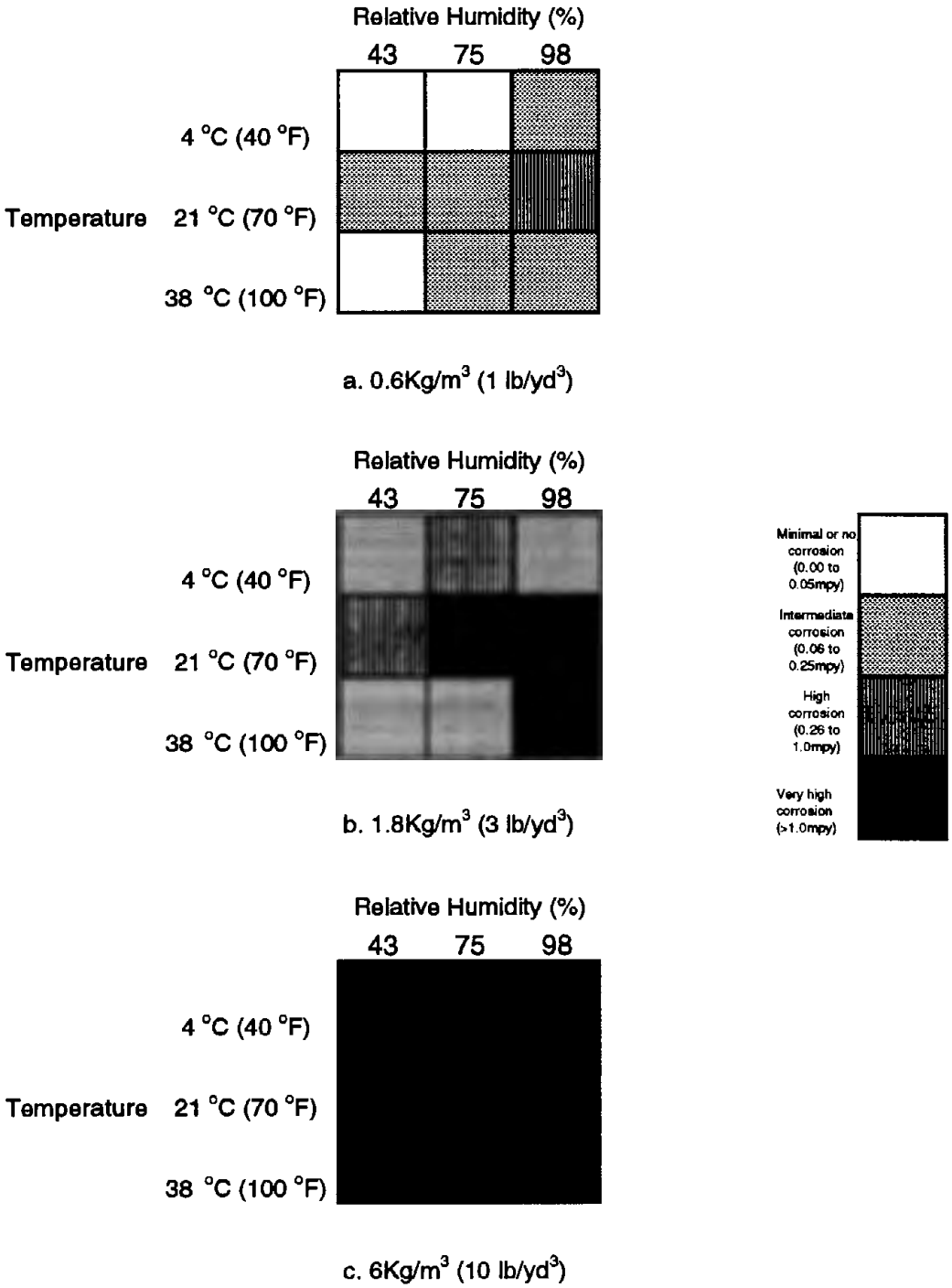

Figure 27. Corrosion rate map as a function of environment for conventional steel in mortar B-2 (calcium aluminate cement).

Note: 1.0 mpy = 25.4 μm/yr.

Table 25. Summary of effects of independent variable on the measured dependent variables.

Independent Variable	Dependent Variable								
	Rapid Chloride Permeability	Resistivity	Compressive Strength	Corrosion Rate Moderate	Corrosion Rate Aggressive	Corrosion Potential * Moderate	Corrosion Potential * Aggressive	Chloride at Steel Surface Moderate	Chloride at Steel Surface Aggressive
Water-Cement Ratio	↑	↓	↓	↑	↑	↑	↑	⬌	↑
Air Content	⬌	⬌	↓	⬌	↓	↑	↑	⬌	⬌
Coarse Aggregate**	↓	↑	↑	↓	↓	⬌	↑	⬌	⬌
Fine Aggregate**	↓	↑	↑	↓	↓	⬌	⬌	⬌	⬌
Mineral Admixture	↓↑	↓↑	↓↑	↓↑	↓↑	⬌	↓↑	↓↑	↓↑
Cement Type	↓↑	↓↑	↓↑	↓↑	↓↑	↓↑	↓↑	↓↑	↓↑

↓ : Decrease in dependent variable with an increase in independent variable.

↑ : Increase in dependent variable with an increase in independent variable.

⬌ : No trend in dependent variable with an increase in independent variable.

↓↑ : Significant change in dependent variable with change in independent variable.

* : Increase in corrosion potential is an increasingly more negative potential.

** : Increasing aggregate refers to increasing absorbent resistance

(going from limestone to quartz or glacial sand to quartz increases absorbent resistance).

Moderate: Moderate environment (21 °C (70 °F) - 75% Relative Humidity - 1.8 Kg/m^3 (3 lb/yd^3) chloride).

Aggressive: Aggressive environment (38 °C (100 °F) - 98% Relative Humidity - 6 Kg/m3 (10 lb/yd3) chloride).

desired. All of the independent variables examined had a significant effect on one or more of the dependent variables measured.

The dependent variable chloride at the steel surface is the amount of chloride measured at the completion of the corrosion tests in a 1.6 mm (0.062 in) layer of concrete adjacent to the steel surface. In the corrosion tests, the concretes underwent a severe vacuum assisted drying cycle prior to ponding in an attempt to get uniform chlorides to the steel surface. It might be expected that these data would be related to the rapid chloride permeability test. However, the rapid chloride permeability is performed under saturated conditions which are significantly different from those in the corrosion tests. The data indicate that aggregate type (fine and coarse) has little effect on the chloride at the steel surface, while the aggregate type had a large effect on the rapid chloride permeability data. This difference likely is due to the manner in which the chloride was driven into the concrete by the differential moisture gradient setup by the severe drying conditions used in the corrosion tests. Even with the severe conditions of the corrosion tests, significant effects on the chloride at the steel surface were observed for mineral admixture and cement type.

CORRELATIONS AMONG DEPENDENT VARIABLES

A correlation matrix was performed on the data for the dependent variables given in table 25. Correlations were calculated for all the data together and for only the portland cement data as a subset. Only a few weak correlations were observed with the exception of rapid chloride permeability and resistivity. Corrosion rate for the moderate and aggressive environments gave a positive correlation coefficient, as did the final chloride for the two environments. This indicates that trends in the behavior for the two environments were related, which was expected. The correlations between corrosion rate and potential and between rapid chloride permeability and resistivity are discussed below.

Corrosion Rate Versus Potential

The polarization behavior of a metal in an electrolyte is characterized by plotting logarithm of current verses potential. The anodic polarization curve characterizes the corrosion behavior as a function of potential since the anodic current is a measure of the corrosion rate. Steel in concrete is characterized by an active - passive behavior: (1) at positive potentials steel is passive and (2) at sufficiently negative potentials steel can become active. In this study, a range of concrete compositions were tested in two different environments, and the corrosion rate and corrosion potential were measured. The correlation analysis indicated only weak correlations between logarithm of corrosion rate and potential. But it was interesting that the correlation coefficient for the moderate environment data was negative and that for the aggressive environment was positive.

Figure 28a and 28b show the data for the moderate and aggressive environments respectively. Although there is significant scatter in the data, these relationships are of interest. The scatter is understandable since these data represent many different concretes of varying mix compositions. The data in figure 28a (moderate environment) indicate that at positive potentials, corrosion rates are low (<0.01 mpy, 0.254 μm/yr), as would be expected for passive conditions. At more negative potentials corrosion rates are much higher. These data are indicative of corrosion rates increasing as the potential becomes more negative, while the metal surface goes from a passive to active corrosion condition. This is the typical observation for steel in chloride contaminated concrete. For real structures, this relationship is accentuated by the presence of macrocells within the concrete structure. No macrocell due to significant chloride concentration gradients is present on the steel tested in this experimental setup.

In figure 28b (aggressive environment), the observed relationship between corrosion rate and potential is the opposite to what is normally expected and observed above for the moderate environment. However, this is the typical relationship observed for active metal corrosion, i.e. corrosion rate decreases as the potential becomes more negative. For the aggressive environment (high chlorides), the steel surface is predominantly active and the behavior in the absence of macrocells is typical for active corrosion. For tests that permit macrocell corrosion, the more negative potentials would increase the difference in the driving potential of the macrocell and corrosion rate would likely to increase with more negative potentials. Therefore, the lack of macrocells in this particular experimental setup tends to enhance the observed corrosion rate - potential relationship.

In addition, figures 28a and b show that for the wide range of concrete conditions investigated in task B, the corrosion rate at any given potential can vary over two to three orders of magnitude. This makes it impossible to predict corrosion rate from a potential measurement alone.

To carry the analysis farther, data from the task A for mortars A2 and B2 were also included and shown in figure 29a. Including the task A data does not change the types of concretes included, but increases the range of environments tested. The task A data did not change the upper and lower bounds for the data significantly from those shown in figure 28. Figure 29a represents corrosion data from a very large range of concrete mix components and environments. In figure 29a the shaded area between 0.05 and 0.25 mpy (1.3 μm/yr and 6.4 μm/yr) represents an intermediate corrosion rate. Below 0.05 mpy (1.3 μm/yr) corrosion is negligible and greater than 0.25 mpy (6.4 μm/yr) corrosion becomes significant. Figure 30 shows a series of photographs of test specimens with a range of measured corrosion rates.

Based on figure 29a, the following observations can be made. Concrete can not be considered a generic material from which general conclusions concerning corrosion behavior can be made. The actual corrosion behavior is dependent on concrete mix components and environment. The rate of corrosion can vary over as

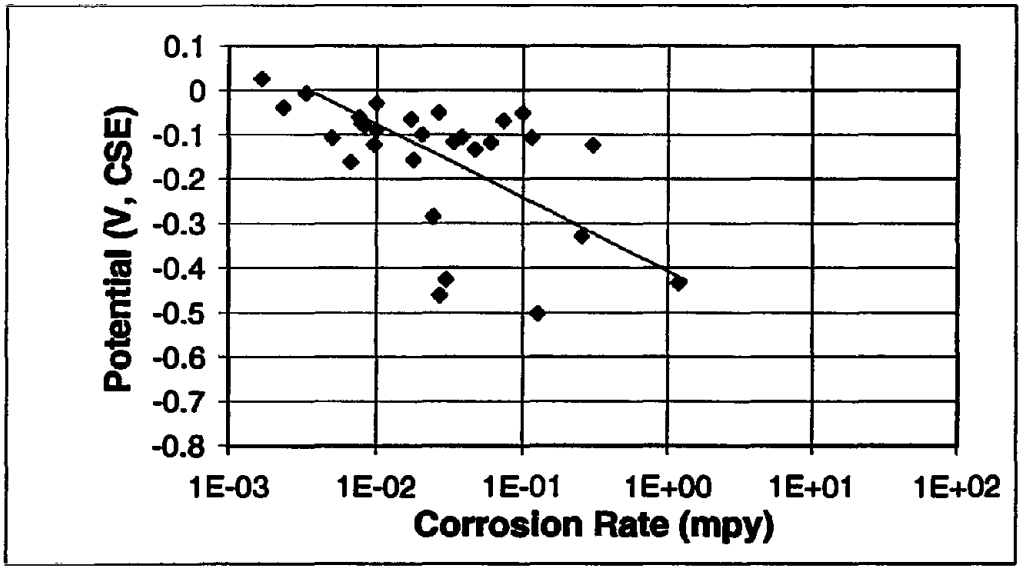

Figure 28a. Moderate environment data.

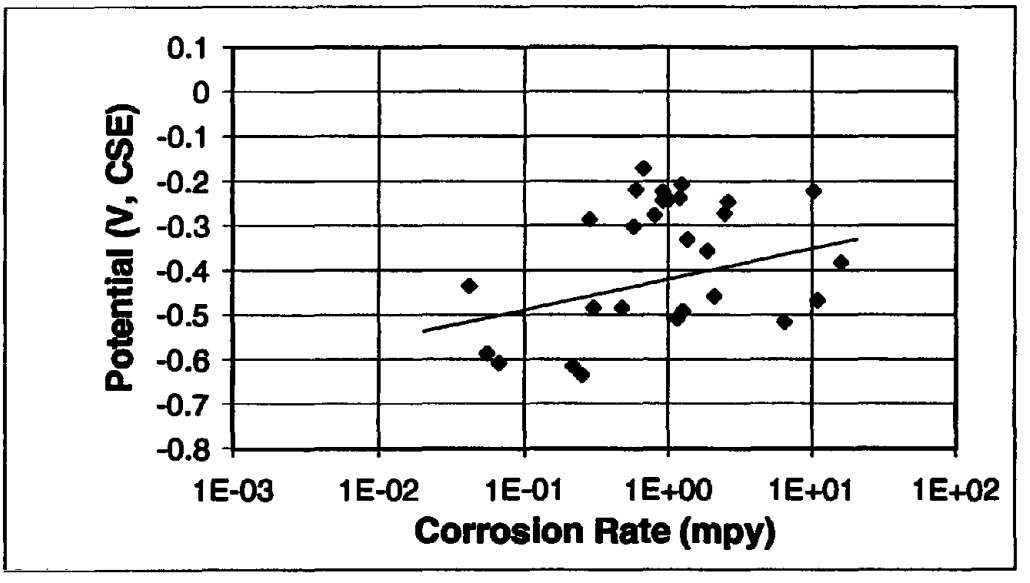

Figure 28b. Aggressive environment data.

Figure 28. Logarithm of corrosion rate versus potential for task B data.
Note: 1 mpy = 25.4 μm/yr

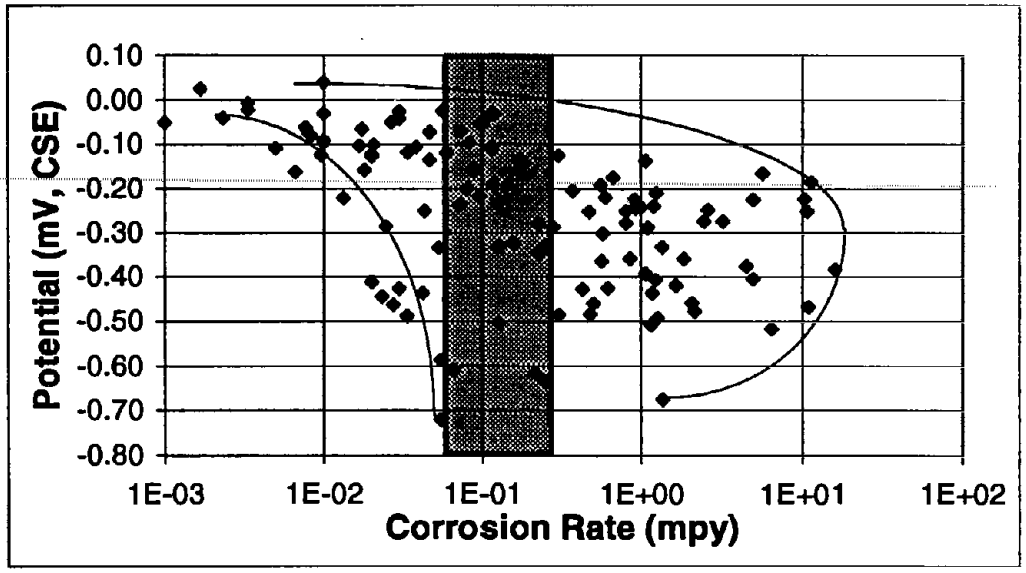

29a. Corrosion rates (minimal - intermediate - high).

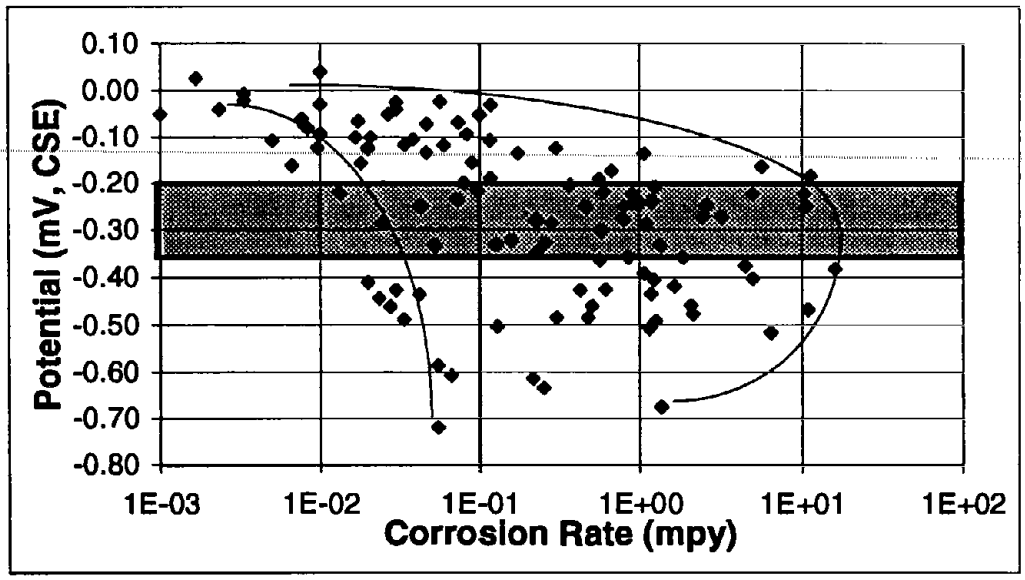

29b. Potential criteria for active corrosion.

Figure 29. Potential versus logarithm of corrosion rate for all data in tasks A and B.
Note: 1 mpy = 25.4 μm/yr

a. 1.3 µm/yr (0.05 mpy)

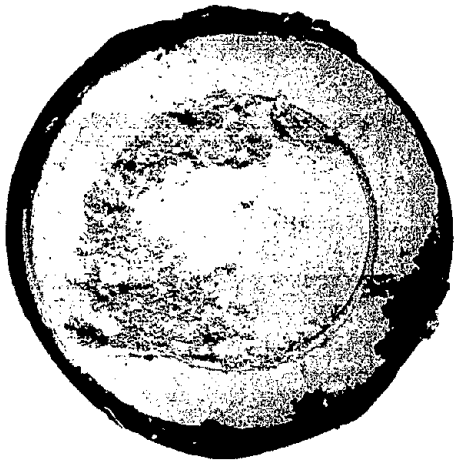

Mix 11 - 3

b. 7.1 µm/yr (0.28 mpy)

Mix 3 - 3

c. 305 µm/yr (12 mpy)

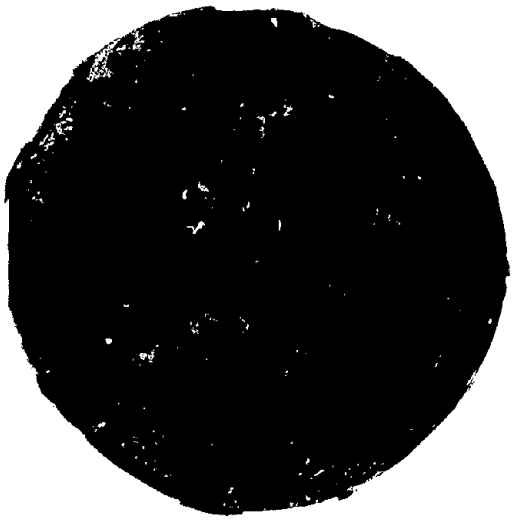

Mix 4 - 1

Figure 30. Photographs of typical corrosion in the aggressive environment in task B.

much as three orders of magnitude at a given potential depending on the concrete mix components and the environment.

The above discussion and data presented reflects on the use of a potential criterion for establishing corrosion behavior. This is important from a practical standpoint since the potential criterion is presently being used. The shaded area in figure 29b outlines the potential criterion in use based on ASTM no 876. The criterion states that at potentials more positive than the shaded area active (>-0.20V) corrosion is not likely and at potentials more negative than the shaded area (<-0.35V) active corrosion is likely. The data presented in figure 29b indicates that even at potentials between -0.10 and -0.20V active corrosion can be significant depending on the concrete mix components and the environment. At first glance, this suggests that the potential criterion may not be suitable. The fact that macrocells control corrosion in most concrete structures is critical to this analysis. The role of macrocells is to increase corrosion in the more negative potential areas and decrease corrosion in the more positive potential areas. This role of the macrocell tends to separate the corrosion process into anodic and cathodic sites based on potential. This makes the use of a potential criterion more applicable. In fact, experience indicates that the ASTM standard is applicable in many circumstances on concrete structures. However, the data presented here indicates that significant differences in corrosion rates are possible depending on the concrete components and the environment.

Rapid Chloride Permeability Versus Resistivity

A very strong correlation was found between rapid chloride permeability and 1/resistivity (0.60 for all data and 0.99 for portland cement data as a subset). Figure 31 shows rapid chloride permeability versus 1/resistivity for all of the portland cement data. This relationship is expected. Furthermore, the excellent agreement suggest that the resistivity test, which is easier to perform than the rapid chloride permeability test, has merit as a qualification test for concrete. This is the same conclusion that was reported by Arup et al. and Feldman et al. [62, 63]

OPTIMIZATION FOR CORROSION RESISTANCE

One of the required outputs for tasks A and B is to identify concretes for testing in task C and to select appropriate environments. Also, a final output to this project is a model for the selection of the most appropriate concrete for a particular application. At this stage of the project, it is desired to select a range of concretes that are expected to perform well and some that are expected to perform poorly in order to establish the predictive capability of tasks A and B. These concretes will be tested in the larger scale and longer term tests to be performed in task C. Two procedures were used for this purpose: (1) predictions based on the general linear main effect models established in task B and (2) selection of optimum concrete mixes from the test matrix of concretes tested in task B. By using some of the concretes from the

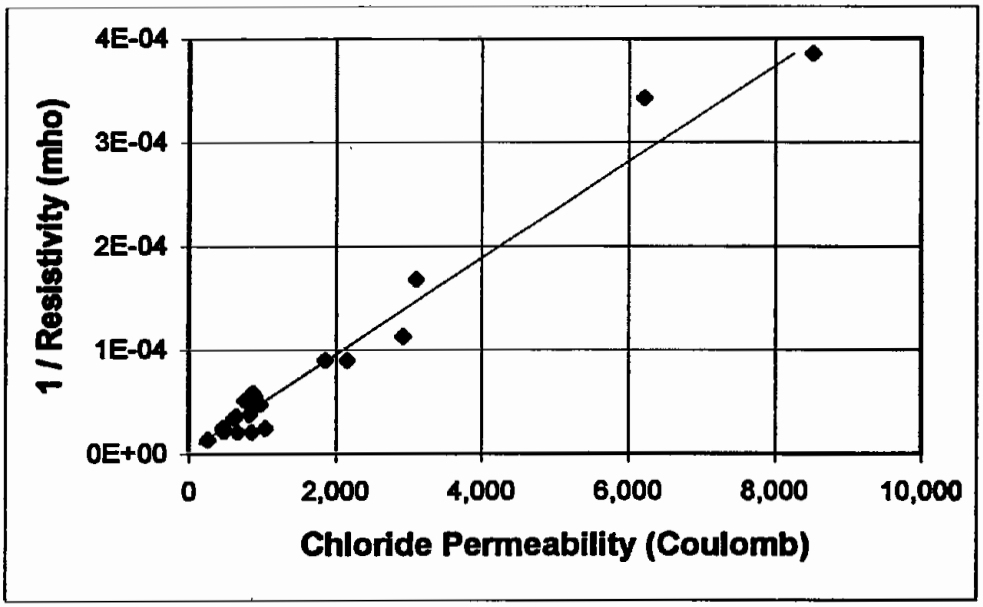

Figure 31. Chloride permeability versus 1 / resistivity.

task B matrix, a relationship can be established between (1) the performance based on the small cells used in task B and (2) the more realistic conditions and the longer exposure time used in task C. By using some concretes designed based on the prediction model, the prediction model itself will be evaluated.

Model Predictions

Concrete deterioration is characterized by three processes:

1. Chloride diffusion to the steel surface.
2. Corrosion of the steel.
3. Cracking/spalling damage to the concrete due to expanding corrosion products.

Chloride permeability was selected as the dependent variable that best describes the process of chloride diffusion. Corrosion rates in the moderate and aggressive environments were selected as the dependent variables that best describe the process of corrosion of steel. For rapid chloride permeability and corrosion rate, the general relationship to concrete deterioration is clear.

It is desirable to have a mechanical property that can be related to damage of the concrete by the mechanical forces developed during the corrosion of the reinforcing steel. Compressive strength was used in task B to characterize the mechanical properties of the concrete. However, no relationship exists between damage and any mechanical property. Developing such a relationship will be examined in task C of this project. In the discussion below, only the corrosion resistance properties of the concrete and rapid chloride permeability were used in the selection of concretes for further study.

Table 26 shows the model estimates for the following dependent variables: (1) corrosion rate in the moderate environment, (2) corrosion rate in the aggressive environment, and (3) rapid chloride permeability. The magnitude of the effect can be determined by adding the model estimate to the intercept value for that particular dependent variable. A negative estimate for a level indicates that the intercept value of the dependent variable would decrease by that amount and a positive estimate would increase the intercept value. To the right of the "Model Estimates," a qualitative ranking is provided entitled "Levels Ranked by Deterioration Resistance." Within each independent variable, the levels are ranked (based on the model estimates) in order of their qualitative concrete deterioration resistance, most resistance first. Based on the magnitude of the effect, an indication is given as to whether the independent variable had a significant effect or not and whether two or more levels produced similar effects. For example, changing the levels of the independent variable "air content" had no appreciable effect on the dependent variables "moderate environment corrosion rate" or "chloride permeability." For "aggressive environment corrosion rate," there was no appreciable difference in 5 or 8 percent air content, but 2 percent gave a higher corrosion rate.

Table 26. Levels of each independent variable ranked according to corrosion resistance for corrosion rate (moderate and aggressive environments) and rapid chloride permeability.

Independent Variable	Level	Model Estimates			Levels Ranked by Concrete Deterioration Resistance		
		Corrosion Rate Moderate Estimate (mpy)	Corrosion Rate Aggressive Estimate (mpy)	Chloride Permeability Estimate (Coulombs)	Corrosion Rate Moderate Estimate	Corrosion Rate Aggressive Estimate	Chloride Permeability Estimate
Intercept		0.426	4.523	3011			
Water-Cement Ratio	0.3	-0.050	-1.919	-1894	0.4	0.3	0.3
	0.4	-0.107	-1.067	-1255	0.3	0.4	0.4
	0.5	0.000	0.000	0	0.5	0.5	0.5
Air Content (%)	2	0.024	1.304	57		2	
	5	-0.066	0.114	199	↔	5	↔
	8	0.000	0.000	0		8	
Coarse Aggregate	Limestone	0.036	1.322	2177	↔	Quartz	Quartz
	Quartz	0.000	0.000	0		Limestone	Limestone
Fine Aggregate	Glacial Sand	0.175	2.186	1288	Quartz	Quartz	Quartz
	Quartz	0.000	0.000	0	Glacial Sand	Glacial Sand	Glacial Sand
Mineral Admixture	Silica Fume	-0.127	-4.109	-734	Silica	Silica	Silica
	None	-0.121	-2.035	2128	none	none	Class C FA
	Class C Fly Ash	-0.108	-0.292	-431	Class C FA	Class F FA	Slag
	GGBF Slag	0.000	0.000	0	Slag	Class C FA	Class F FA
	Class F Fly Ash	0.123	-1.444	1279	Class F FA	Slag	none
Cement Type	Type I Low C3A E	-0.404	-2.234	-3118	E	A	E
	Type I Low Alkali C	-0.373	-2.378	-2414	C	C	B
	Type I High C3A D	-0.371	-0.557	-1743	D	E	C
	Type I High Alkali A	-0.314	-2.385	-1430	A	D	D
	Lumnite B	-0.218	2.976	-2783	B	F	A
	Mag Phosphate F	0.000	0.000	0	F	B	F

| : No significant difference in magnitude of effect

↔ : Independent variable does not effect dependent variable.

Note : 1 mpy = 25.4 μm/yr

For the "moderate environment corrosion rate" dependent variable, cement types E, C, and D have similar effects on the value of corrosion rate, cements A and B are next, with cement F producing the highest corrosion rate. Cement F is also near the worst corrosion rate based on the "aggressive environment corrosion rate" variable and the worst rapid chloride permeability. Therefore the model would predict that cement F would provide the highest concrete deterioration of the cements tested when exposed to a chloride environment. Cement E is one of the best performers based on the three dependent variables given in table 26. Likewise, silica mineral admixture was the best performer of the admixtures based on all three dependent variables. Quartz aggregate was the best performer for both coarse and fine aggregates in improving concrete deterioration resistance.

The overall concrete deterioration resistance of cement A is somewhat more difficult to determine since it is the most corrosion resistant in the aggressive environment but has one of the highest chloride permeabilities. The good corrosion resistance might be explained by the high alkali content of cement A, but the overall performance of the concrete might be compromised by the higher chloride permeability. The same difficulty in evaluating the overall performance of "no (none) mineral admixture" is true. The condition of "no mineral admixture" was good for lowering corrosion rate (both environments), but produced the highest rapid chloride permeability.

Based on the model predictions, concretes can be designed that have a range of properties. Four concretes are shown in table 27 that were selected based on the model predictions. In these selections, air content was not considered as a critical variable since the magnitude of its effect was small. The following basis was used for selection:

1. Maximize concrete deterioration resistance.
2. Medium concrete deterioration resistance (medium corrosion rate - low rapid chloride permeability).
3. Medium concrete deterioration resistance (low corrosion rate - medium rapid chloride permeability).
4. Minimize concrete deterioration resistance.

Task B Test Matrix Optimization

In the above analysis, concretes were selected based on the model predictions of the statistical models. In this section, experimental data are used to rank the performance of the individual concretes tested in task B. The three dependent variables (chloride permeability, corrosion rate - moderate environment, corrosion rate - aggressive environment) used above in the model predictions are the same as used in this section to rank concretes based on the experimental data.

Table 27. Selection of task C concrete mix designs based on linear main-effect term model predictions.

Independent Variable	Level	Model Predictions			
		Maximize Concrete Deterioration Resistance	Medium Concrete Deterioration Resistance	Medium Concrete Deterioration Resistance	Minimize Concrete Deterioration Resistance
		Low CR-Mod Low CR-Agg Low Perm	Low CR-Mod Med CR-Agg Low Perm	Low CR-Mod Low CR-Agg Med Perm	High CR-Mod High CR-Agg High Perm
Water-Cement Ratio	0.3 0.4 0.5	0.3	0.4	0.4	0.4
Air Content (%)	2 5 8				
Coarse Aggregate	Limestone Quartz	Quartz	Quartz	Quartz	Limestone
Fine Aggregate	Glacial Sand Quartz	Quartz	Quartz	Quartz	Glacial Sand
Mineral Admixture	Silica Fume None Class C Fly Ash GGBF Slag Class F Fly Ash	Silica	Class C FA	None	Slag
Cement Type	Type I Low C3A E Type I Low Alkali C Type I High C3A D Type I High Alkali A Lumnite B Mag Phosphate F	E	C	E	D
Corrosion Rate - Moderate Prediction (mpy) :		-0.15	-0.16	-0.21	0.16
Corrosion Rate - Aggressive Prediction (mpy) :		-3.74	0.79	-0.81	6.41
Chloride Permeability Prediction (Coulombs) :		-2735	-1089	766	3478

Note : 1 mpy = 25.4 μm/yr
CR-Mod : Corrosion rate - moderate environment.
CR-Agg : Corrosion rate - aggressive environment.
Perm : Chloride permeability

An optimization equation to predict the concrete deterioration resistance can be based on any number of variables. In this analysis, three variables were selected: (1) chloride permeability, (2) corrosion rate - moderate environment, and (3) corrosion rate - aggressive environment. The critical component to this type of prediction model is how much weight is placed on each variable. The first step in optimizing for concrete deterioration resistance was to normalize the data using the following equation:

$$\text{Normalized Value} = (\text{Value} - \text{Minimum})/(\text{Maximum} - \text{Minimum}) \qquad (2)$$

This type of normalization is required to permit the handling of variables of different types, and it sets the range of each variable between 1 (maximum value) and 0 (minimum value). Once normalized, equations can be used to weight the importance of the dependent variables and a ranking of concrete deterioration resistance can be calculated simply by summing the normalized values times the weighting factor. The simple concrete deterioration resistance (CDR) equation used in this analysis was to give each of the three variables equal weighting. See the equation below:

$$\text{CDR} = (0.33 \times \text{Moderate CR}) + (0.33 \times \text{Aggressive CR}) + (0.33 \times \text{Permeability}) \qquad (3)$$

Other equations could be developed that weight permeability greater, but it was felt that the equal weightings given above would provide a good first estimate for ranking the task B concretes.

Table 28 gives the average and normalized values for the dependent variables, "corrosion rate - moderate environment," "corrosion rate - aggressive environment," "chloride permeability," and "compressive strength." Although compressive strength was not used in the equation to rank, or optimize, the concretes, it was included since it is desirable to have a range of compressive strengths in the concretes selected for task C testing. Table 28 also gives the results of the above equation used to rank the corrosion deterioration resistance. The data in table 28 was sorted based on the ranking, from best corrosion deterioration resistance to worst. Table 29 gives 14 concretes: 9 concretes that gave the best concrete deterioration resistance and 5 concretes that gave poor performance. One of the few observed trends is that all of the best nine performing concretes have a mineral additive. However, three of the five worst performing concretes also have a mineral admixture. Several of the concretes selected for examination in task C were based on the results shown in tables 28 and 29.

TASK C WORK PLAN

Task C has several goals, including:

1. Evaluate the mechanical aspect of the concrete deterioration resistance.
2. Provide input on the optimization models for estimating concrete deterioration resistance.

Table 28. Optimizing concrete deterioration resistance based on the mix designs tested in task B.

Concrete Mix	Average Values				Normalized Values				CDR Ranking*
	Moderate Corrosion Rate (mpy)	Aggressive Corrosion Rate (mpy)	Rapid Chloride Permeability (Coulombs)	Compressive Strength (psi)	Moderate Corrosion Rate (mpy)	Aggressive Corrosion Rate (mpy)	Rapid Chloride Permeability (Coulombs)	Compressive Strength (psi)	0.33 x Mod CR** Plus 0.33 x Agg CR*** Plus 0.33 x Perm****
11	0.01	0.04	645	7,150	0.01	0.00	0.03	0.51	0.014
18	0.03	0.67	230	10,065	0.03	0.04	0.00	0.77	0.022
30	0.02	0.06	850	10,785	0.02	0.00	0.05	0.83	0.023
3	0.01	0.59	605	8,870	0.00	0.03	0.03	0.66	0.023
24	0.00	0.57	863	9,435	0.00	0.03	0.05	0.71	0.029
10	0.02	1.15	299	8,040	0.01	0.07	0.01	0.59	0.030
5R	0.01	1.20	472	10,400	0.01	0.07	0.02	0.80	0.033
15R	0.05	0.48	663	6,490	0.04	0.03	0.04	0.45	0.034
1	0.07	0.47	460	12,650	0.06	0.03	0.02	1.00	0.036
23	0.04	0.28	1,037	10,035	0.03	0.01	0.07	0.77	0.038
9	0.01	1.00	965	7,560	0.01	0.06	0.06	0.55	0.043
6	0.01	1.26	893	11,690	0.00	0.08	0.05	0.91	0.045
26	0.01	1.24	888	5,755	0.01	0.08	0.05	0.39	0.045
12	0.02	1.35	759	5,975	0.02	0.08	0.04	0.41	0.048
16	0.01	2.09	438	7,965	0.01	0.13	0.02	0.58	0.050
28	0.11	0.91	260	10,590	0.10	0.05	0.00	0.82	0.051
2	0.10	0.80	815	7,635	0.08	0.05	0.05	0.55	0.060
25	0.03	1.86	1,059	3,625	0.02	0.11	0.07	0.20	0.069
8	0.13	0.07	1,486	4,710	0.11	0.00	0.10	0.29	0.071
27	0.00	0.91	2,149	6,590	0.00	0.05	0.16	0.46	0.071
13	0.00	0.25	2,933	10,960	0.00	0.01	0.22	0.85	0.079
7	0.03	0.22	2,854	9,110	0.02	0.01	0.22	0.68	0.083
19	0.03	2.48	1,854	7,200	0.02	0.15	0.13	0.51	0.103
17	0.06	2.61	3,111	5,725	0.05	0.16	0.24	0.38	0.149
29	0.01	0.30	8,520	5,175	0.01	0.02	0.69	0.33	0.235
21	0.30	6.46	981	7,125	0.25	0.40	0.06	0.51	0.239
22	0.02	10.26	6,218	8,800	0.01	0.64	0.49	0.66	0.382
4	0.25	16.01	539	5,090	0.21	1.00	0.03	0.33	0.413
20	1.18	10.93	12,332	1,425	1.00	0.68	1.00	0.00	0.893

Note : 1.0 mpy = 0.0254 mm per year.
Note : 1.0 psi = 6.89 kPa
*CDR : Corrosion deterioration resistance.
**CR-Mod : Corrosion rate - moderate environment.
***CR-Agg : Corrosion rate - aggressive environment.
****Perm : Chloride permeability

Table 29. Selection of task C concrete mix designs based on optimization of task B test matrix results.

Independent Variable	Level	Optimization of Task B Mix Designs										
		Maximize Concrete Deterioration Resistance	Maximize Concrete Deterioration Resistance	Maximize Concrete Deterioration Resistance	Maximize Concrete Deterioration Resistance	Maximize Concrete Deterioration Resistance	Maximize Concrete Deterioration Resistance	Maximize Concrete Deterioration Resistance	Maximize Concrete Deterioration Resistance	Minimize Concrete Deterioration Resistance	Minimize Concrete Deterioration Resistance	Minimize Concrete Deterioration Resistance
		Mix Design 11	Mix Design 18	Mix Design 30	Mix Design 15R	Mix Design 10	Mix Design 1	Mix Design 3	Mix Design 24	Mix Design 22	Mix Design 4	Mix Design 29
Water-Cement Ratio	0.3		0.3	0.3			0.3	0.3	0.3			
	0.4					0.4				0.4		
	0.5	0.5			0.5						0.5	0.5
Air Content (%)	2											
	5											
	8											
Coarse Aggregate	Limestone		Limestone						Limestone	Limestone		Limestone
	Quartz	Quartz		Quartz	Quartz	Quartz	Quartz	Quartz			Quartz	
Fine Aggregate	Glacial Sand				Glacial Sand			Glacial Sand		Glacial Sand		
	Quartz	Quartz	Quartz	Quartz		Quartz	Quartz		Quartz		Quartz	Quartz
Mineral Admixture	Silica Fume		Silica		Silica							
	None									None		None
	Class C Fly Ash					Class C FA	Class C FA	Class C FA				
	GGBF Slag								Slag		Slag	
	Class F Fly Ash	Class F FA		Class F FA								
Cement Type	Type I Low C3A E	E							E			
	Type I Low Alkali C				C			C				
	Type I High C3A D			D						D		
	Type I High Alkali A						A					A
	Lumnite B		B			B					B	
	Mag Phosphate F											
Corrosion Rate - Moderate Prediction (mpy) :		0.15	0.07	0.13	0.10	-0.01	-0.05	0.07	0.01	0.04	0.208	0.027
Corrosion Rate - Aggressive Prediction (mpy) :		0.85	2.79	1.16	0.22	6.14	-0.07	2.12	1.69	-0.15	7.499	1.425
Chloride Permeability Prediction (Coulombs) :		1172	-223	653	1151	-1458	-744	-440	176	5606	228	5686

Note : 1 mpy = 25.4 μm/yr
CR-Mod : Corrosion rate - moderate environment.
CR-Agg : Corrosion rate - aggressive environment.
Perm : Chloride permeability

3. Evaluate the accuracy of the prediction models developed in task B.
4. Evaluate the effect of macrocell couples on the corrosion rate predictions made in task B.
5. Provide longer term exposures than in tasks A and B.

The following is the task C work plan.

Test Specimen Design

Two types of specimens are used in the task C work. The standard specimen is used to evaluate the long-term corrosion performance of reinforcing steel in concrete. The repair/patch specimen is used to evaluate the corrosion performance of adjacent reinforcing steel in repair/patch material and chloride containing concrete.

Standard Specimen. The standard specimen used in the task C work for evaluating concrete materials is shown in figure 32. The sides of the specimen are coated with an epoxy. The concrete surface above reinforcing steel bars nos 1 and 2 is ponded with a 15 percent chloride solution. The concrete surface above reinforcing steel bars no 3 is ponded with deionized water. In this arrangement, concrete containing reinforcing steel bars nos 1 and 2 will become high chloride containing concrete compared to concrete containing reinforcing steel bar no 3. Therefore, a couple will be set up between reinforcing steel bars nos 2 and 3 when coupled together. The couple simulates top mat reinforcing steel or top-to-bottom mat reinforcing steel that have chloride gradients in the concrete. The ends of the reinforcing steel bars are coated with a coal tar epoxy coating to insulate the transition of the steel into the concrete specimen. This coating extends into the concrete by 38-mm (1.5 in). The cover of the concrete to the top of the reinforcing steel bar is 19-mm (0.75-in). The bottom of the concrete specimen will be left open to the atmosphere (no coating). This will promote drying of the concrete from the bottom, creating a moisture gradient from the top of the concrete specimen (ponded) to the bottom. It is expected that this will enhance chloride diffusion into the concrete.

Repair/Patch Specimens. The repair/patch specimens are similar to the standard specimens with the following exceptions. Chlorides will be mixed into the standard concrete to pre-contaminate the concrete with chlorides. This will create a corrosive environment for the reinforcing steel from the start of the test. A temporary partition will be placed in the mold so the standard concrete can be cast separate from the repair/patch concrete. The standard concrete will be poured first and allowed to set. The partition will be removed and the repair/patch concrete will be cast (see figure 33). The primary measurement will be between the reinforcing steel bars nos 1 and 2, repair/patch concrete and standard concrete containing chloride. The pond above these two reinforcing steel bars will be the chloride containing solution. Over time, the chloride concentration will increase in the repair/patch concrete and the pre-contaminated standard concrete.

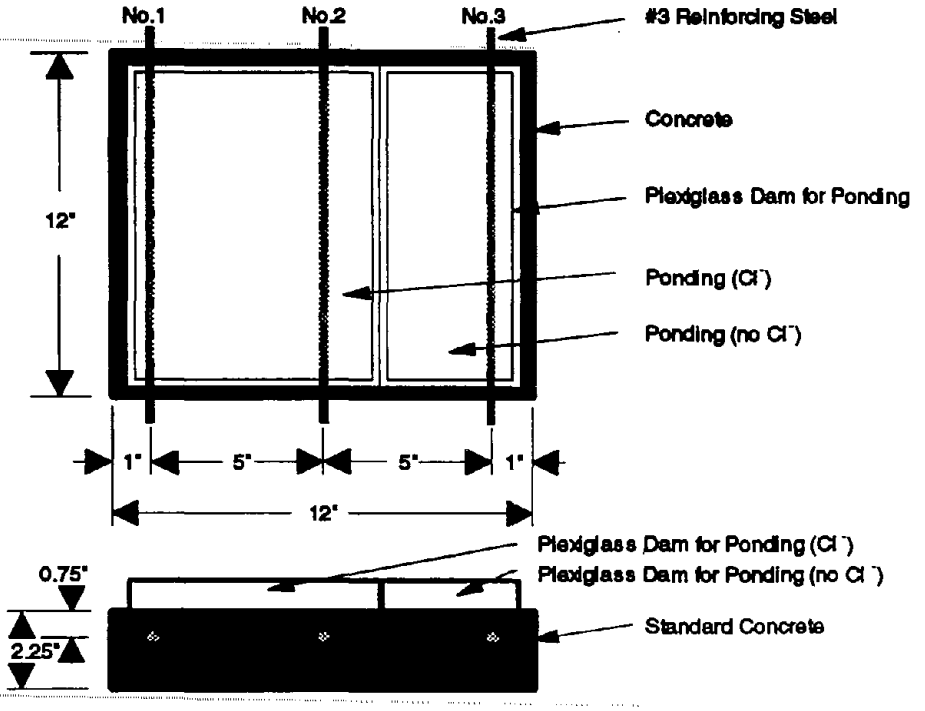

Figure 32. Standard concrete specimen used for task C long-term tests.

Standard Concretes

Ten concretes were selected to be examined in task C using the standard specimens (figure 32). Four repair/patch materials were selected (figure 33). Eight different concrete mixes were identified based on the task B work (nos 1, 3, 11, 15R, 22, 24, 29, and 31). The mix components for these concretes are shown in table 30. Concrete no 31 was not tested in task B, but is based on the results of the statistical model predictions. Concrete no 31 was selected to give the combination of lowest corrosion rates and chloride permeability.

Concretes nos 1, 3, 11, 15R, and 24 were selected to have good concrete deterioration resistance. Concretes nos 22 and 29 were selected to have poorer concrete deterioration resistance. The selections were based on optimization of the actual measured values.

In all 29 of the concretes tested in task B, the cement paste (total cementitious phases plus water) was maintained at 30 volume percent. The effect of variations in the cement paste content on (1) the rate on chloride ingress, (2) corrosion rate, and (3) rate of corrosion related distress will be evaluated in task C. To accomplish this, concrete no 1 (table 30) will be prepared at a cement paste content of 25 volume percent (concrete no 37) and 40 volume percent (concrete no 38). To achieve the desired cement paste content, the coarse and fine aggregates were varied in equal proportions.

Repair/Patch Concretes

Four repair/patch concretes are being examined using the specimen design shown in figure 33. These four concrete chemistries are shown in table 31 along with the standard concrete that has the chloride mixed-in (concrete no 13 from task B). One of the repair/patch concretes (concrete no 40) is a commercially available (magnesium phosphate cement - Master Builders Set-45). Repair concrete 41 is a typical repair/patch concrete using a calcium aluminate cement. Repair concretes nos 42 and 43 were selected based on the task B testing and analysis. These were concretes nos 1 and 31 and represent the concretes expected to have the best resistance to corrosion deterioration based on task B data. These mixes have the desired properties of a repair/patch material, low permeability and low corrosion rates. The low permeability (high resistivity) will minimize any macrocell couple effect. The standard concrete pre-contaminated with chlorides and used in the specimens for evaluating the repair/patch concretes will be mix no 13 from task B. Mix no 13 has intermediate values for corrosion rate and chloride permeability.

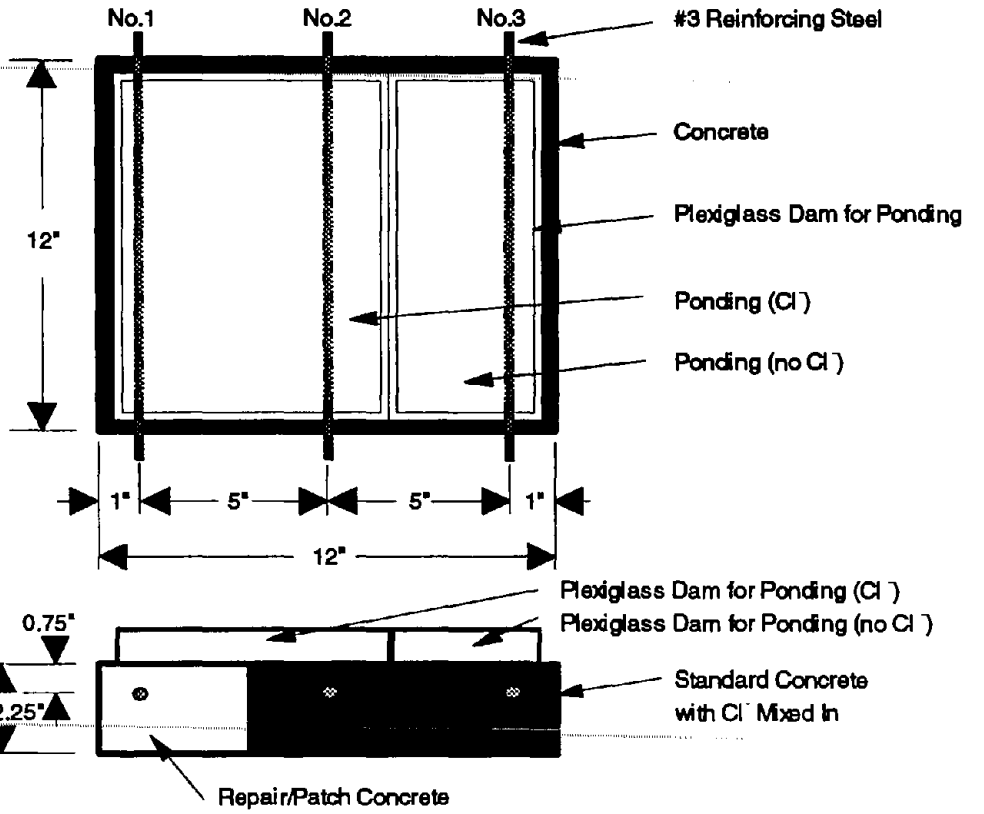

Figure 33. Repair/patch concrete specimen used for task C long-term tests.

Table 30. Concrete mix designs selected for task C concretes.

Independent Variable	Concretes									
	Mix Design 1	Mix Design 3	Mix Design 11	Mix Design 15R	Mix Design 22	Mix Design 24	Mix Design 29	Mix Design 31	Mix Design 37	Mix Design 38
Water-Cement Ratio	0.3	0.3	0.5	0.5	0.4	0.3	0.5	0.3	0.3	0.3
Air Content (%)	2	6	2	6	2	6	6	5	2	2
Coarse Aggregate	Quartz	Quartz	Quartz	Quartz	Limestone	Limestone	Limestone	Quartz	Quartz	Quartz
Fine Aggregate	Quartz	Glacial Sand	Quartz	Glacial Sand	Glacial Sand	Quartz	Quartz	Quartz	Quartz	Quartz
Mineral Admixture	Class C FA	Class C FA	Class F FA	Silica	None	Slag	None	Silica	Class C FA	Class C FA
Cement Type	A	C	E	C	D	E	A	E	A	A
Cement Paste %vol	30	30	30	30	30	30	30	30	25	40

A: Type I High Alkali
C: Type I Low Alkali
D: Type I High C_3A
E: Type I Low C_3A

Table 31. Repair/patch concrete mix designs selected for task C.

Independent Variable	Standard Concrete Chlorides Mixed In	Repair/Patch Concretes			
	Mix Design 13 (Task B)	Mix Design 40	Mix Design 41	Mix Design 42	Mix Design 43
Water-Cement Ratio	0.4	(*)	0.35	0.3	0.3
Air Content (%)	5	2	5	2	5
Coarse Aggregate	Quartz	Quartz	Quartz	Quartz	Quartz
Fine Aggregate	Quartz	p	Quartz	Quartz	Quartz
Mineral Admixture	none	p	none	Class C FA	Silica
Cement Type	C	Set-45	B	A	E
Cement Paste %vol	30	p	30	30	30

p: Proprietary
(*): 7.3% water based on dry Set-45.
A: Type I High Alkali
B: Calcium Aluminate Cement
C: Type I Low Alkali
E: Type I Low C_3A

Environment

For tasks A and B, chlorides were diffused into the concrete prior to exposure to the desired environment. The environment was controlled by constant temperature and constant relative humidity (external) exposure. No ponding was required during the test because the desired concentration of chlorides was achieved prior to the exposure. For task C a more conventional means of introducing chlorides into the concrete (i.e., ponding with a chloride solution, either cyclic or constant ponding) will be utilized. Ponding with chlorides makes external humidity control meaningless. For the task C tests, the conditions selected are 38 °C (100 °F) and 50 percent external relative humidity. The high temperature enhances both the corrosion rate of the reinforcing steel and the diffusion of chlorides into the concrete. The 50 percent relative humidity promotes drying of the exposed concrete that is not ponded or coated. When the concrete specimens are ponded, drying of the bottom of the concrete will enhance diffusion of the chlorides into the concrete by establishing a moisture gradient in the 57mm (2.25 in) thickness of the concrete specimen. When the specimens are not ponded, the low relative humidity will promote drying of the concrete that will enhance chloride ingress into the concrete during the ponding cycle.

Exposure

Eight concrete specimens are being cast for each standard concrete and repair/patch concrete to be examined in task C. These eight specimens will be divided into two groups for the purpose of exposures. The first group will undergo the following exposure (continuous ponding).

1. Cure for a minimum of 28 days in 100 percent humidity room.
2. Place in the 38 °C (100 °F) - 50 percent RH environment.
3. Pond continuously during exposure with a 15 percent NaCl solution.

In this exposure, the concrete will dry from the bottom setting up a moisture gradient that enhances the ingress of chlorides into the concrete. The internal relative humidity will be monitored during the exposure. It is expected that this exposure will provide a high internal relative humidity condition.

The second group of four specimens will undergo a cyclic ponding exposure.

1. Cure for a minimum of 28 days in 100 percent humidity room.
2. Dry such that 50 percent of the total free water is removed from the concrete.
3. Pond with 15 percent NaCl solution for 14 days.
4. Remove ponding solution and permit to dry for 7 days.
5. Continue to repeat ponding-drying cycle for the remaining exposure time.

This exposure is designed to provide a more severe environment for chloride ingress into the concrete by the cyclic wet-dry exposure. The length of the cycle was selected to permit monitoring of the corrosion activity during this cyclic exposure.

Also the length of the cycle and the low relative humidity of the external environment will permit drying of the concrete to greater depths, which is the key to enhancing chloride ingress into the concrete (based on tasks A and B and preliminary experiments using the resistivity depth meter described later in this report). It is expected that this exposure condition will be more severe than the constant ponding exposure from the standpoint of chloride ingress into the concrete. Also, cracking damage may be more severe in the cyclic exposure. Internal relative humidity will be monitored in these tests. It will be interesting to note how the internal relative humidity changes with respect to the cyclic exposure.

Measurements

Measurements will be divided into the following three categories: (1) rate of chloride ingress, (2) rate of corrosion, and (3) rate of corrosion-induced damage.

Rate of Chloride Ingress. The following measurements will be made.

1. Resistance versus depth as function of time will be performed using the devise shown in figure 34. The resistance versus depth device will permit resistance changes to be measured in 6.4mm (0.25 in) increments. Following some time to permit steady-state values to be achieved, changes in resistance will be related to the chloride ingress into the concrete matrix (end of ponding cycle) or to depth of drying (end of drying cycle). One specimen of each exposure condition of each concrete has been fitted with a resistance versus depth device.

2. Acid Soluble Chloride versus depth as function of time will be measured two to three times during the exposure period to calibrate the resistance versus depth device and provide an independent measure of chloride ingress. Measurements will be made on the same specimen that contains the resistance versus depth device. Chlorides concentrations will be measured at depths corresponding to the depths measured by the resistance versus depth device.

3. Resistivity of the concrete will be measured following 1-, 7-, 28-day, 3-, 6-, 12-, 18-, and 24-month exposures at 100-percent humidity. These measurements are performed on small cup samples specially designed for a two pin resistivity measurement.

Rate of Corrosion. The following measurements will be made.

1. Coupled current measurements will be made between steel specimens nos 2 and 3 (standard specimens, figure 32) or nos 1 and 2 (repair/patch specimens, figure 33). Coupled currents will be measured using a data acquisition system on a daily basis for the task C tests.

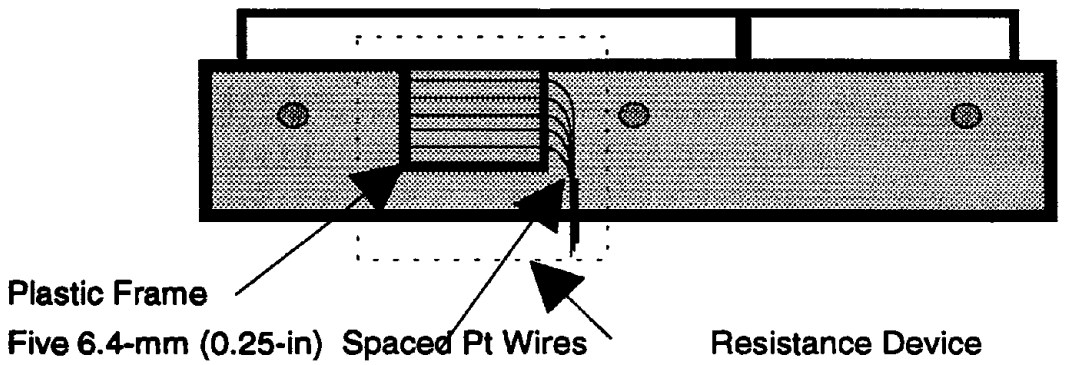

Figure 34. Resistance versus depth device.

2. Linear polarization resistance (LPR) measurements will be made for specimens nos 1, 2 and 3 (uncoupled) for both specimen types (standard and repair/patch). Solution resistance correction will be made and measurements will be performed periodically based on the results of the coupled current measurements. A three electrode technique will be performed using a $Cu/CuSO_4$ (CCS) reference electrode and a platinum counter electrode. For the cyclic tests, measurements will be performed during both the wet and dry cycle.

3. Potential measurements will be made with respect to a CCS reference electrode performed in conjunction with the LPR measurements.

Rate of Corrosion-Induced Damage. The following measurements will be made to characterize the mechanical properties of the concretes (which may in-turn be related to damage) and to measure damage directly.

1. Compressive strength will be measured on 102- by 203-mm (4- by 8-in) cylinders following 28-day, 6-, 12-, and 24-month exposures at 100-percent humidity.

2. Modulus of elasticity will be measured on 102- by 203-mm (4- by 8-in) cylinders following 28-day, 6-, 12-, and 24-month exposures at 100-percent humidity.

3. Flexural strength will be measured on 102- by 102- by 356-mm (4- by 4- by 14-in) beams following 28-day, 6-, 12-, and 24-month exposures at 100-percent humidity.

4. Permeable void volume (ASTM 642) will be measured on 102- by 102- by 356-mm (4- by 4- by 14-in) beams following 28-day, 6-, 12-, and 24-month exposures at 100-percent humidity.

5. An ultrasonic pulse velocity measurement technique will be performed on the exposed concrete slabs to assess the onset and extent of damage in the concrete. Measurements will be performed on a similar frequency as the LPR measurements.

Concrete Chemistry

Efforts will be made to correlate chloride ingress, corrosion rate, and damage rate with chemical and mineralogical properties of the concretes. To accomplish this, the following measurements will be made.

1. pH of the concrete specimens undergoing corrosion exposure (at the reinforcing steel depth) will be measured periodically using the same specimen that is used for chloride measurements.

2. Petrographic analysis (ASTM C856) will be performed on selected specimens at 12- and 24-month exposures.

3. Chemical/ mineralogical characterization will be performed on selected specimens at 12- and 24-month exposures.

APPENDIX - A
Test Matrices For Task A

Test matrix for mortar A2 and conventional reinforcing steel.

Concrete	Cell	Temp		Relative Humidity	Chlorides	
		(F)	(C)	(%)	(lb/yd³)	(Kg/m³)
A2	48	40	4	43	1	0.6
A2	10	40	4	43	1	0.6
A2	11	40	4	43	1	0.6
A2	na	70	21	43	1	0.6
A2	na	70	21	43	1	0.6
A2	3	70	21	43	1	0.6
A2	55	100	38	43	1	0.6
A2	57	100	38	43	1	0.6
A2	56	100	38	43	1	0.6
A2	51	40	4	75	1	0.6
A2	49	40	4	75	1	0.6
A2	50	40	4	75	1	0.6
A2	4	70	21	75	1	0.6
A2	5	70	21	75	1	0.6
A2	6	70	21	75	1	0.6
A2	59	100	38	75	1	0.6
A2	58	100	38	75	1	0.6
A2	60	100	38	75	1	0.6
A2	53	40	4	98	1	0.6
A2	54	40	4	98	1	0.6
A2	52	40	4	98	1	0.6
A2	7	70	21	98	1	0.6
A2	8	70	21	98	1	0.6
A2	9	70	21	98	1	0.6
A2	61	100	38	98	1	0.6
A2	62	100	38	98	1	0.6
A2	63	100	38	98	1	0.6
A2	65	40	4	43	3	1.8
A2	64	40	4	43	3	1.8
A2	66	40	4	43	3	1.8
A2	74	70	21	43	3	1.8
A2	73	70	21	43	3	1.8
A2	75	70	21	43	3	1.8
A2	83	100	38	43	3	1.8
A2	84	100	38	43	3	1.8
A2	85	100	38	43	3	1.8
A2	68	40	4	75	3	1.8
A2	69	40	4	75	3	1.8
A2	67	40	4	75	3	1.8
A2	77	70	21	75	3	1.8
A2	78	70	21	75	3	1.8
A2	79	70	21	75	3	1.8
A2	86	100	38	75	3	1.8
A2	87	100	38	75	3	1.8
A2	88	100	38	75	3	1.8
A2	72	40	4	98	3	1.8
A2	71	40	4	98	3	1.8
A2	70	40	4	98	3	1.8
A2	80	70	21	98	3	1.8
A2	81	70	21	98	3	1.8
A2	82	70	21	98	3	1.8
A2	89	100	38	98	3	1.8
A2	91	100	38	98	3	1.8
A2	90	100	38	98	3	1.8
A2	92	40	4	43	10	6
A2	94	40	4	43	10	6
A2	93	40	4	43	10	6
A2	101	70	21	43	10	6
A2	102	70	21	43	10	6
A2	103	70	21	43	10	6
A2	111	100	38	43	10	6
A2	112	100	38	43	10	6
A2	110	100	38	43	10	6
A2	95	40	4	75	10	6
A2	97	40	4	75	10	6
A2	96	40	4	75	10	6
A2	104	70	21	75	10	6
A2	105	70	21	75	10	6
A2	106	70	21	75	10	6
A2	115	100	38	75	10	6
A2	114	100	38	75	10	6
A2	113	100	38	75	10	6
A2	99	40	4	98	10	6
A2	98	40	4	98	10	6
A2	100	40	4	98	10	6
A2	109	70	21	98	10	6
A2	108	70	21	98	10	6
A2	107	70	21	98	10	6
A2	117	100	38	98	10	6
A2	116	100	38	98	10	6
A2	118	100	38	98	10	6

Test matrix for mortar B2 and conventional reinforcing steel.

Concrete	Cell	Temp		Relative Humidity	Chlorides	
		(F)	(C)	(%)	(lb/yd^3)	(Kg/m^3)
B2	43	40	4	43	1	0.6
B2	44	40	4	43	1	0.6
B2	45	40	4	43	1	0.6
B2	54	70	21	43	1	0.6
B2	55	70	21	43	1	0.6
B2	56	70	21	43	1	0.6
B2	61	100	38	43	1	0.6
B2	62	100	38	43	1	0.6
B2	63	100	38	43	1	0.6
B2	40	40	4	75	1	0.6
B2	41	40	4	75	1	0.6
B2	42	40	4	75	1	0.6
B2	49	70	21	75	1	0.6
B2	50	70	21	75	1	0.6
B2	51	70	21	75	1	0.6
B2	58	100	38	75	1	0.6
B2	59	100	38	75	1	0.6
B2	60	100	38	75	1	0.6
B2	37	40	4	98	1	0.6
B2	38	40	4	98	1	0.6
B2	39	40	4	98	1	0.6
B2	46	70	21	98	1	0.6
B2	47	70	21	98	1	0.6
B2	48	70	21	98	1	0.6
B2	52	100	38	98	1	0.6
B2	53	100	38	98	1	0.6
B2	57	100	38	98	1	0.6
B2	70	40	4	43	3	1.8
B2	71	40	4	43	3	1.8
B2	72	40	4	43	3	1.8
B2	79	70	21	43	3	1.8
B2	80	70	21	43	3	1.8
B2	81	70	21	43	3	1.8
B2	88	100	38	43	3	1.8
B2	89	100	38	43	3	1.8
B2	90	100	38	43	3	1.8
B2	66	40	4	75	3	1.8
B2	68	40	4	75	3	1.8
B2	69	40	4	75	3	1.8
B2	76	70	21	75	3	1.8
B2	77	70	21	75	3	1.8
B2	78	70	21	75	3	1.6
B2	85	100	38	75	3	1.8
B2	86	100	38	75	3	1.8
B2	87	100	38	75	3	1.8
B2	64	40	4	98	3	1.8
B2	65	40	4	98	3	1.8
B2	67	40	4	98	3	1.8
B2	73	70	21	98	3	1.8
B2	74	70	21	98	3	1.6
B2	75	70	21	98	3	1.8
B2	82	100	38	98	3	1.8
B2	83	100	38	98	3	1.8
B2	84	100	38	98	3	1.8
B2	99	40	4	43	10	6
B2	100	40	4	43	10	6
B2	101	40	4	43	10	6
B2	108	70	21	43	10	6
B2	109	70	21	43	10	6
B2	110	70	21	43	10	6
B2	117	100	38	43	10	6
B2	118	100	38	43	10	6
B2	96	40	4	75	10	6
B2	97	40	4	75	10	6
B2	98	40	4	75	10	6
B2	105	70	21	75	10	8
B2	106	70	21	75	10	6
B2	107	70	21	75	10	6
B2	114	100	38	75	10	6
B2	115	100	38	75	10	6
B2	116	100	38	75	10	6
B2	93	40	4	98	10	6
B2	94	40	4	98	10	6
B2	95	40	4	98	10	6
B2	102	70	21	98	10	6
B2	103	70	21	98	10	6
B2	104	70	21	98	10	6
B2	111	100	38	98	10	6
B2	112	100	38	98	10	6
B2	113	100	38	98	10	6
B2	113b	100	38	98	10	6

Test matrix for concrete A5 and conventional reinforcing steel.

Concrete	Cell	Temp		Relative Humidity	Chlorides	
		(F)	(C)	(%)	(lb/yd³)	(Kg/m³)
A5	10	70	21	75	1	0.6
A5	11	70	21	75	1	0.6
A5	12	70	21	75	1	0.6
A5	13	70	21	98	1	0.6
A5	14	70	21	98	1	0.6
A5	15	70	21	98	1	0.6
A5	16	70	21	75	3	1.8
A5	17	70	21	75	3	1.8
A5	18	70	21	75	3	1.8
A5	19	70	21	98	3	1.8
A5	20	70	21	98	3	1.8
A5	21	70	21	98	3	1.8
A5	22	70	21	75	10	6
A5	23	70	21	75	10	6
A5	24	70	21	75	10	6
A5	25	70	21	98	10	6
A5	26	70	21	98	10	6
A5	27	70	21	98	10	6

Test matrix for mortar A2-PST and prestressing steel tendons.

Concrete	Cell	Temp		Relative Humidity	Chlorides	
		(F)	(C)	(%)	(lb/yd³)	(Kg/m³)
A2 PST	1	70	21	75	1	0.6
A2 PST	2	70	21	75	1	0.6
A2 PST	3	70	21	75	1	0.6
A2 PST	4	70	21	98	1	0.6
A2 PST	5	70	21	98	1	0.6
A2 PST	6	70	21	98	1	0.6
A2 PST	7	70	21	75	3	1.6
A2 PST	8	70	21	75	3	1.8
A2 PST	9	70	21	75	3	1.8
A2 PST	10	70	21	98	3	1.8
A2 PST	11	70	21	98	3	1.8
A2 PST	12	70	21	98	3	1.8
A2 PST	13	70	21	75	10	6
A2 PST	14	70	21	75	10	6
A2 PST	15	70	21	75	10	6
A2 PST	16	70	21	98	10	6
A2 PST	17	70	21	98	10	6
A2 PST	18	70	21	98	10	6

APPENDIX -B
Concrete Property Data

Table 32. Rapid chloride permeability measurements on 51-mm (2-in) thick portion of 102-mm (4-in) diameter by 203-mm (8-in) long cylinder specimens prepared from experimental concretes on the FHWA project (DTFH61-92-R-00137)

Specimen Identification Number	Cementitious Matrix	Coarse Aggregate	Water-Cement Ratio	Rapid Chloride Permeability, Coulombs	
				28-Days	90-Days
				Average	Average
1	Type I Portland Cement, High Alkali Content	Quartz	0.3	871	460
2	Type I Portland Cement, High Alkali Content	Limestone	0.3	2349	815
3	Type I Portland Cement, Low Alkali Content + Class C Flyash	Quartz	0.3	1695	605
4	Calcium Aluminate Cement + GGBF Slag	Quartz	0.5	2116	539
5R	Type I Portland Cement, High C_3A Content + Microsilica	Quartz	0.5	863	472
6	Type I Portland Cement, Low C_3A Content	Quartz	0.3	1274	893
7	Magnesium Phosphate Cement + Microsilica	Quartz	0.4	5796	2854
8	Magnesium Phosphate Cement	Quartz	0.5	2457	1486
9	Type I Portland Cement, High C_3A Content + GGBF Slag	Quartz	0.4	2353	965
10	Calcium Aluminate Cement + Class C Flyash	Quartz	0.4	512	299
11	Type I Portland Cement, Low C_3A + Class F Flyash	Quartz	0.5	3325	645
12	Type I Portland Cement, Low C_3A + Microsilica	Limestone	0.4	1081	759
13	Type I Portland Cement, Low Alkali Content	Quartz	0.4	3728	2933
15R	Type I Portland Cement, Low Alkali Content + Microsilica	Quartz	0.5	1353	663
16	Calcium Aluminate Cement	Quartz	0.3	701	438
17	Type I Portland Cement, High C_3A Content + Class C Flyash	Limestone	0.5	8656	3111
18	Calcium Aluminate Cement + Microsilica	Limestone	0.3	462	230

Table 32. Rapid chloride permeability measurements on 51-mm (2-in) thick portion of 102-mm (4-in) diameter by 203-mm (8-in) long cylinder specimens prepared from experimental concretes on the FHWA project (DTFH61-92-R-00137) **(Continued)**

Specimen Identification Number	Cementitious Matrix	Coarse Aggregate	Water-Cement Ratio	Rapid Chloride Permeability, Coulombs	
				28-Days	90-Days
				Average	Average
19	Type I Portland Cement, Low Alkali Content + GGBF Slag	Limestone	0.5	4027	1854
20	Magnesium Phosphate Cement + Class F Flyash	Limestone	0.5	13,164	12,332
21	Calcium Aluminate Cement + Class F Flyash	Quartz	0.4	1090	981
22	Type I Portland Cement, High C_3A Content	Limestone	0.4	8202	6218
23	Type I Portland Cement, High Alkali Content + GGBF Slag	Quartz	0.4	826	1037
24	Type I Portland Cement, Low C_3A Content + GGBF Slag	Limestone	0.3	1132	863
25	Magnesium Phosphate Cement + Class C Flyash	Limestone	0.4	3008	1059
26	Type I Portland Cement, Low C_3A Content + Class C Flyash	Quartz	0.5	3533	888
27	Type I Portland Cement, Low Alkali Content + Class F Flyash	Limestone	0.4	6757	2149
28	Type I Portland Cement, High Alkali Content + Microsilica	Quartz	0.4	338	260
29	Type I Portland Cement, High Alkali Content	Limestone	0.5	11,272	8520
30	Type I Portland Cement, High C_3A Content +	Quartz	0.3	4958	850

* Per AASHTO Designation T277-83, The Standard Method of Test For Rapid Determination of the Chloride Permeability of Concrete To Be Determined

(a) Vacuum Saturated
(b) 24 Hour H_2O soak

Table 33. Compressive strength measurements on 51-mm (2-in) cubes prepared from experimental concretes on the FHWA Project on (DTFH61-92-R-00137)

Specimen Identification Number	Cementitious Matrix	Coarse Aggregate	Water-Cement Ratio	Compressive Strength, psi			
				7-Days	28-Days	90-Days	365-Days
				Average	Average	Average	Average
1	Type I Portland Cement, High Alkali Content	Quartz	0.3	9365	11,340	12,650	TBD
2	Type I Portland Cement, High Alkali Content	Limestone	0.3	4650	6715	7635	TBD
3	Type I Portland Cement, Low Alkali Content + Class C Flyash	Quartz	0.3	7300	8965	8865	TBD
4	Calcium Aluminate Cement + GGBF Slag	Quartz	0.5	4240	4300	5090	TBD
5R	Type I Portland Cement, High C_3A Content + Microsilica	Quartz	0.5	7060	9890	10,400	TBD
6	Type I Portland Cement, Low C_3A Content	Quartz	0.3	9810	12,010	11,690	TBD
7	Magnesium Phosphate Cement + Microsilica	Quartz	0.4	3810	5335	9110	TBD
8	Magnesium Phosphate Cement	Quartz	0.5	2785	3790	4710	TBD
9	Type I Portland Cement, High C_3A Content + GGBF Slag	Quartz	0.4	4260	6875	7560	TBD
10	Calcium Aluminate Cement + Class C Flyash	Quartz	0.4	6335	8465	8040	TBD
11	Type I Portland Cement, Low C_3A + Class F Flyash	Quartz	0.5	3725	5240	7150	TBD
12	Type I Portland Cement, Low C_3A + Microsilica	Limestone	0.4	4500	5615	5975	TBD
13	Type I Portland Cement, Low Alkali Content	Quartz	0.4	8050	10,135	10,960	TBD
15R	Type I Portland Cement, Low Alkali Content + Microsilica	Quartz	0.5	4540	6335	6490	TBD
16	Calcium Aluminate Cement	Quartz	0.3	5875	7215	7965	TBD

Table 33. Compressive strength measurements on 51-mm (2-in) cubes prepared from experimental concretes on the FHWA Project on (DTFH61-92-R-00137) (**Continued**)

Specimen Identification Number	Cementitious Matrix	Coarse Aggregate	Water-Cement Ratio	Compressive Strength, psi			
				7-Days	28-Days	90-Days	365-Days
				Average	Average	Average	Average
17	Type I Portland Cement, High C_3A Content + Class C Flyash	Limestone	0.5	3790	5190	5725	TBD
18	Calcium Aluminate Cement + Microsilica	Limestone	0.3	6700	8765	10,065	TBD
19	Type I Portland Cement, Low Alkali Content + GGBF Slag	Limestone	0.5	3440	6110	7200	TBD
20	Magnesium Phosphate Cement + Class F Flyash	Limestone	0.5	685	910	1425	TBD
21	Calcium Aluminate Cement + Class F Flyash	Quartz	0.4	6440	6740	7125	TBD
22	Type I Portland Cement, High C_3A Content	Limestone	0.4	7460	8290	8800	TBD
23	Type I Portland Cement, High Alkali Content + GGBF Slag	Quartz	0.4	7025	9050	10,035	TBD
24	Type I Portland Cement, Low C_3A Content + GGBF Slag	Limestone	0.3	6765	8450	9435	TBD
25	Magnesium Phosphate Cement _ Class C Flyash	Limestone	0.4	1585	2750	3625	TBD
26	Type I Portland Cement, Low C_3A Content + Class C Flyash	Quartz	0.5	3200	4500	5755	TBD
27	Type I Portland Cement, Low Alkali Content + Class F Flyash	Limestone	0.4	3515	4750	6590	TBD
28	Type I Portland Cement, High Alkali Content + Microsilica	Quartz	0.4	9140	10,290	10,590	TBD
29	Type I Portland Cement, High Alkali Content	Limestone	0.5	4035	4715	5175	TBD
30	Type I Portland Cement, High C_3A Content + Class F Flyash	Quartz	0.3	7390	9500	10,785	TBD

*TBD = To Be Determined

Table 34. Electrical resistivity measurements on experimental concretes: FHWA project (DTFH61-92-R-00137)

Concrete No.	Electrical Resistivity					
	1-Day	7-Days	28-Days	90-Days	180-Days	365-Days
	Ohm•cm	Ohm•cm	Ohm•cm	Ohm•cm	Ohm•cm	Ohm•c
1	1850	9465	20,165	40,330	82,305	TBD
2	615	3045	7821	26,750	61,730	TBD
3	2490	7035	13,580	29,425	57,615	TBD
4	9875	16,255	16,460	31,685	44,445	TBD
5Rb	1380	4035	28,190	47,325	43,210	36,625
6b	5350	12345	15,430	18,150	21,195	TBD
7	2200	4485	9465	189,300	368,310	TBD
8	1315	2100	9260	57,615	905,350	TBD
9	1480	4525	11,730	21,195	27,160	26,750
10	1730	102,880	187,245	226,335	14,405	TBD
11b	3250	4525	9055	27,985	55,555	94,650
12b	1810	5350	16,460	19,755	20,780	TBD
13	3785	7405	8435	8850	9,055	9,260
15Rb	2595	5145	29,220	49,385	51,400	TBD
16b	25,100	53,500	106,995	185,185	226,340	TBD
17	1400	1810	3130	5965	8,850	14,200
18b	24,895	65,845	113,170	197,530	294,240	TBD
19	2430	3130	6585	11,100	13,170	15,225
20	1235	1440	2800	23,455	2,551,440	TBD
21b	27,900	42,385	36,420	34,980	51,400	TBD
22	1645	2345	2595	2920	3,705	TBD
23	1315	10,290	23,870	41,150	53,500	TBD
24b	1995	6585	13,990	17,285	20,575	TBD
25	1175	1255	16,870	41,975	115,225	261,315
26b	2160	4320	9465	22,840	34,155	TBD

Table 34. Electrical resistivity measurements on experimental concretes: FHWA project (DTFH61-92-R-00137) **(Continued)**

Concrete No.	Electrical Resistivity					
	1-Day	7-Days	28-Days	90-Days	180-Days	365-Days
	Ohm•cm	Ohm•cm	Ohm•cm	Ohm•cm	Ohm•cm	Ohm•c
27	2430	3990	4735	11,110	18,520	TBD
28	1500	15,845	67,900	76,130	76,132	TBD
29	965	2100	2595	2595	41,150	TBD
30	945	5760	11,935	49,385	117,285	TBD

APPENDIX - C
Statistical Analysis Data Sheets For Task B

90-Day Rapid Chloride Permeability

General Linear Models Procedure
Class Level Information

Class	Levels	Values
W_C	3	0.3 0.4 0.5
AIR	3	2 5 8
COARSE	2	LS Q
FINE	2	G Q
MINERAL	5	FA_C FA_F MS None Slag
CEMENT	6	A B C D E F

Number of observations in data set = 58
General Linear Models Procedure

Dependent Variable: CL90

Source	DF	Sum of Squares	Mean Square	F Value	Pr > F
Model	15	266937599.20279000	17795839.94685260	5.14	0.0001
Error	42	145403915.14203700	3461997.97957232		
Corrected Total	57	412341514.34482700			

R-Square	C.V.	Root MSE	CL90 Mean
0.647370	97.80263	1860.64450650	1902.44827586

Source	DF	Type III SS	Mean Square	F Value	Pr > F
W_C	2	29984887.81392110	14992443.90696050	4.33	0.0195
AIR	2	373059.72255424	186529.86127712	0.05	0.9476
COARSE	1	59622026.44894130	59622026.44894130	17.22	0.0002
FINE	1	19721979.00154500	19721979.00154500	5.70	0.0216
MINERAL	4	67873182.72429340	16968295.68107330	4.90	0.0025
CEMENT	5	46540908.01008710	9308181.60201742	2.69	0.0339

Parameter		Estimate	T for H0: Parameter=0	Pr > |T|	Std Error of Estimate
INTERCEPT		3010.771530 B	2.77	0.0083	1086.744270
W_C	0.3	-1893.597274 B	-2.78	0.0081	680.747057
	0.4	-1255.088170 B	-2.12	0.0403	593.115200
	0.5	0.000000 B	.	.	.
AIR	2	57.115391 B	0.09	0.9301	646.982914
	5	199.108284 B	0.32	0.7526	627.535534
	8	0.000000 B	.	.	.
COARSE	LS	2177.162083 B	4.15	0.0002	524.627197
	Q	0.000000 B	.	.	.
FINE	G	1287.644202 B	2.39	0.0216	539.490791
	Q	0.000000 B	.	.	.
MINERAL	FA_C	-430.846342 B	-0.51	0.6115	841.997617
	FA_F	1279.382631 B	1.54	0.1321	833.131010
	MS	-734.931192 B	-0.89	0.3812	830.394481
	None	2128.177692 B	2.58	0.0135	825.249980
	Slag	0.000000 B	.	.	.
CEMENT	A	-1430.144237 B	-1.51	0.1393	948.998625
	B	-2783.832055 B	-2.85	0.0067	976.501976
	C	-2414.762270 B	-2.60	0.0128	928.823519
	D	-1743.785348 B	-1.90	0.0647	919.022079
	E	-3118.360449 B	-3.25	0.0023	960.185021
	F	0.000000 B	.	.	.

NOTE: The X'X matrix has been found to be singular and a generalized inverse was used to solve the normal equations. Estimates followed by the letter 'B' are biased, and are not unique estimators of the parameters.

90-Day Rapid Chloride Permeability

General Linear Models Procedure
Least Squares Means

W_C	CL90 LSMEAN	T for H0: LSMEAN(i)=LSMEAN(j) / Pr > |T| i/j	1	2	3
0.3	1468.19445	1	.	-0.95219	-2.78165
				0.3464	0.0081
0.4	2106.70356	2	0.952188	.	-2.1161
			0.3464		0.0403
0.5	3361.79173	3	2.781646	2.116095	.
			0.0081	0.0403	

AIR	CL90 LSMEAN	T for H0: LSMEAN(i)=LSMEAN(j) / Pr > |T| i/j	1	2	3
2	2283.93741	1	.	-0.2243	0.08828
				0.8236	0.9301
5	2425.93031	2	0.224304	.	0.317286
			0.8236		0.7526
8	2226.82202	3	-0.08828	-0.31729	.
			0.9301	0.7526	

COARSE	CL90 LSMEAN	T / Pr > |T| H0: LSMEAN1=LSMEAN2
LS	3400.81095	4.149922
		0.0002
Q	1223.64887	

FINE	CL90 LSMEAN	T / Pr > |T| H0: LSMEAN1=LSMEAN2
G	2956.05201	2.386777
		0.0216
Q	1668.40781	

MINERAL	CL90 LSMEAN	T for H0: LSMEAN(i)=LSMEAN(j) / Pr > |T| i/j	1	2	3	4	5
FA_C	1433.02701	1		-2.19582	0.396056	-3.34553	-0.5117
				0.0337	0.6941	0.0017	0.6115
FA_F	3143.25599	2	2.195818	.	2.565015	-1.09739	1.535632
			0.0337		0.0140	0.2787	0.1321
MS	1128.94216	3	-0.39606	-2.56502	.	-3.71749	-0.88504
			0.6941	0.0140		0.0006	0.3812
None	3992.05105	4	3.345531	1.097394	3.717493	.	2.578828
			0.0017	0.2787	0.0006		0.0135
Slag	1863.87336	5	0.511695	-1.53563	0.885039	-2.57883	.
			0.6115	0.1321	0.3812	0.0135	

CEMENT	CL90 LSMEAN	T for H0: LSMEAN(i)=LSMEAN(j) / Pr > |T| i/j	1	2	3	4	5	6
A	2797.23307	1	.	1.570477	1.152977	0.368119	1.979477	-1.507
				0.1238	0.2554	0.7146	0.0543	0.1393
B	1443.54525	2	-1.57048	.	-0.43036	-1.21475	0.392347	-2.85082
			0.1238		0.6691	0.2312	0.6968	0.0067
C	1812.61504	3	-1.15298	0.430365	.	-0.79678	0.83479	-2.59981
			0.2554	0.6691		0.4301	0.4086	0.0128
D	2483.59196	4	-0.36812	1.214751	0.796784	.	1.612966	-1.89744
			0.7146	0.2312	0.4301		0.1142	0.0647
E	1109.01686	5	-1.97948	-0.39235	-0.83479	-1.61297	.	-3.24767
			0.0543	0.6968	0.4086	0.1142		0.0023
F	4227.37731	6	1.507003	2.850821	2.599807	1.897436	3.247666	.
			0.1393	0.0067	0.0128	0.0647	0.0023	

NOTE: To ensure overall protection level, only probabilities associated with pre-planned comparisons should be used.

90-Day Compressive Strength

General Linear Models Procedure
Class Level Information

Class	Levels	Values
W_C	3	0.3 0.4 0.5
AIR	3	2 5 8
COARSE	2	LS Q
FINE	2	G Q
MINERAL	5	FA_C FA_F MS None Slag
CEMENT	6	A B C D E F

Number of observations in data set = 58

FHWA BRIDGE DECKS - 90 Day Data from Dave Lankard 8
16:38 Thursday, October 20, 1994

General Linear Models Procedure

Dependent Variable: STR90

Source	DF	Sum of Squares	Mean Square	F Value	Pr > F
Model	15	330377271.97595200	22025151.46506350	25.82	0.0001
Error	42	35832038.36887490	853143.77068750		
Corrected Total	57	366209310.34482700			

R-Square	C.V.	Root MSE	STR90 Mean
0.902154	12.07940	923.65782121	7646.55172414

Source	DF	Type III SS	Mean Square	F Value	Pr > F
W_C	2	100895514.32626000	50447757.16313020	59.13	0.0001
AIR	2	32214803.20012970	16107401.60006480	18.88	0.0001
COARSE	1	36367598.95401180	36367598.95401180	42.63	0.0001
FINE	1	17529737.92496740	17529737.92496740	20.55	0.0001
MINERAL	4	35035121.13497190	8758780.28374297	10.27	0.0001
CEMENT	5	77438711.03656320	15487742.20731260	18.15	0.0001

Parameter		Estimate	T for H0: Parameter=0	Pr > |T|	Std Error of Estimate
INTERCEPT		3495.673744 B	6.48	0.0001	539.4796488
W_C	0.3	3610.081663 B	10.68	0.0001	337.9352376
	0.4	1958.102219 B	6.65	0.0001	294.4331879
	0.5	0.000000 B	.	.	.
AIR	2	1688.811425 B	5.26	0.0001	321.1741020
	5	1684.255852 B	5.41	0.0001	311.5200684
	8	0.000000 B	.	.	.
COARSE	LS	-1700.374997 B	-6.53	0.0001	260.4344955
	Q	0.000000 B	.	.	.
FINE	G	-1213.971084 B	-4.53	0.0001	267.8130543
	Q	0.000000 B	.	.	.
MINERAL	FA_C	-381.937444 B	-0.91	0.3661	417.9829526
	FA_F	-1075.329434 B	-2.60	0.0128	413.5814073
	MS	1305.892463 B	3.17	0.0029	412.2229446
	None	280.317375 B	0.68	0.4976	409.6691205
	Slag	0.000000 B	.	.	.
CEMENT	A	3469.626803 B	7.36	0.0001	471.1002018
	B	1176.111748 B	2.43	0.0196	484.7533661
	C	2970.054250 B	6.44	0.0001	461.0849114
	D	3247.291965 B	7.12	0.0001	456.2192981
	E	2639.658361 B	5.54	0.0001	476.6533326
	F	0.000000 B	.	.	.

NOTE: The X'X matrix has been found to be singular and a generalized inverse was used to solve the normal equations. Estimates followed by the letter 'B' are biased, and are not unique estimators of the parameters.

90-Day Compressive Strength

General Linear Models Procedure
Least Squares Means

W_C	STR90 LSMEAN	T for H0: LSMEAN(i)=LSMEAN(j) / Pr > |T| i/j	1	2	3
0.3	9049.18391	1	.	4.962638 0.0001	10.68276 0.0001
0.4	7397.20446	2	-4.96264 0.0001	.	6.650413 0.0001
0.5	5439.10224	3	-10.6828 0.0001	-6.65041 0.0001	.

AIR	STR90 LSMEAN	T for H0: LSMEAN(i)=LSMEAN(j) / Pr > |T| i/j	1	2	3
2	7859.61920	1	.	0.014497 0.9885	5.258243 0.0001
5	7855.06363	2	-0.0145 0.9885	.	5.406573 0.0001
8	6170.80778	3	-5.25824 0.0001	-5.40657 0.0001	.

COARSE	STR90 LSMEAN	T / Pr > |T| H0: LSMEAN1=LSMEAN2
LS	6444.97604	-6.52899 0.0001
Q	8145.35104	

FINE	STR90 LSMEAN	T / Pr > |T| H0: LSMEAN1=LSMEAN2
G	6688.17799	-4.5329 0.0001
Q	7902.14908	

MINERAL	STR90 LSMEAN	T for H0: LSMEAN(i)=LSMEAN(j) / Pr > |T| i/j	1	2	3	4	5
FA_C	6887.43750	1	.	1.793384 0.0801	-4.42836 0.0001	-1.74409 0.0885	-0.91376 0.3661
FA_F	6194.04551	2	-1.79338 0.0801	.	-6.10822 0.0001	-3.53068 0.0010	-2.60004 0.0128
MS	8575.26741	3	4.428357 0.0001	6.108224 0.0001	.	2.682452 0.0104	3.167928 0.0029
None	7549.69232	4	1.744087 0.0885	3.530682 0.0010	-2.68245 0.0104	.	0.684253 0.4976
Slag	7269.37494	5	0.913763 0.3661	2.600043 0.0128	-3.16793 0.0029	-0.68425 0.4976	.

CEMENT	STR90 LSMEAN	T for H0: LSMEAN(i)=LSMEAN(j) / Pr > |T| i/j	1	2	3	4	5	6
A	8514.33315	1	.	5.360026 0.0001	1.17843 0.2453	0.525672 0.6019	1.960362 0.0566	7.364944 0.0001
B	6220.81810	2	-5.36003 0.0001	.	-4.21394 0.0001	-4.87309 0.0001	-3.45777 0.0013	2.426206 0.0196
C	8014.76060	3	-1.17843 0.2453	4.213944 0.0001	.	-0.66319 0.5108	0.789659 0.4342	6.441448 0.0001
D	8291.99831	4	-0.52567 0.6019	4.873091 0.0001	0.66319 0.5108	.	1.436318 0.1583	7.117831 0.0001
E	7684.36471	5	-1.96036 0.0566	3.457772 0.0013	-0.78966 0.4342	-1.43632 0.1583	.	5.5379 0.0001
F	5044.70635	6	-7.36494 0.0001	-2.42621 0.0196	-6.44145 0.0001	-7.11783 0.0001	-5.5379 0.0001	.

NOTE: To ensure overall protection level, only probabilities associated with pre-planned comparisons should be used.

90-Day Electrical Resistivity

General Linear Models Procedure

Dependent Variable: EL90

Source	DF	Sum of Squares	Mean Square	F Value	Pr > F
Model	15	62104163198.45820000	4140277546.56388000	2.26	0.0191
Error	42	76904292736.02450000	1831054588.95296000		
Corrected Total	57	139008455934.48200000			

R-Square	C.V.	Root MSE	EL90 Mean
0.446765	131.5608	42790.82365359	32525.51724138

Source	DF	Type III SS	Mean Square	F Value	Pr > F
W_C	2	4349098790.98922000	2174549395.49461000	1.19	0.3150
AIR	2	312624079.14022600	156312039.57011300	0.09	0.9183
COARSE	1	1641422225.19422000	1641422225.19422000	0.90	0.3492
FINE	1	1449484438.46787000	1449484438.46787000	0.79	0.3787
MINERAL	4	14060137053.42310000	3515034263.35579000	1.92	0.1249
CEMENT	5	33609918122.34040000	6721983624.46808000	3.67	0.0076

Parameter		Estimate	T for H0: Parameter=0	Pr > |T|	Std Error of Estimate
INTERCEPT		33574.59996 B	1.34	0.1864	24992.78194
W_C	0.3	23392.96646 B	1.49	0.1426	15655.71885
	0.4	13817.71527 B	1.01	0.3169	13640.37453
	0.5	0.00000 B	.	.	.
AIR	2	-3.96463 B	-0.00	0.9998	14879.21614
	5	-5142.14480 B	-0.36	0.7234	14431.96821
	8	0.00000 B	.	.	.
COARSE	LS	-11423.45698 B	-0.95	0.3492	12065.29769
	Q	0.00000 B	.	.	.
FINE	G	-11038.94092 B	-0.89	0.3787	12407.12839
	Q	0.00000 B	.	.	.
MINERAL	FA_C	19506.96334 B	1.01	0.3195	19364.13508
	FA_F	415.15682 B	0.02	0.9828	19160.22217
	MS	43119.92187 B	2.26	0.0292	19097.28790
	None	8182.55652 B	0.43	0.6686	18978.97543
	Slag	0.00000 B	.	.	.
CEMENT	A	-29450.31839 B	-1.35	0.1844	21824.92823
	B	31074.05521 B	1.38	0.1738	22457.44617
	C	-33325.58907 B	-1.56	0.1262	21360.94415
	D	-31221.79614 B	-1.48	0.1471	21135.53210
	E	-35721.13931 B	-1.62	0.1132	22082.19129
	F	0.00000 B	.	.	.

NOTE: The X'X matrix has been found to be singular and a generalized inverse was used to solve the normal equations. Estimates followed by the letter 'B' are biased, and are not unique estimators of the parameters.

90-Day Electrical Resistivity

General Linear Models Procedure
Least Squares Means

W_C	EL90 LSMEAN	Pr > |T| HO: LSMEAN(i)=LSMEAN(j) i/j	1	2	3
0.3	41825.1194	1	.	0.5380	0.1426
0.4	32249.8682	2	0.5380	.	0.3169
0.5	18432.1530	3	0.1426	0.3169	

AIR	EL90 LSMEAN	Pr > |T| HO: LSMEAN(i)=LSMEAN(j) i/j	1	2	3
2	32547.1187	1	.	0.7259	0.9998
5	27408.9385	2	0.7259	.	0.7234
8	32551.0834	3	0.9998	0.7234	

COARSE	EL90 LSMEAN	Pr > |T| HO: LSMEAN1=LSMEAN2
LS	25123.9851	0.3492
Q	36547.4420	

FINE	EL90 LSMEAN	Pr > |T| HO: LSMEAN1=LSMEAN2
G	25316.2431	0.3787
Q	36355.1840	

MINERAL	EL90 LSMEAN	Pr > |T| HO: LSMEAN(i)=LSMEAN(j) i/j	1	2	3	4	5
FA_C	36097.7572	1	.	0.2926	0.1883	0.5232	0.3195
FA_F	17005.9506	2	0.2926	.	0.0227	0.6646	0.9828
MS	59710.7157	3	0.1883	0.0227	.	0.0552	0.0292
None	24773.3504	4	0.5232	0.6646	0.0552	.	0.6686
Slag	16590.7938	5	0.3195	0.9828	0.0292	0.6686	

CEMENT	EL90 LSMEAN	Pr > |T| HO: LSMEAN(i)=LSMEAN(j) i/j	1	2	3	4	5	6
A	17826.1931	1		0.0039	0.8445	0.9284	0.7508	0.1844
B	78350.5667	2	0.0039	.	0.0022	0.0029	0.0015	0.1738
C	13950.9224	3	0.8445	0.0022	.	0.9140	0.9022	0.1262
D	16054.7153	4	0.9284	0.0029	0.9140	.	0.8195	0.1471
E	11555.3722	5	0.7508	0.0015	0.9022	0.8195	.	0.1132
F	47276.5115	6	0.1844	0.1738	0.1262	0.1471	0.1132	

NOTE: To ensure overall protection level, only probabilities associated with pre-planned comparisons should be used.

Moderate Environment - Measured Chlorides

General Linear Models Procedure
Class Level Information

Class	Levels	Values
W_C	3	0.3 0.4 0.5
MOD_AIR	3	2 5 8
COARSE	2	LS Q
FINE	2	G Q
MINERAL	5	FA_C FA_F MS None Slag
CEMENT	6	A B C D E F

Number of observations in data set = 86

General Linear Models Procedure

Dependent Variable: CL

Source	DF	Sum of Squares	F Value	Pr > F
Model	15	47.36523689	2.90	0.0013
Error	70	76.12790264		
Corrected Total	85	123.49313953		

R-Square	C.V.	CL Mean
0.383545	56.22904	1.85465116

Moderate Environment - Measured Chlorides

Source	DF	Type III SS	F Value	Pr > F
W_C	2	8.99408145	4.14	0.0201
MOD_AIR	2	3.80889475	1.75	0.1811
COARSE	1	0.00000426	0.00	0.9984
FINE	1	4.15537688	3.82	0.0546
MINERAL	4	8.14541355	1.87	0.1249
CEMENT	5	13.71436934	2.52	0.0371

Parameter		Estimate	T for H0: Parameter=0	Pr > |T|	Std Error of Estimate
INTERCEPT		2.370476487 B	4.22	0.0001	0.56190338
W_C	0.3	-0.266018832 B	-0.78	0.4380	0.34105043
	0.4	-0.802014787 B	-2.76	0.0073	0.29034866
	0.5	0.000000000 B	.	.	.
MOD_AIR	2	0.569382163 B	1.50	0.1392	0.38063401
	5	0.499794293 B	1.70	0.0936	0.29403244
	8	0.000000000 B	.	.	.
COARSE	LS	0.000477562 B	0.00	0.9984	0.24138612
	Q	0.000000000 B	.	.	.
FINE	G	0.485035342 B	1.95	0.0546	0.24813675
	Q	0.000000000 B	.	.	.
MINERAL	FA_C	-0.779145337 B	-1.96	0.0537	0.39702816
	FA_F	0.084586609 B	0.22	0.8254	0.38192742
	MS	-0.512430202 B	-1.35	0.1829	0.38094483
	None	-0.098701416 B	-0.26	0.7954	0.37912833
	Slag	0.000000000 B	.	.	.
CEMENT	A	-0.483457615 B	-1.07	0.2877	0.45125144
	B	-0.909403387 B	-1.96	0.0541	0.46421068
	C	-0.149994715 B	-0.34	0.7357	0.44251250
	D	0.116128853 B	0.27	0.7877	0.42960914
	E	-1.010568380 B	-2.17	0.0332	0.46527857
	F	0.000000000 B	.	.	.

NOTE: The X'X matrix has been found to be singular and a generalized inverse was used to solve the normal equations. Estimates followed by the letter 'B' are biased, and are not unique estimators of the parameters.

Moderate Environment - Measured Chlorides

General Linear Models Procedure
Least Squares Means

W_C	CL LSMEAN	Pr > |T| H0: LSMEAN(i)=LSMEAN(j) i/j	1	2	3
0.3	2.03625232	1	.	0.0880	0.4380
0.4	1.50025636	2	0.0880	.	0.0073
0.5	2.30227115	3	0.4380	0.0073	.

MOD_AIR	CL LSMEAN	Pr > |T| H0: LSMEAN(i)=LSMEAN(j) i/j	1	2	3
2	2.15924995	1	.	0.8446	0.1392
5	2.08966208	2	0.8446	.	0.0936
8	1.58986779	3	0.1392	0.0936	.

COARSE	CL LSMEAN	Pr > |T| H0: LSMEAN1=LSMEAN2
LS	1.94649872	0.9984
Q	1.94602116	

FINE	CL LSMEAN	Pr > |T| H0: LSMEAN1=LSMEAN2
G	2.18877761	0.0546
Q	1.70374227	

MINERAL	CL LSMEAN	LSMEAN Number
FA_C	1.42825267	1
FA_F	2.29198462	2
MS	1.69496781	3
None	2.10869660	4
Slag	2.20739801	5

Pr > |T| H0: LSMEAN(i)=LSMEAN(j)

i/j	1	2	3	4	5
1	.	0.0254	0.4791	0.0742	0.0537
2	0.0254	.	0.1016	0.6064	0.8254
3	0.4791	0.1016	.	0.2446	0.1829
4	0.0742	0.6064	0.2446	.	0.7954
5	0.0537	0.8254	0.1829	0.7954	.

Moderate Environment - Corrosion Rate

General Linear Models Procedure

Dependent Variable: RATE

Source	DF	Sum of Squares	F Value	Pr > F
Model	15	2.77944464	3.64	0.0001
Error	70	3.56711349		
Corrected Total	85	6.34655814		

R-Square	C.V.	RATE Mean
0.437945	252.7823	0.08930233

Source	DF	Type III SS	F Value	Pr > F
W_C	2	0.15011197	1.47	0.2363
MOD_AIR	2	0.09534964	0.94	0.3972
COARSE	1	0.02408674	0.47	0.4940
FINE	1	0.54184432	10.63	0.0017
MINERAL	4	0.77061002	3.78	0.0077
CEMENT	5	1.19249355	4.68	0.0010

Parameter		Estimate		T for H0: Parameter=0	Pr > |T|	Std Error of Estimate
INTERCEPT		0.4261200016	B	3.50	0.0008	0.12163209
W_C	0.3	-.0498929876	B	-0.68	0.5014	0.07382528
	0.4	-.1066292978	B	-1.70	0.0942	0.06285016
	0.5	0.0000000000	B	.	.	.
MOD_AIR	2	0.0237337552	B	0.29	0.7742	0.08239372
	5	-.0662126419	B	-1.04	0.3018	0.06364756
	8	0.0000000000	B	.	.	.
COARSE	LS	0.0359234771	B	0.69	0.4940	0.05225151
	Q	0.0000000000	B	.	.	.
FINE	G	0.1751481027	B	3.26	0.0017	0.05371278
	Q	0.0000000000	B	.	.	.
MINERAL	FA_C	-.1077582942	B	-1.25	0.2141	0.08594247
	FA_F	0.1230856044	B	1.49	0.1410	0.08267370
	MS-	-.1266978885	B	-1.54	0.1289	0.08246100
	None	-.1214070342	B	-1.48	0.1435	0.08206780
	Slag	0.0000000000	B	.	.	.
CEMENT	A	-.3136458911	B	-3.21	0.0020	0.09767988
	B	-.2178960545	B	-2.17	0.0335	0.10048510
	C	-.3729578219	B	-3.89	0.0002	0.09578821
	D	-.3710379063	B	-3.99	0.0002	0.09299510
	E	-.4035476124	B	-4.01	0.0002	0.10071626
	F	0.0000000000	B	.	.	.

NOTE: The X'X matrix has been found to be singular and a generalized inverse was used to solve the normal equations. Estimates followed by the letter 'B' are biased, and are not unique estimators of the parameters.

Moderate Environment - Corrosion Rate

General Linear Models Procedure
Least Squares Means

W_C	RATE LSMEAN	Pr > |T| H0: LSMEAN(i)=LSMEAN(j) i/j	1	2	3
0.3	0.14120010	1	.	0.4004	0.5014
0.4	0.08446379	2	0.4004	.	0.0942
0.5	0.19109309	3	0.5014	0.0942	.

MOD_AIR	RATE LSMEAN	Pr > |T| H0: LSMEAN(i)=LSMEAN(j) i/j	1	2	3
2	0.17681238	1	.	0.2441	0.7742
5	0.08686598	2	0.2441	.	0.3018
8	0.15307863	3	0.7742	0.3018	.

COARSE	RATE LSMEAN	Pr > |T| H0: LSMEAN1=LSMEAN2
LS	0.15688074	0.4940
Q	0.12095726	

FINE	RATE LSMEAN	Pr > |T| H0: LSMEAN1=LSMEAN2
G	0.22649305	0.0017
Q	0.05134495	

MINERAL	RATE LSMEAN	LSMEAN Number
FA_C	0.07771623	1
FA_F	0.30856012	2
MS	0.05877663	3
None	0.06406749	4
Slag	0.18547452	5

Pr > |T| H0: LSMEAN(i)=LSMEAN(j)

Dependent Variable: RATE

i/j	1	2	3	4	5
1	.	0.0062	0.8161	0.8671	0.2141
2	0.0062	.	0.0020	0.0021	0.1410
3	0.8161	0.0020	.	0.9449	0.1289
4	0.8671	0.0021	0.9449	.	0.1435
5	0.2141	0.1410	0.1289	0.1435	.

Moderate Environment - Corrosion Rate

CEMENT	RATE LSMEAN	LSMEAN Number
A	0.10512065	1
B	0.20087049	2
C	0.04580872	3
D	0.04772864	4
E	0.01521893	5
F	0.41876654	6

Pr > |T| H0: LSMEAN(i)=LSMEAN(j)

i/j	1	2	3	4	5	6
1	.	0.2688	0.4811	0.4978	0.2901	0.0020
2	0.2688	.	0.0770	0.0856	0.0412	0.0335
3	0.4811	0.0770	.	0.9818	0.7177	0.0002
4	0.4978	0.0856	0.9818	.	0.7087	0.0002
5	0.2901	0.0412	0.7177	0.7087	.	0.0002
6	0.0020	0.0335	0.0002	0.0002	0.0002	.

Moderate Environment - Corrosion Potential

General Linear Models Procedure

Dependent Variable: POTENT

Source	DF	Sum of Squares	F Value	Pr > F
Model	15	1.41452033	14.07	0.0001
Error	70	0.46900525		
Corrected Total	85	1.88352558		

R-Square	C.V.	POTENT Mean
0.750996	-54.90985	-0.14906977

Source	DF	Type III SS	F Value	Pr > F
W_C	2	0.01899589	1.42	0.2492
MOD_AIR	2	0.03493186	2.61	0.0809
COARSE	1	0.00958523	1.43	0.2357
FINE	1	0.01354131	2.02	0.1596
MINERAL	4	0.02579182	0.96	0.4337
CEMENT	5	1.23804500	36.96	0.0001

Parameter	Estimate	T for H0: Parameter=0	Pr > |T|	Std Error of Estimate
INTERCEPT	-.5550944262 B	-12.59	0.0001	0.04410406
W_C	0.3			
	0.0425833501 B	1.59	0.1162	0.02676921
	0.4			
	0.0298326257 B	1.31	0.1948	0.02278960
	0.5			
	0.0000000000 B	.	.	.
MOD_AIR	2 0.0567659213 B	1.90	0.0615	0.02987614
	5 0.0465350181 B	2.02	0.0476	0.02307874
	8 0.0000000000 B	.	.	.
COARSE	LS0.0226616102 B	1.20	0.2357	0.01894651
	Q 0.0000000000 B	.	.	.
FINE	G -.0276884427 B	-1.42	0.1596	0.01947637
	Q 0.0000000000 B	.	.	.
MINERAL	FA_C			
	0.0246286098 B	0.79	0.4320	0.03116293
	FA_F			
	0.0362617171 B	1.21	0.2305	0.02997766
	MS0.0012010163 B	0.04	0.9681	0.02990054
	None			
	0.0439055996 B	1.48	0.1446	0.02975796
	Slag			
	0.0000000000 B	.	.	.
CEMENT	A 0.3929721888 B	11.09	0.0001	0.03541894
	B 0.312910546 B	8.59	0.0001	0.03643611
	C 0.4194888588 B	12.08	0.0001	0.03473301
	D 0.3914690079 B	11.61	0.0001	0.03372022
	E 0.3689123843 B	10.10	0.0001	0.03651993
	F 0.0000000000 B			

NOTE: The X'X matrix has been found to be singular and a generalized inverse was used to solve the normal equations. Estimates followed by the letter 'B' are biased, and are not unique estimators of the parameters.

Moderate Environment - Corrosion Potential

General Linear Models Procedure
Least Squares Means

W_C	POTENT LSMEAN	Pr > |T| H0: LSMEAN(i)=LSMEAN(j) i/j	1	2	3
0.3	-0.14509932	1	.	0.6017	0.1162
0.4	-0.15785005	2	0.6017	.	0.1948
0.5	-0.18768268	3	0.1162	0.1948	.

NOTE: To ensure overall protection level, only probabilities associated with pre-planned comparisons should be used.

MOD_AIR	POTENT LSMEAN	Pr > |T| H0: LSMEAN(i)=LSMEAN(j) i/j	1	2	3
2	-0.14121174	1	.	0.7136	0.0615
5	-0.15144264	2	0.7136	.	0.0476
8	-0.19797766	3	0.0615	0.0476	.

COARSE	POTENT LSMEAN	Pr > |T| H0: LSMEAN1=LSMEAN2
LS	-0.15221321	0.2357
Q	-0.17487482	

FINE	POTENT LSMEAN	Pr > |T| H0: LSMEAN1=LSMEAN2
G	-0.17738824	0.1596
Q	-0.14969980	

MINERAL	POTENT LSMEAN	LSMEAN Number
FA_C	-0.16011480	1
FA_F	-0.14848169	2
MS	-0.18354239	3
None	-0.14083781	4
Slag	-0.18474341	5

Pr > |T| H0: LSMEAN(i)=LSMEAN(j)

i/j	1	2	3	4	5
1	.	0.6962	0.4286	0.5152	0.4320
2	0.6962	.	0.2187	0.7841	0.2305
3	0.4286	0.2187	.	0.1273	0.9681
4	0.5152	0.7841	0.1273	.	0.1446
5	0.4320	0.2305	0.9681	0.1446	.

NOTE: To ensure overall protection level, only probabilities associated with pre-planned comparisons should be used.

Moderate Environment - Corrosion Potential

CEMENT	POTENT LSMEAN	LSMEAN Number
A	-0.08486396	1
B	-0.16492579	2
C	-0.05834729	3
D	-0.08636714	4
E	-0.10892376	5
F	-0.47783615	6

Pr > |T| H0: LSMEAN(i)=LSMEAN(j)

i/j	1	2	3	4	5	6
1	.	0.0123	0.3855	0.9609	0.4341	0.0001
2	0.0123	.	0.0011	0.0161	0.0880	0.0001
3	0.3855	0.0011	.	0.3611	0.1024	0.0001
4	0.9609	0.0161	0.3611	.	0.4753	0.0001
5	0.4341	0.0880	0.1024	0.4753	.	0.0001
6	0.0001	0.0001	0.0001	0.0001	0.0001	.

NOTE: To ensure overall protection level, only probabilities associated with pre-planned comparisons should be used.

Aggressive Environment - Measure Chloride

General Linear Models Procedure
Class Level Information

Class	Levels	Values
W_C	3	0.3 0.4 0.5
MOD_AIR	3	2 5 8
COARSE	2	LS Q
FINE	2	G Q
MINERAL	5	FA_C FA_F MS None Slag
CEMENT	6	A B C D E F

Number of observations in data set = 85

Group	Obs	Dependent Variables
1	84	CL
2	85	RATE
3	75	POTENT

NOTE: Variables in each group are consistent with respect to the presence or absence of missing values.

General Linear Models Procedure

Dependent Variable: CL

Source	DF	Sum of Squares	F Value	Pr > F
Model	15	366.47201560	2.46	0.0062
Error	68	675.59305464		
Corrected Total	83	1042.06507024		

R-Square	C.V.	CL Mean
0.351679	44.18048	7.13440476

Aggressive Environment - Measure Chloride

Source	DF	Type III SS	F Value	Pr > F
W_C	2	95.70200830	4.82	0.0111
MOD_AIR	2	1.05972702	0.05	0.9481
COARSE	1	5.73065905	0.58	0.4502
FINE	1	21.12733206	2.13	0.1494
MINERAL	4	78.40029641	1.97	0.1085
CEMENT	5	123.92204425	2.49	0.0392

Parameter		Estimate	T for H0: Parameter=0	Pr > |T|	Std Error of Estimate
INTERCEPT		7.230763917 B	4.25	0.0001	1.69937697
W_C	0.3				
		-2.596059020 B	-2.48	0.0155	1.04523167
	0.4				
		-2.605040508 B	-2.88	0.0053	0.90352350
	0.5				
		0.000000000 B	.	.	.
MOD_AIR	2	-0.042999245 B	-0.04	0.9704	1.15493574
	5	0.252777910 B	0.27	0.7866	0.93014684
	8	0.000000000 B	.	.	.
COARSE	LS	-0.563862115 B	-0.76	0.4502	0.74243556
	Q	0.000000000 B	.	.	.
FINE	G	1.117978944 B	1.46	0.1494	0.76665404
	Q	0.000000000 B	.	.	.
MINERAL	FA_C				
		-0.470118684 B	-0.37	0.7099	1.25843710
	FA_F				
		-0.249766732 B	-0.22	0.8298	1.15767872
	MS	-0.258669231 B	-0.22	0.8230	1.15185556
	None				
		2.137274790 B	1.86	0.0667	1.14707929
	Slag				
		0.000000000 B	.	.	.
CEMENT	A	-0.582892848 B	-0.43	0.6706	1.36438557
	B	1.247497176 B	0.86	0.3914	1.44611511
	C	3.051228681 B	2.28	0.0257	1.33753717
	D	1.790354852 B	1.35	0.1801	1.32183760
	E	0.426654632 B	0.30	0.7625	1.40637532
	F	0.000000000 B	.	.	.

NOTE: The X'X matrix has been found to be singular and a generalized inverse was used to solve the normal equations. Estimates followed by the letter 'B' are biased, and are not unique estimators of the parameters.

Aggressive Environment - Measure Chloride

General Linear Models Procedure
Least Squares Means

W_C	CL LSMEAN	Pr > |T| H0: LSMEAN(i)=LSMEAN(j) i/j	1	2	3
0.3	6.20224064	1	.	0.9926	0.0155
0.4	6.19325916	2	0.9926	.	0.0053
0.5	8.79829966	3	0.0155	0.0053	.

NOTE: To ensure overall protection level, only probabilities associated with pre-planned comparisons should be used.

MOD_AIR	CL LSMEAN	Pr > |T| H0: LSMEAN(i)=LSMEAN(j) i/j	1	2	3
2	6.95167435	1	.	0.7896	0.9704
5	7.24745151	2	0.7896	.	0.7866
8	6.99467360	3	0.9704	0.7866	.

NOTE: To ensure overall protection level, only probabilities associated with pre-planned comparisons should be used.

COARSE	CL LSMEAN	Pr > |T| H0: LSMEAN1=LSMEAN2
LS	6.78266876	0.4502
Q	7.34653088	

FINE	CL LSMEAN	Pr > |T| H0: LSMEAN1=LSMEAN2
G	7.62358929	0.1494
Q	6.50561035	

MINERAL	CL LSMEAN	LSMEAN Number
FA_C	6.36273711	1
FA_F	6.58308906	2
MS	6.57418656	3
None	8.97013058	4
Slag	6.83285579	5

Pr > |T| H0: LSMEAN(i)=LSMEAN(j)

/j	1	2	3	4	5
1	.	0.8527	0.8589	0.0308	0.7099
2	0.8527	.	0.9935	0.0293	0.8298
3	0.8589	0.9935	.	0.0278	0.8230
4	0.0308	0.0293	0.0278	.	0.0667
5	0.7099	0.8298	0.8230	0.0667	.

NOTE: To ensure overall protection level, only probabilities associated with pre-planned comparisons should be used.

General Linear Models Procedure
Least Squares Means

CEMENT	CL LSMEAN	LSMEAN Number
A	5.49289989	1
B	7.32328992	2
C	9.12702142	3
D	7.86614759	4
E	6.50244737	5
F	6.07579274	6

Pr > |T| H0: LSMEAN(i)=LSMEAN(j)

i/j	1	2	3	4	5	6
1	.	0.1456	0.0028	0.0513	0.3944	0.6706
2	0.1456	.	0.1547	0.6763	0.5280	0.3914
3	0.0028	0.1547	.	0.2972	0.0291	0.0257
4	0.0513	0.6763	0.2972	.	0.2724	0.1801
5	0.3944	0.5280	0.0291	0.2724	.	0.7625
6	0.6706	0.3914	0.0257	0.1801	0.7625	.

NOTE: To ensure overall protection level, only probabilities associated with pre-planned comparisons should be used.

Aggressive Environment - Corrosion Rate

General Linear Models Procedure

Dependent Variable: RATE

Source	DF	Sum of Squares	F Value	Pr > F
Model	15	638.52474987	3.04	0.0009
Error	69	964.84549249		
Corrected Total	84	1603.37024235		

R-Square	C.V.	RATE Mean
0.398239	161.6574	2.31317647

Source	DF	Type III SS	F Value	Pr > F
W_C	2	35.13479969	1.26	0.2911
MOD_AIR	2	14.85370541	0.53	0.5903
COARSE	1	32.50017760	2.32	0.1319
FINE	1	81.76710998	5.85	0.0182
MINERAL	4	142.71192972	2.55	0.0467
CEMENT	5	261.70916525	3.74	0.0047

Parameter		Estimate	T for H0: Parameter=0	Pr > |T|	Std Error of Estimate
INTERCEPT		4.523357938 B	2.24	0.0280	2.01518548
W_C	0.3				
		-1.918887207 B	-1.57	0.1221	1.22580194
	0.4				
		-1.066884710 B	-1.01	0.3156	1.05546058
	0.5				
		0.000000000 B	.	.	.
MOD_AIR	2	1.304515224 B	0.95	0.3430	1.36619363
	5	0.113790397 B	0.10	0.9177	1.09774986
	8	0.000000000 B	.	.	.
COARSE	LS	1.321626497 B	1.52	0.1319	0.86690241
	Q	0.000000000 B	.	.	.
FINE	G	2.186330812 B	2.42	0.0182	0.90413003
	Q	0.000000000 B	.	.	.
MINERAL	FA_C				
		-2.915415882 B	-1.97	0.0529	1.48045787
	FA_F				
		-1.444566721 B	-1.05	0.2966	1.37342028
	MS	-4.108941679 B	-3.01	0.0037	1.36627585
	None				
		-2.034775017 B	-1.50	0.1392	1.36019794
	Slag				
		0.000000000 B	.	.	.
CEMENT	A	-2.385244772 B	-1.47	0.1451	1.61833657
	B	2.975576325 B	1.73	0.0873	1.71559859
	C	-2.377688880 B	-1.50	0.1386	1.58678993
	D	-0.557258591 B	-0.36	0.7187	1.54066422
	E	-2.234530301 B	-1.34	0.1849	1.66837976
	F	0.000000000 B			

NOTE: The X'X matrix has been found to be singular and a generalized inverse was used to solve the normal equations. Estimates followed by the letter 'B' are biased, and are not unique estimators of the parameter

General Linear Models Procedure
Least Squares Means

W_C	RATE LSMEAN	Pr > |T| HO: LSMEAN(i)=LSMEAN(j) i/j	1	2	3
0.3	1.96728703	1	.	0.4575	0.1221
0.4	2.81928953	2	0.4575	.	0.3156
0.5	3.88617424	3	0.1221	0.3156	.

NOTE: To ensure overall protection level, only probabilities associated with pre-planned comparisons should be used.

MOD_AIR	RATE LSMEAN	Pr > |T| HO: LSMEAN(i)=LSMEAN(j) i/j	1	2	3
2	3.72266361	1	.	0.3599	0.3430
5	2.53193879	2	0.3599	.	0.9177
8	2.41814839	3	0.3430	0.9177	.

NOTE: To ensure overall protection level, only probabilities associated with pre-planned comparisons should be used.

COARSE	RATE LSMEAN	Pr > |T| HO: LSMEAN1=LSMEAN2
LS	3.55173018	0.1319
Q	2.23010368	

FINE	RATE LSMEAN	Pr > |T| HO: LSMEAN1=LSMEAN2
G	3.98408234	0.0182
Q	1.79775152	

MINERAL	RATE LSMEAN	LSMEAN Number
FA_C	2.07624091	1
FA_F	3.54709007	2
MS	0.88271511	3
None	2.95688177	4
Slag	4.99165679	5

Pr > |T| H0: LSMEAN(i)=LSMEAN(j)

i/j	1	2	3	4	5
1	.	0.2933	0.3956	0.5297	0.0529
2	0.2933	.	0.0431	0.6439	0.2966
3	0.3956	0.0431	.	0.1055	0.0037
4	0.5297	0.6439	0.1055	.	0.1392
5	0.0529	0.2966	0.0037	0.1392	.

NOTE: To ensure overall protection level, only probabilities associated with pre-planned comparisons should be used.

General Linear Models Procedure
Least Squares Means

CEMENT	RATE LSMEAN	LSMEAN Number
A	1.26886320	1
B	6.62968429	2
C	1.27641909	3
D	3.09684938	4
E	1.41957767	5
F	3.65410797	6

Pr > |T| H0: LSMEAN(i)=LSMEAN(j)

i/j	1	2	3	4	5	6
1	.	0.0005	0.9957	0.1944	0.9144	0.1451
2	0.0005	.	0.0006	0.0219	0.0011	0.0873
3	0.9957	0.0006	.	0.1955	0.9186	0.1386
4	0.1944	0.0219	0.1955	.	0.2468	0.7187
5	0.9144	0.0011	0.9186	0.2468	.	0.1849
6	0.1451	0.0873	0.1386	0.7187	0.1849	.

NOTE: To ensure overall protection level, only probabilities associated with pre-planned comparisons should be used.

Aggressive Environment - Corrosion Potential

General Linear Models Procedure

Dependent Variable: POTENT

Source	DF	Sum of Squares	F Value	Pr > F
Model	15	1.08873800	6.85	0.0001
Error	59	0.62473667		
Corrected Total	74	1.71347467		

R-Square	C.V.	POTENT Mean
0.635398	-27.68159	-0.37173333

Source	DF	Type III SS	F Value	Pr > F
W_C	2	0.05393284	2.55	0.0869
MOD_AIR	2	0.15988103	7.55	0.0012
COARSE	1	0.22924447	21.65	0.0001
FINE	1	0.00750168	0.71	0.4034
MINERAL	4	0.39508575	9.33	0.0001
CEMENT	5	0.31929414	6.03	0.0001

Parameter	Estimate	T for H0: Parameter=0	Pr > |T|	Std Error of Estimate
INTERCEPT	-.6328098599 B	-10.93	0.0001	0.05790589
W_C	0.3			
	0.0829266690 B	2.21	0.0308	0.03746642
	0.4			
	0.0442711910 B	1.47	0.1463	0.03007402
	0.5			
	0.0000000000 B	.	.	.
MOD_AIR	2 0.1575405661 B	3.88	0.0003	0.04060869
	5 0.0549023235 B	1.67	0.1002	0.03286941
	8 0.0000000000 B	.	.	.
COARSE	LS0.1185407817 B	4.65	0.0001	0.02547656
	Q 0.0000000000 B	.	.	.
FINE	G 0.0228908982 B	0.84	0.4034	0.02719607
	Q 0.0000000000 B	.	.	.
MINERAL	FA_C			
	0.0490792754 B	1.07	0.2903	0.04599693
	FA_F			
	-.1442503651 B	-3.55	0.0008	0.04067813
	MS-.0370096191 B	-0.96	0.3410	0.03855675
	None			
	-.1653192372 B	-4.08	0.0001	0.04052889
	Slag			
	0.0000000000 B	.	.	.
CEMENT	A 0.2344275068 B	4.80	0.0001	0.04884332
	B 0.1650146833 B	3.43	0.0011	0.04812317
	C 0.1878158902 B	3.99	0.0002	0.04705630
	D 0.2121140418 B	4.87	0.0001	0.04356959
	E 0.2031644728 B	4.00	0.0002	0.05078833
	F 0.0000000000 B			

NOTE: The X'X matrix has been found to be singular and a generalized inverse was used to solve the normal equations. Estimates followed by the letter 'B' are biased, and are not unique estimators of the parameters.

MINERAL	POTENT LSMEAN	LSMEAN Number
FA_C	-0.23271173	1
FA_F	-0.42604137	2
MS	-0.31880062	3
None	-0.44711024	4
Slag	-0.28179100	5

Pr > |T| H0: LSMEAN(i)=LSMEAN(j)

i/j	1	2	3	4	5
1	.	0.0001	0.0476	0.0001	0.2903
2	0.0001	.	0.0056	0.5837	0.0008
3	0.0476	0.0056	.	0.0008	0.3410
4	0.0001	0.5837	0.0008	.	0.0001
5	0.2903	0.0008	0.3410	0.0001	.

NOTE: To ensure overall protection level, only probabilities associated with pre-planned comparisons should be used.

FHWA - Neil Thompson, Cortest 12
Task B, Temperature=100, Relative Humidity=98
MOD_AIR: Air changed in 5 cases to match actual air
11:06 Monday, June 5, 1995

General Linear Models Procedure

Least Squares Means

CEMENT	POTENT LSMEAN	LSMEAN Number
A	-0.27395292	1
B	-0.34336574	2
C	-0.32056454	3
D	-0.29626638	4
E	-0.30521595	5
F	-0.50838043	6

Pr > |T| H0: LSMEAN(i)=LSMEAN(j)

i/j	1	2	3	4	5	6
1	.	0.1272	0.2852	0.6030	0.4787	0.0001
2	0.1272	.	0.6106	0.2739	0.3987	0.0011
3	0.2852	0.6106	.	0.5655	0.7272	0.0002
4	0.6030	0.2739	0.5655	.	0.8399	0.0001
5	0.4787	0.3987	0.7272	0.8399	.	0.0002
6	0.0001	0.0011	0.0002	0.0001	0.0002	.

NOTE: To ensure overall protection level, only probabilities associated with pre-planned comparisons should be used

General Linear Models Procedure
Least Squares Means

W_C	POTENT LSMEAN	Pr > |T| H0: LSMEAN(i)=LSMEAN(j) i/j	1	2	3
0.3	-0.30076361	1	.	0.2691	0.0308
0.4	-0.33941909	2	0.2691	.	0.1463
0.5	-0.38369028	3	0.0308	0.1463	.

NOTE: To ensure overall protection level, only probabilities associated with pre-planned comparisons should be used.

MOD_AIR	POTENT LSMEAN	Pr > |T| H0: LSMEAN(i)=LSMEAN(j) i/j	1	2	3
2	-0.25456472	1	.	0.0091	0.0003
5	-0.35720297	2	0.0091	.	0.1002
8	-0.41210529	3	0.0003	0.1002	.

NOTE: To ensure overall protection level, only probabilities associated with pre-planned comparisons should be used.

COARSE	POTENT LSMEN	Pr > |T| H0: LSMEAN1=LSMEAN2
LS	-0.28202060	0.0001
Q	-0.40056138	

FINE	POTENT LSMEAN	Pr > |T| H0: LSMEAN1=LSMEAN2
G	-0.32984554	0.4034
Q	-0.35273644	

APPENDIX - D
Statistical Analysis Description

The analyses performed used the statistical package SAS. The most common procedure used is the general linear model (seen as GLM in SAS programming statements). GLM fits a continuous dependent variable (e.g., strength) to a user specified function of independent variables (e.g., aggregate, cement, air). The independent variable may be treated as either continuous variables such as length or as discrete categorical variables such as cement type. It is possible to treat some variables in either way, e.g., if air content is used at 3 discrete levels, it may be treated as a categorical variable.

In the SAS GLM procedure a MODEL statement is given showing the functional form of the equation for which GLM will estimate the least-squares coefficients. All independent variables to be treated as categorical variables are declared in a SAS CLASS statement; otherwise, SAS assumes them to be continuous variables. The functional form specified by the SAS MODEL statement allows a wide variety of function forms from a linear only model to ones involving polynomial terms (such as quadratic) or interaction terms between two or more independent variables.

When the number of samples must be limited for economic reasons and there exist a fair number of independent variables a model is usually developed only for the linear (or main effects) terms. One must keep in mind that prior to analyzing the experimental data with SAS, the important step of developing the experimental design must be given adequate attention. This program used the software package ECHIP to aid in the development of the experimental design. Recall that the experimental design is the specification of the values that each independent variable will be set to for each sample (concrete mix design). Without proper attention given to the experimental design, the quality of useful information that may be gleaned from the statistical analysis is limited.

For this project , a design (using ECHIP) was developed as a main effects model using D-optimality as a tool in the design development. The design was built to extract maximal quality estimates on numerous parameters given relatively small number of trials.

After the data is collected, SAS creates an equation for the model specified by the user. This model may be used to predict outcomes of future trials though care should be exercised not to extrapolate out of the original experimental region. For example, one would not want to use our models to estimate Air contents of 1.0 since this is completely out of the range of the experimental design.

In addition to an overall equation that combines the effects of all independent variables, SAS can generate comparisons of predicted means (least squares means) to estimate the relative effect of each level of any categorical independent variable. If the design is perfectly balanced (such as a fractional factorial), SAS also could be used to statistically compare the sample means using procedures such as the Duncan's procedure. The sample means do not change with different models as the least squares means might.

The best way to discuss the output analysis is to walk through a sample output. For this purpose, the re-run of the CL28 (28 day chloride permeability) will be used. The two page SAS output is attached at the end of this write up. Inserts of these two pages will be used throughout is the walk-through to better illustrate certain points.

Below is the first part of the SAS GLM output. After the initial title cards and date and time of the SAS run, GLM lists all categorical independent variables with their levels. These are the independent variables given in the CLASS statement if you looked at the SAS programming statements. Independent variables treated as continuous would not be listed here. Looking at the initial GLM output, one can see that W_C (Water to Cement ratio) has 3 discrete levels (0.3, 0.4, and 0.5). Also given is the number of observations used in the analysis. In this case 58 observations were used (duplicates from 29 trials).

```
FHWA - Re-run with corrected CL28 data for Trial 29                    2
                                Original AIR          07:47 Tuesday, August 30, 1994
                             Cl 28 day Permeability

                        General Linear Models Procedure
                            Class Level Information

                   Class      Levels     Values

                   W_C             3     0.3 0.4 0.5

                   AIR             3     2 5 8

                   COARSE          2     LS Q

                   FINE            2     G Q

                   MINERAL         5     FA_C FA_F MS None Slag

                   CEMENT          6     A B C D E F

                    Number of observations in data set = 58
```

The next part of the GLM output provides overall statistics on the model that was fit to the data. It does not go into a separate look at each independent variable. Each dependent measure (variable) has a certain amount of variability. In this particular case, CL28 results are not all the same and thus have a measurable amount of sample variability. In a simple statistical sense, one can estimate this by computing a sample variance (or more usually a sample standard deviation that is the square root of the sample variance.)

The sample variance quantifies the spread or dispersion of the 58 CL28 values. The purpose of the GLM (or a regression or analysis of variance {ANOVA or AOV depending on the book}) is to partition this variably into two parts: a part that can be explained by the independent variables; and a second part that is unexplained or termed error. A Total sum of squares (let's call it TSS for Total Sum of Squares) (represented by the *Corrected Total* row in the GLM output below) is analogous to the sample variance. The TSS is just (N-1) * sample variance where N is the same size (58 in this case). This sum of squares (SS) has N-1 degrees of freedom (because the real mean had to be estimated by the sample mean thus resulting in a 1 degree of freedom loss) and is called Corrected Total SS because it has been corrected for the

loss of the degree of freedom. Many stat books just call it the Total Sum of Squares without using the corrected term. This gives, (58-1) * 11,034,820.02 = 628,984,757 which equals the SS value in the Corrected Total row below. The more of this sample variance (or its analogue the TSS) that the model can account for, the better the model is for predicting CL28.

The TSS = 628,984,757 in the third row below after the "Source" line was divided into the Model SS and Error SS seen in the first and second rows after the "Source" line. Each of the three SS has its degrees of freedom (DF in printout) given, and the Model SS and Error SS have their Mean Squares computed (just the SS divided by the DF). The ratio of the Model Mean Square to the Error Mean Square results in the F statistic (F Value in printout) with its corresponding probability (Pr > F in printout). Large F values (definition of large depends on the DF of both the Model SS and Error SS) imply that our model is doing something worthwhile. Prior to sophisticated software, statisticians would look up the computed F values in the F tables that were developed for a few critical significance levels and determine whether the F test was statistically significant. In modern times, this is not necessary as the software gives up the *p value* which is 1 minus the significance level. It should be pointed out that SAS never prints anything below .0001 for the p values. One could say that our F value of 8.34 for degrees of freedom 15 and 42 is significant at the 99.99% level. Thus in this case the model is performing a useful service to us.

One should not get over-enthused by the overall model F test. It is important to examine and should be treated as a necessary test to pass before going into the later detailed statistical analyses; however, it does not guarantee that our model is a great predictor or say anything about the individual significance of any of our independent variables let alone their levels (e.g., the 3 air levels).

Below the SS table that we discussed above are some other sample summary statistics. The R^2 (R-Square in printout) is just the ratio of the Model SS to the Total SS. High values (approaching 1.0) indicate that the model is accounting for a good deal of the variability of the dependent variable CL28.

The coefficient of variation (C.V. in printout) is just the ratio of the Root MSE to the dependent variable sample mean (CL28 Mean in printout). The Root MSE is the root mean squared error which is the square root of the Error Mean Square. It can be interesting to compare this to the sample standard deviation. The sample standard deviation is 3321.87 which is higher than our Root MSE of 1940.36 which again is giving us a feel for the reduction in unexplained variability due to the use of the proposed model. (The Root MSE can also be roughly used to develop confidence intervals around the predicted model.) In rough terms ±2 * Root MSE gives a 955 confidence interval about the model's predictions. Thus this would correspond to almost ± 4000 for CL28. This appears very wide, however, one must also consider the range of CL28 values used in the analysis. The wide range is seen by the CL28 minimum and maximum values given below.

Minimum	Maximum
336.0000000	13325.00

FHWA - Re-run with corrected CL28 data for Trial 29 3
Original AIR 07:47 Tuesday, August 30, 1994
Cl 28 day Permeability

General Linear Models Procedure

Dependent Variable: CL28

Source	DF	Sum of Squares	Mean Square	F Value	Pr > F
Model	15	470855325.14016500	31390355.00934430	8.34	0.0001
Error	42	158129416.25638600	3764986.10134254		
Corrected Total	57	628984741.39655100			

R-Square	C.V.	Root MSE	CL28 Mean
0.748596	57.48120	1940.35720973	3375.63793103

The next part of the GLM output delves a little further into the model proposed. This section given below examines the *overall* effect of each independent variable. At this point GLM is not examining the levels within each independent variable (this will come later). Only the Type III SS is presented here.

Each independent variable has its own row which ends with an overall significance test (F Value and corresponding p value). The DF, SS, and Mean Square columns follow the logic presented earlier. In this particular output, all variables except FINE (Fine aggregate) are statistically significant at the 95% confidence level since their p values are less that .05.

Source	DF	Type III SS	Mean Square	F Value	Pr > F
W_C	2	72797389.27782680	36398694.63891340	9.67	0.0004
AIR	2	22800642.72956450	11400321.36478220	3.03	0.0591
COARSE	1	116471087.48530800	116471087.48530800	30.94	0.0001
FINE	1	6988226.43635656	6988226.43635656	1.86	0.1803
MINERAL	4	95532589.59817010	23883147.39954250	6.34	0.0004
CEMENT	5	81781152.34933210	16356230.46986640	4.34	0.0028

The next part of the SAS GLM gives the statistical equation that has been developed for the proposed model. The coefficients are least squares coefficients that have been estimated by trying to minimize the sum of the squared differences between the predicted and actual CL28 values for the 58 observations. In GLM with the categorical variables, it should be pointed out that the equation and its coefficients are not unique; however the predicted outcomes are unique. This means that the base case used for each independent can be changed and with a change the coefficients may change but the model will still predict the same exact values for each of the 58 data points.

In the output given there is a separate row for each parameter estimated. This includes an intercept term, as well as, each level within each independent variable. The model's predicted equation is just these coefficients. One would use the appropriate coefficients for a given case. For example if W_C = 0.3, only the W_C coefficient in the 0.3 row would be used. The other two W_C coefficients would not be used. By default SAS uses the highest (alphabetically) level to be the base case. The base case coefficient is zero. The t-tests (T for H0: Parameter = 0 in printout) compare the other levels one by one to the base case only. For example the t-test for W_C = 0.3 performs a statistical comparison between W_C level 0.3 and the base case level 0.5. It tells us nothing about how level 0.3 compares to level 0.4. Focus on the next to last column with Pr > |T| if you want to compare each level to the base case. The t-test is just the ratio of the Estimate column to the Std Error of Estimate column.

Parameter		Estimate	T for H0: Parameter=0	Pr > |T|	Std Error of Estimate
INTERCEPT		3719.530805 B	3.28	0.0021	1133.301967
W_C	0.3	-2932.002229 B	-4.13	0.0002	709.911246
	0.4	-1988.725799 B	-3.22	0.0025	618.525114
	0.5	0.000000 B	.	.	.
AIR	2	-76.603604 B	-0.11	0.9101	674.700598
	5	1349.022615 B	2.06	0.0455	654.420064
	8	0.000000 B	.	.	.
COARSE	LS	3042.961523 B	5.56	0.0001	547.102985
	Q	0.000000 B	.	.	.
FINE	G	766.485802 B	1.36	0.1803	562.603357
	Q	0.000000 B	.	.	.
MINERAL	FA_C	929.433904 B	1.06	0.2959	878.070014
	FA_F	2553.350848 B	2.94	0.0053	868.823548
	MS	-624.612168 B	-0.72	0.4747	865.969783
	None	2616.931538 B	3.04	0.0041	860.604884
	Slag	0.000000 B	.	.	.
CEMENT	A	-1478.202430 B	-1.49	0.1427	989.655100
	B	-3579.439892 B	-3.51	0.0011	1018.336734
	C	-1968.928119 B	-2.03	0.0484	968.615662
	D	-459.407399 B	-0.48	0.6342	958.394314
	E	-3223.072833 B	-3.22	0.0025	1001.320737
	F	0.000000 B	.	.	.

The following part of the printout (given here are only the W_C part of the least squares means) allows all possible comparisons between the least squares means of the levels within each independent variable. Recall that the above printout with the model equation only compared each level to its respective base case. One does need to be careful about protecting the overall experiment-wise Type I error rates when comparing too many means using such tables below.

The matrix below has a row and column for each level of W_C. It is a symmetric matrix. The 3 levels of W_C are 0.3, 0.4, and 0.5 which are rows 1, 2, and 3, respectively in the matrix below. Likewise columns 1, 2, and 3 (just labeled 1, 2, 3) are the W_C levels 0.3, 0.4, and 0.5, respectively. Any pair wise comparison of the least square means may be gleaned from this matrix for W_C for the dependent measure CL28. Actually what is termed a row is really a pair of associated rows with t-tests and their p values. As an example of how to use this particular least squares mean matrix, W_C level 0.3 is significantly different from level 0.5 at the 95% confidence level, but it is not significantly different from the 0.4 level of W_C. The p value are the keys here.

General Linear Models Procedure

Least Squares Means

W_C	CL28 LSMEAN	T for H0: LSMEAN(i)=LSMEAN(j) / Pr > |T| i/j	1	2	3
0.3	2426.57095	1	.	-1.34889 0.1846	-4.1301 0.0002
0.4	3369.84738	2	1.34889 0.1846	.	-3.21527 0.0025
0.5	5358.57318	3	4.130097 0.0002	3.215271 0.0025	.

General Linear Models Procedure
Class Level Information

Class	Levels	Values
W_C	3	0.3 0.4 0.5
AIR	3	2 5 8
COARSE	2	LS Q
FINE	2	G Q
MINERAL	5	FA_C FA_F MS None Slag
CEMENT	6	A B C D E F

Number of observations in data set = 58

General Linear Models Procedure

Dependent Variable: CL28

Source	DF	Sum of Squares	Mean Square	F Value	Pr > F
Model	15	470855325.14016500	31390355.00934430	8.34	0.0001
Error	42	158129416.25638600	3764986.10134254		
Corrected Total	57	628984741.39655100			

R-Square	C.V.	Root MSE	CL28 Mean
0.748596	57.48120	1940.35720973	3375.63793103

Source	DF	Type III SS	Mean Square	F Value	Pr > F
W_C	2	72797389.27782680	36398694.63891340	9.67	0.0004
AIR	2	22800642.72956450	11400321.36478220	3.03	0.0591
COARSE	1	116471087.48530800	116471087.48530800	30.94	0.0001
FINE	1	6988226.43635656	6988226.43635656	1.86	0.1803
MINERAL	4	95532589.59817010	23883147.39954250	6.34	0.0004
CEMENT	5	81781152.34933210	16356230.46986640	4.34	0.0028

Parameter		Estimate	T for H0: Parameter=0	Pr > |T|	Std Error of Estimate
INTERCEPT		3719.530805 B	3.28	0.0021	1133.301967
W_C	0.3	-2932.002229 B	-4.13	0.0002	709.911246
	0.4	-1988.725799 B	-3.22	0.0025	618.525114
	0.5	0.000000 B	.	.	.
AIR	2	-76.603604 B	-0.11	0.9101	674.700598
	5	1349.022615 B	2.06	0.0455	654.420064
	8	0.000000 B	.	.	.
COARSE	LS	3042.961523 B	5.56	0.0001	547.102985
	Q	0.000000 B	.	.	.
FINE	G	766.485802 B	1.36	0.1803	562.603357
	Q	0.000000 B	.	.	.
MINERAL	FA_C	929.433904 B	1.06	0.2959	878.070014
	FA_F	2553.350848 B	2.94	0.0053	868.823548
	MS	-624.612168 B	-0.72	0.4747	865.969783
	None	2616.931538 B	3.04	0.0041	860.604884
	Slag	0.000000 B	.	.	.
CEMENT	A	-1478.202430 B	-1.49	0.1427	989.655100
	B	-3579.439892 B	-3.51	0.0011	1018.336734
	C	-1968.928119 B	-2.03	0.0484	968.615662
	D	-459.407399 B	-0.48	0.6342	958.394314
	E	-3223.072833 B	-3.22	0.0025	1001.320737
	F	0.000000 B	.	.	.

General Linear Models Procedure
Least Squares Means

W_C	CL28 LSMEAN	T for H0: LSMEAN(i)=LSMEAN(j) / Pr > |T| i/j	1	2	3
0.3	2426.57095	1		-1.34889	-4.1301
				0.1846	0.0002
0.4	3369.84738	2	1.34889	.	-3.21527
			0.1846		0.0025
0.5	5358.57318	3	4.130097	3.215271	.
			0.0002	0.0025	

AIR	CL28 LSMEAN	T for H0: LSMEAN(i)=LSMEAN(j) / Pr > |T| i/j	1	2	3
2	3217.58723	1	.	-2.15953	-0.11354
				0.0366	0.9101
5	4643.21345	2	2.159525	.	2.061402
			0.0366		0.0455
8	3294.19084	3	0.113537	-2.0614	.
			0.9101	0.0455	

COARSE	CL28 LSMEAN	T / Pr > |T| H0: LSMEAN1=LSMEAN2
LS	5239.81127	5.561954
		0.0001
Q	2196.84975	

FINE	CL28 LSMEAN	T / Pr > |T| H0: LSMEAN1=LSMEAN2
G	4101.57341	1.362391
		0.1803
Q	3335.08761	

MINERAL	CL28 LSMEAN	T for H0: LSMEAN(i)=LSMEAN(j) / Pr > |T| i/j	1	2	3	4	5
FA_C	3552.74359	1	.	-1.99934	1.940918	-2.11551	1.058496
				0.0521	0.0590	0.0404	0.2959
FA_F	5176.66053	2	1.999345	.	3.880551	-0.07883	2.93886
			0.0521		0.0004	0.9375	0.0053
MS	1998.69752	3	-1.94092	-3.88055	.	-4.03595	-0.72129
			0.0590	0.0004		0.0002	0.4747
None	5240.24122	4	2.115513	0.078826	4.035951	.	3.040805
			0.0404	0.9375	0.0002		0.0041
Slag	2623.30968	5	-1.0585	-2.93886	0.721286	-3.0408	.
			0.2959	0.0053	0.4747	0.0041	

CEMENT	CL28 LSMEAN	T for H0: LSMEAN(i)=LSMEAN(j) / Pr > |T| i/j	1	2	3	4	5	6
A	4024.96986	1	.	2.337598	0.551028	-1.14663	1.961857	-1.49365
				0.0242	0.5845	0.2580	0.0564	0.1427
B	1923.73239	2	-2.3376	.	-1.80083	-3.49442	-0.40079	-3.51499
			0.0242		0.0789	0.0011	0.6906	0.0011
C	3534.24417	3	-0.55103	1.800834	.	-1.71891	1.426862	-2.03272
			0.5845	0.0789		0.0930	0.1610	0.0484
D	5043.76489	4	1.146631	3.494421	1.718913	.	3.109738	-0.47935
			0.2580	0.0011	0.0930		0.0034	0.6342
E	2280.09945	5	-1.96186	0.40079	-1.42686	-3.10974	.	-3.21882
			0.0564	0.6906	0.1610	0.0034		0.0025
F	5503.17229	6	1.493654	3.514987	2.032724	0.479351	3.218822	.
			0.1427	0.0011	0.0484	0.6342	0.0025	

NOTE: To ensure overall protection level, only probabilities associated with pre-planned comparisons should be used.

REFERENCES

1. Schiessl, P., "Influence of the Composition of Concrete on the Corrosion Protection of the Reinforcement," American Concrete Institute Special Publication SP-100, *Concrete Durability*, Vol. 2, 1987, pp. 1633-1650.

2. Whiting, D. and Dziadzic, W., "Resistance to Chloride Infiltration of Superplasticized Concrete as Compared with Currently Used Overlay Systems," *Construction Technology Laboratories Final Report to The Ohio Department of Transportation*, Columbus, OH, May 1989, pp. 1-86.

3. Ryan, J. P., "Relationship of Fly Ash and Corrosion," *Proceedings of the American Concrete Institute*, Volume 47, February, 1951, pp. 481-484.

4. Dhir, R. K., et al., "Diffusion of Chlorides into Concrete - Influence of Fly Ash Quality," *Cement and Concrete Research*, Vol. 21, 1991, pp. 1091-1102.

5. Short, N. R. and Phee, C. L., "Diffusion of Chloride Ions in Portland and Blended Cement Pastes," *Silicates Industriels*, Vol. 10, 1982, pp. 237-240.

6. Hope, B. B. and Ip, A., "Corrosion of Steel and Concrete Made with Slag Cement," *ACI Materials Journal*, November-December, 1987, pp. 525-531.

7. Frey, R., et al., "Kinetic Method to Analyze Chloride Diffusion in Various Concretes," *Cement and Concrete Research*, Vol. 24, No. 5, 1994, pp. 863-873.

8. Al-Amoudi, O., "Durability of Reinforced Concrete in a Aggressive Sabkha Environments," American Concrete Institute, *Material Journal*, May-June 1995, pp. 236-245.

9. Lorentz, T. and French, C., "Corrosion of Reinforcing Steel in Concrete; Effects of Materials, Mix Composition, and Cracking," American Concrete Institute, *Materials Journal*, March-April 1995, pp. 181-190.

10. Ngala, V., et al., "Diffusion in Cementitious Materials: II - Further Investigations of Chloride and Oxygen Diffusion in Well-Cured OPC and OPC/30% PFA Pastes," *Cement and Concrete Research*, Vol. 25, No. 4, 1995, pp. 819-826.

11. Saito, M. and Ishimori, H., "Chloride Permeability of Concrete Under Static and Repeated Compressive Loading," *Cement and Concrete Research*, Vol. 25, No. 4, 1995, pp. 803-808.

12. Halamickova, P., et al., "Water Permeability and Chloride Ion Diffusion in Portland Cement Mortars: Relationship to Sand Content and Critical Pore Diameter,"*Cement and Concrete Research*, Vol. 25, No. 4, 1995, pp. 790-802.

13. Andrade, C., et al., "Calculation of Chloride Diffusivity in Concrete from Migration Experiments in Non-Steady-State Conditions," *Cement and Concrete Research*, Vol. 24, No. 7, 1994, pp. 1214-1228.

14. Johansen, V., et al., "Chloride Transport in Concrete," *Concrete International*, American Concrete Institute, July, 1995, pp. 43-44.

15. Chatterji, S., "On the Applicability of Fick's Second Law to Chloride Ion Migration Through Portland Cement Concrete," *Cement and Concrete Research*, Vol. 25, No. 2, 1995, pp. 299-303.

16. Barneyback, R. S. and Diamond, S., *Cement and Concrete Research*, Vol. 11, 1981, pp. 279.

17. Diamond, S., "Chloride Concentrations in Concrete Pore Solutions Resulting from Calcium and Sodium Chloride Admixtures," *Cement, Concrete, and Aggregates*, Vol. 8, No. 2, Winter 1986, pp. 97-102.

18 Glasser, F. P., et al., "Modification of Cement Pore Fluid Compositions by Pozzolonic Additives," *Cement and Concrete Research*, Vol. 18, 1988, pp. 165-178.

19. Hansson, C. M., et al., "The Effect of Chloride Cation Type on the Corrosion of Steel in Concrete by Chloride Salts," *Cement and Concrete Research*, Vol. 15, 1985, pp. 65-73.

20. Kayyali, O. A., "Chloride Penetration in the Ratio of Cl^-/OH^- in the Pores of Cement Paste," *Cement and Concrete Research*, Vol. 18, 1988, pp. 895-900.

21. Tritthart, J., "Changes in Pore Water Composition and in Total Chloride Content at Different Levels of Cement Paste Plates Under Different Storage Conditions," *Cement and Concrete Research*, Vol. 22, 1992, pp. 129-138.

22. Kawamura, M., et al., "Effects of a Fly Ash on Pore Solution Composition in Calcium and Sodium Chloride-Bearing Mortars," *Cement and Concrete Research*, Vol. 18, 1988, pp. 763-773.

23. Goni, S. and Andrade, C., "Synthetic Concrete Pore Solution Chemistry and Rebar Corrosion Rate in the Presence of Chlorides," *Cement and Concrete Research*, Vol. 20, 1990, pp. 525-539.

24. Andersson, K., et al., "Chemical Composition of Cement Pore Solutions," *Cement and Concrete Research*, Vol. 19, 1989, pp.327-332.

25. Duchesne, J. and Berube, M. A., "Evaluation of the Validity of the Pore Solution Expression Method from Hardened Cement Pastes and Mortars," *Cement and Concrete Research*, Vol. 24, No. 3, 1994, pp. 456-462.

26. Rasheeduzzafar, et al., "Effect of Cement Composition on Chloride Binding and Corrosion of Reinforcing Steel in Concrete," *Cement and Concrete Research*, Vol. 21, 1991, pp. 777-794.

27. Clear, K. C., "Chloride at the Threshold," *Report of Kenneth C. Clear, Inc.*, March 1983, pp. 1-11.

28. Arya, C., et al., "Factors Influencing Chloride Binding in Concrete," *Cement and Concrete Research*, Vol. 20, 1990, pp. 291-300.

29. Tritthart, J., "Chloride Binding in Cement, I: Investigations to Determine the Composition of Pore Water in Hardened Concrete," *Cement and Concrete Research*, Vol. 19, 1989, pp. 586-594.

30. Tritthart, J., "Chloride Binding in Cement, II: The Influence of the Hydroxide Concentration in the Pore Solution of Hardened Cement Paste on Chloride Binding," *Cement and Concrete Research*, Vol. 19, 1989, pp. 683-691.

31. Page, et al., "The Influence of Different Cements on Chloride-Induced Corrosion of Reinforcing Steel," *Cement and Concrete Research*, Vol. 16, 1986, pp. 79-86.

32. Arya, C. and Xu, Y., "Effect of Cement Type on Chloride Binding and Corrosion of Steel in Concrete," *Cement and Concrete Research*, Vol. 25, No. 4, 1995, pp. 893-902.

33. Byfors, K., et al., "Pore Solution Expression as a Method to Determine the Influence of Mineral Additives on Chloride Binding," *Cement and Concrete Research*, Vol. 16, 1986, pp. 760-770.

34. Suryavanshi, A., et al., "The Binding of Chloride Ions by Sulfate-Resistant Portland Cement," *Cement and Concrete Research*, Vol. 25, No. 3, 1995, pp. 581-592.

35. Haque, M. and Kayyala, O.. "Free and Water-Soluble Chloride in Concrete," *Cement and Concrete Research*, Vol. 25, No. 3, 1995, pp. 531-542.

36. Enevoldsen, J., et al., "Binding of Chloride in Mortar Containing Admixed or Penetrated Chlorides," *Cement and Concrete Research*, Vol. 24, No. 8, 1994, pp. 1525-1533.

37. Chatterji, S., "A Discussion of the Paper 'The Effectiveness of Supplementary Cementing Materials in Suppressing Expansion Due to ASR, Part II: Pore Solution Chemistry by Duchesne and Berube,'" *Cement and Concrete Research*, Vol. 24, No. 8, 1994, pp. 1577-1578.

38. Fraczek, J., "A Review of Electrochemical Principles as Applied to Corrosion of Steel in a Concrete or Crowd Environment," American Concrete Institute Special Publication SP-102, *Corrosion Concrete in Chlorides*, 1987, pp. 13-19.

39. Hope, B.B., et al., "Corrosion Rates of Steel in Concrete," *Cement and Concrete Research*, Vol. 16, 1986, pp. 771-781.

40. Hope B. B. and Ip, A. K., "Corrosion and Electrical Impedance in Concrete," *Cement and Concrete Research*, Vol. 15, 1985, pp. 525-534.

41. Alonso, C., et al., "Relation Between Resistivity and Corrosion Rate of Reinforcements in Carbonated Mortar Made with Several Cement Types," *Cement and Concrete Research*, Vol. 8, 1988, pp. 687-698.

43. Arya, C. and Vassie, P., "Influence of Cathode to Anode Area Ratio and Separation Distance on Galvanic Corrosion Current of Steel in Concrete Containing Chlorides," *Cement and Concrete Research*, Vol. 25, No. 5, 1995, pp. 989-998.

43. Enevoldsen, J., et al., "The Influence of Internal Relative Humidity on the Rate of Corrosion of Steel Embedded in Concrete and Mortar," *Cement and Concrete Research*, Vol. 24, No. 7, 1994, pp. 1373-1382.

44. Hussain, S. and Rasheeduzzafar, "Effect of Temperature on Pore Solution Composition in Plain Cements," *Cement and Concrete Research*, Vol. 23, 1993, 1357-1368.

45. Gu, P., et al., "Effect of Uneven Porosity Distribution in Cement Paste and Mortar on Reinforcing Steel Corrosion," *Cement and Concrete Research*, Vol. 24, No. 6, 1994, pp. 1055-1064.

46. Gonzalez, J., et al., "Comparison of Rates of General Corrosion and Maximum Pitting Penetration on Concrete Embedded Steel Reinforcement," *Cement and Concrete Research*, Vol. 25, No. 2, 1995, pp. 257-264.

47. Lopez, W., et. al., "Influence of Temperature on the Life of Rebars", *Cement and Concrete Research*, Vol. 23, 1993, pp. 1130-1140.

48. Arup, A., Sorensen, B., Fredericksen, J., and Thaulow, N., "The Rapid Chloride Permeability Test - An Assessment," *Corrosion/93*, Paper no 334, NACE, Houston, TX, (1993).

49. Feldman, R.F., Chan, G.W., Brousseau, R.J., and Tumidajski, P.J., "Investigation of the Rapid Permeability Test,: *ACI Materials Journal*, May/June, 1994, p. 246.